Evaluation of Erosion Wear of Ash Handling Pipes

A thesis report submitted in partial fulfilment of the requirements for the award of degree of

Master of Engineering

In

PRODUCTION AND INDUSTRIAL

By:

Abrar Ali Khan

Roll no. 801082001

under the supervision of

Dr.S.K.Mohapatra

(Senior Professor, MED, Thapar University, Patiala)

(June 2012)

Mechanical Engineering Department

Thapar University, Patiala-147004

DECLARATION

I hereby certify that the work which is being presented in this report entitled "**Evaluation of Erosion Wear of Ash Handling Pipes**", in partial fulfilment of the requirements for the award of degree of Master of Engineering in Mechanical Engineering with specialization in **PRODUCTION AND INDUSTRIAL ENGINEERING** submitted in **Mechanical Engineering Department** of Thapar university, Patiala, is an authentic record of my own work carried out under the supervision of **Dr. S. K. Mohapatra** and refers to other researcher's studies which are duly listed in the reference section.

The matter presented in this thesis has not been submitted for the award of any other degree of this or any other university.

Date : 13/07/2012

Place: Patiala

(Abrar Ali Khan)

This is to certify that the above statement made by the candidate is correct and true to the best of my knowledge.

Supervisor :

Dr. S.K. Mohapatra

Dean of Academic Affairs

Thapar University Patiala

Counter Signed by

Dr. Ajay Batish

Professor & Head

Mechanical Engineering Department

Thapar University, Patiala

Dr. S.K. Mohapatra

Dean of Academic Affairs

Thapar University, Patiala

ACKNOWLEDGEMENT

This thesis has been a very inspiring, challenging but always exciting and interesting experience.I takes this opportunity to thank all those who helped me in the completion of this work.

This work would not have been possible without the encouragement and able guidance of Dr.S.K.Mohapatra, Senior Professor and Dean of Academic Affairs, Thapar University, Patiala. His enthusiasm and optimism made this experience both rewarding and enjoyable. Most of the novel ideas and solutions in this work are the result of numerous stimulating discussions we had. His feedback and editorial comments were valuable for the writing or this thesis.

I am grateful to Dr. Ajay Batish, Professor and Head of Department of Mechanical Engineering Department for providing me with the facilities in the Department, which helped in completion of my work.

I would like to thank Mr. Satish Kumar, Assiatant Professor, MED, for his novel ideas and solutions which helped me through this journey of my thesis work. His support and encouragement kept me moving towards the completion of this work.

It would be inappropriate to end this without thanking the faculty members and employees of Mechanical Department, Thapar University, Patiala as their everlasting support is a crucial aspect in the completion of my thesis work, specially Mr.Sukhbir Singh, Mr.Narinder Singh(lab attendants).

I take pride in being blessed with the best parents without whose sacrifice, affectionate blessing, everlasting desire and round the clock support, this would have not been possible. I would like to thank my grandparents for their encouragement which made me reach the end with the same zeal with which I started this project. I also thank my brother and cousins for their timely cooperation.

I am also grateful to all my friends for accompanying me during the most pivotal times and standing by me through thick and thin.

But most importantly i would like to thank the Almighty God for giving me strength and ability.

ABSTRACT

Erosion wear is a very common problem in the ash handling pipelines of the coal fired thermal power plants. Mild steel is most commonly used as the piping material in thermal power plants because of its low price and good mechanical properties. Therefore, mild steel was chosen as one of the testing material. Steel 202 was chosen as the second testing material. Steel 202 is cheap and has better properties than mild steel. Erosion wear plays an important role in design and operation of slurry transport system. The present work reports experimental investigation on slurry erosion of mild steel and steel 202 with and without tungsten carbide coating in a slurry pot tester with fly ash and bottom ash slurry mixed in water as erodent. The coating was done with high velocity oxy-fuel (HVOF) thermal coating of thickness of 250μ-300μ. Effect of parameters such as speed at 700, 1000 and 1400rpm with concentration of fly ash at 20%, 40% and 60% by weight in water and for time duration of 60, 90, 120,150 and 180 minutes was calculated. Analysis of weight-loss data and examination of eroded surfaces by scanning electron microscopy was done for coated and uncoated material. Steel 202 reported less erosion wear than mild steel .WC coated mild steel and steel 202 reported less erosion wear than uncoated mild steel and steel 202. The analysis of eroded samples was done using SEM. Signatures of microcutting, fracture of well-bonded WC grains, and fragmentations were observed on the eroded surface of WC-12Co coating, while signatures of formation of ploughing, lips, shearing of platelet, formation of crater, and micro-cutting were observed on the eroded surface of bare mild steel and steel 202.

LIST OF CONTENTS

LIST OF FIGURES

LIST OF TABLES

CHAPTER-1

INTRODUCTION

1.1 WEAR:

Wear is loss of material from a component due to mechanical interaction with another object. Wear reduces the service life of equipment. The rate of removal is generally slow, but steady and continuous. The material intrinsic surface properties such as hardness, strength, ductility, work hardening etc. are very important factors for wear resistance, but other factors like surface finish, lubrication, load, speed, corrosion, temperature and properties of the opposing surface etc. are equally important.

1.2 TYPES OF WEAR:

Figure 1.1 shows the five main categories of wear and the specific wear mechanisms that occur in each category. Each specific mode of wear looks different to the next, and may be distinguished relatively easily.

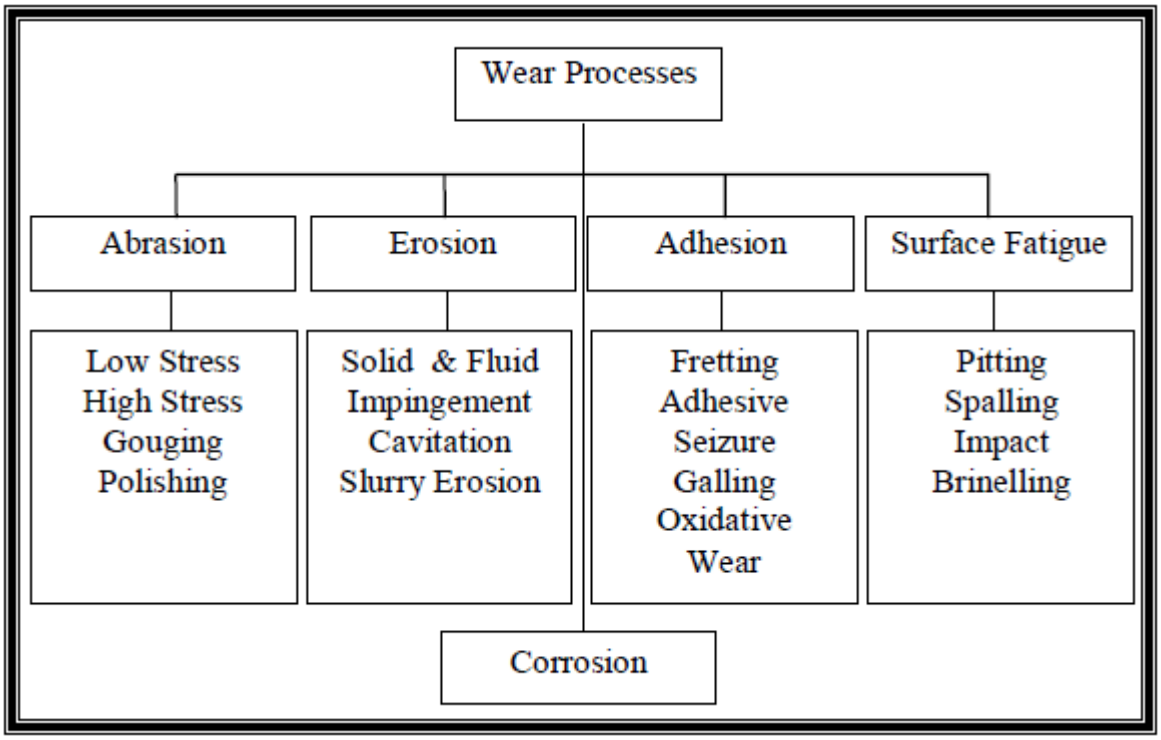

Figure: 1.1 Types of wear

1.2.1 Abrasive Wear:

Abrasive wear occurs when material is removed from one surface by another harder material, leaving hard particles of debris between the two surfaces. It can also be called scratching, gouging or scoring depending on the severity of wear. Two body abrasive wear occurs when one surface (usually harder than the second) cuts material away from the second, although this mechanism very often changes to three body abrasion as the wear debris then acts as an abrasive between the two surfaces. The abrasive wear produced by the hard, sharp surface sliding against the softer one produces a groove in the softer surface.

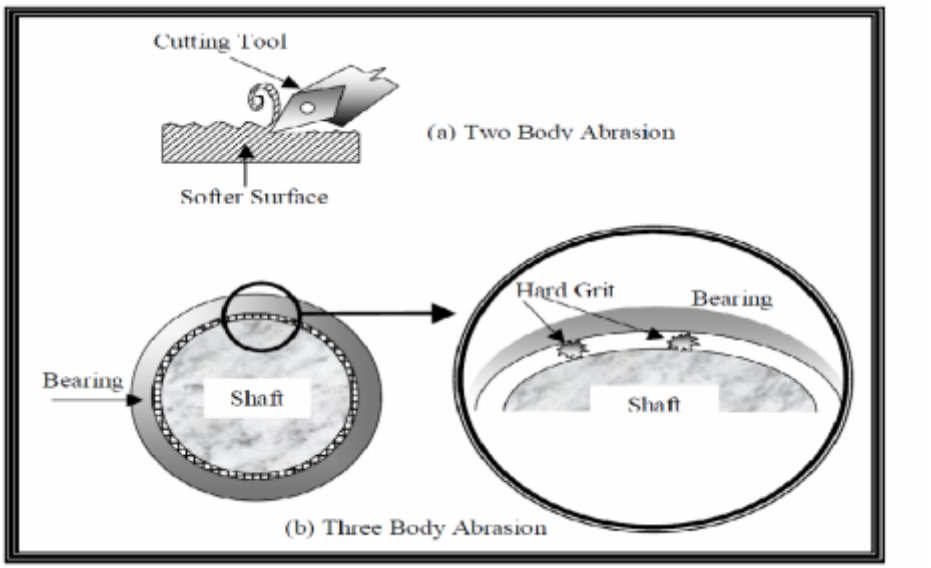

Figure 1.2 Schematic of abrasive wear phenomenon

1.2.2 ADHESIVE WEAR:

Adhesive wear is produced when interfacial adhesive junctions lock together as two surfaces slide across each other under pressure. As normal pressure is applied, local pressure at the asperities become extremely high. Often the yield stress is exceeded, and the asperities deform plastically until the real area of contact has increased sufficiently to support the applied load, as shown in figure 3. In the absence of lubricants, asperities cold-weld together or else junctions shear and form new junctions. If the junctions formed between the sliding surfaces do not break along its original interface then a chunk from one of the sliding surface will be transferred to the other surface. For adhesive wear to occur it is necessary for the surfaces to be in intimate contact

with each other. Surfaces which are held apart by lubricating films, oxide films etc. reduce the tendency for adhesion to occur.

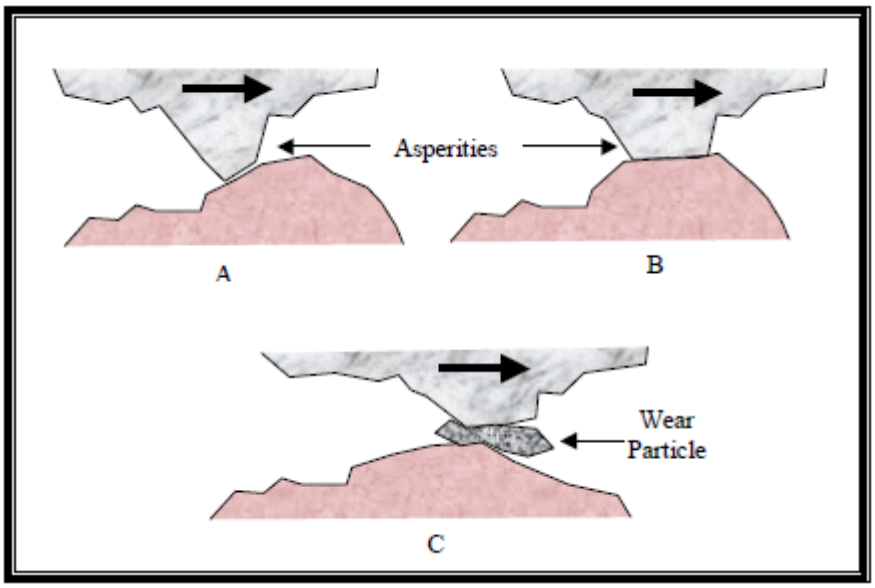

Figure 1.3 Schematic of adhesion wears process

1.2.3 CORROSIVE WEAR:

Corrosion is the gradual destruction of material, usually metals, by chemical reaction with its environment. Most metals react with the oxygen in atmosphere to form oxides. These oxides form layer or scales over the surface. These scales are very loosely bonded to the surface. The scales can be very easily removed from the surface of the material. Corrosion can be concentrated locally to form a pit or crack, or it can extend across a wide area more or less uniformly corroding the surface.

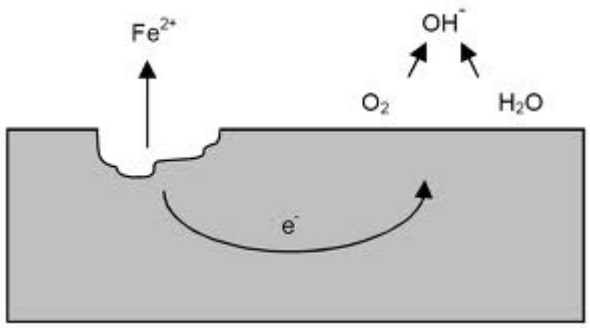

Figure: 1.4 Localized corrosion developing on a metal

Because corrosion is a diffusion controlled process, it occurs on exposed surfaces. Corrosion can be reduced by coating the surface of the material using different processes.

1.2.4 SURFACE FATIGUE

Surface fatigue is a process by which the surface of a material is weakened by cyclic loading, which is one type of general material fatigue. Fatigue wear is produced when the wear particles are detached by cyclic crack growth of microcracks on the surface. When mechanical machinery move in periodical motion, stresses to the metal surfaces occur, often leading to fatigue of material. All repeating stresses in a rolling or sliding contact can give rise to fatigue failure. These effects are mainly based on the action of stresses in or below the surfaces, without the need of direct physical contact of the surface under consideration. When two surface slides across each other, the maximum shear stress lies in some distance below the surface, causing microcracks, which lead to failure of the component. These microcracks are either superficial cracks or subsurface cracks.

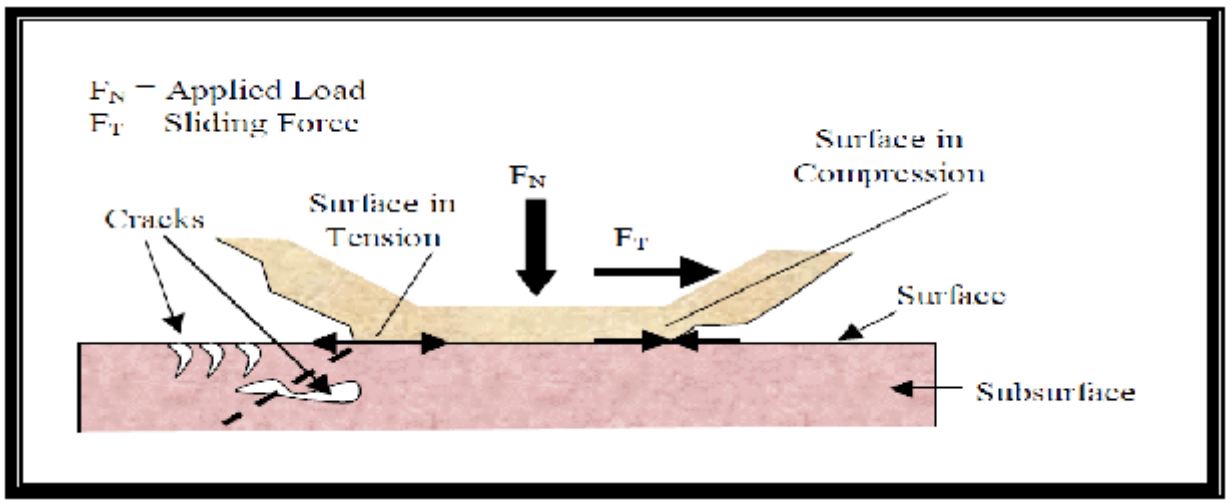

Figure: 1.5 Schematic of fatigue wear

1.2.5 Erosion Wear:

This kind of wear occurs due to impingement of solid particles on the surface. it occurs due to mechanical interaction of impinging solid particles on the surface. Erosive wear can be described as an extremely short sliding motion and is executed within a short time interval. Erosion wear results from particle impingement or cavitation shocks against a surface, but not from the

trapping of loose particles between sliding contact surface. Erosion is particularly insidious because it tends to concentrate its effect, and can cause damage quickly with little warning-i.e. a hole punched through the elbow of a pipe carrying a slurry or gas suspension of particles. Erosion is very difficult to predict, and therefore difficult to control. Because it is not as pervasive as abrasion, and more confined to specific situations. Erosion wear causes a big problem in industries like thermal power plants, hydro power plants, mineral industries etc.

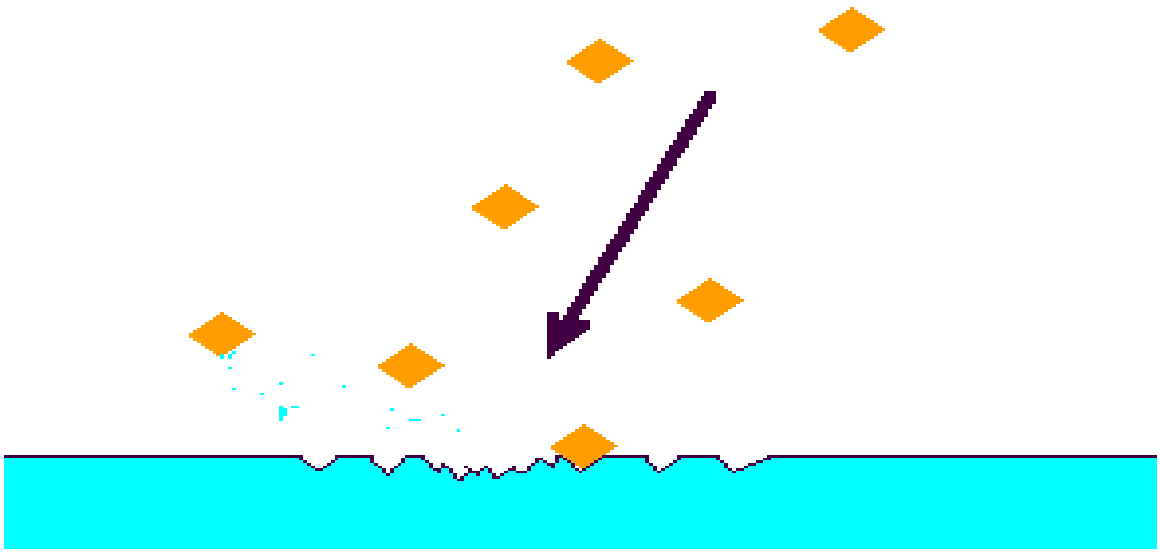

Figure: 1.6 Schematic of erosion wear

1.3 TYPES OF EROSION WEAR:

Erosion wear can be classified on the basis of interaction between target surface and the impacting substance. Following are the types of erosion wear:

1.3.1 SOLID PARTICLE EROSION:

In this, only particles entrained in gas are considered. Solid particle erosion is to be expected whenever hard particles are entrained in a medium that impinges a solid at any significant velocity Repeated impact by airborne solid particles causes erosion and degradation of materials known as solid particle erosion. Erosion damage depends on the particle impact velocity, the mechanical properties of the particles and target, the mass flux of particles, their size and shape.

1.3.2 CAVITATION EROSION:

Cavitation is the formation and then immediate implosion of cavities in a liquid. Cavitation is a significant cause of wear in some engineering contexts. Cavities in contact or close to a solid surface will collapse asymmetrically forming a micro jet of liquid directed toward the solid. Also, the cavities do not act independently, but collapse in concert. This effect leads to an enhanced effect such that the pressures produced by these collapses may cause localized deformation and/or removal of material from a surface in the vicinity of the cavities. The collapse of a cavity cluster starts at the outer perimeter and proceeds inwards. Much of the energy produced by the outer cavities is transferred inwards. The intensity of the collapse of the inner cavities will thus be very high. Also, there will be a significant, localized, temperature increase (up to 5000 K) associated with the collapse. When entering high pressure areas, cavitation bubbles that implode on a metal surface cause cyclic stress. This result in surface fatigue of the metal causing a type of wear also called "cavitation erosion"

1.3.3 LIQUID IMPINGEMENT EROSION:

Liquid impingement erosion has been defined as “progressive loss of original material from a solid surface due to continued exposure to impacts by liquid drops or jets. Liquid impingement erosion connotes repeated impacts or collisions between the surface being eroded and small discrete liquid bodies. The significance of these discrete impacts is that they generate impulsive contact pressure on the solid target, far higher than produced by steady flows and thus the endurance limit and even the yield strength of the target material can be easily exceeded.

1.3.4 SLURRY EROSION:

The term “slurry erosion” is strictly defined as that type of wear, or loss of mass, that is experienced by a material exposed to a high-velocity stream of slurry. This erosion occurs either when the material moves at a certain velocity through the slurry or when the slurry moves past the material at a certain velocity. There are different slurry erosion modes which are as follows:

(a) Abrasion-corrosion (b) Scouring wear (c) Crushing and grinding (d) High-velocity erosion
(e) Low-velocity erosion (f) Saltation erosion (g) Cavitation

1.4 MECHANISMS OF EROSION WEAR:

The Commonly accepted erosion mechanisms are classified as:

1. Cutting
2. Ploughing
3. Extrusion and forging
4. Subsurface deformation and cracking

1.4.1 CUTTING EROSION

If the particles are very sharp it causes cutting erosion and a micromachining action occurs when particles interact with the material surface. Minimal plastic deformation of the surface region occurs in slurry pipeline because of two mechanisms namely corrosion and erosion. These mechanisms are quite different in various manners.

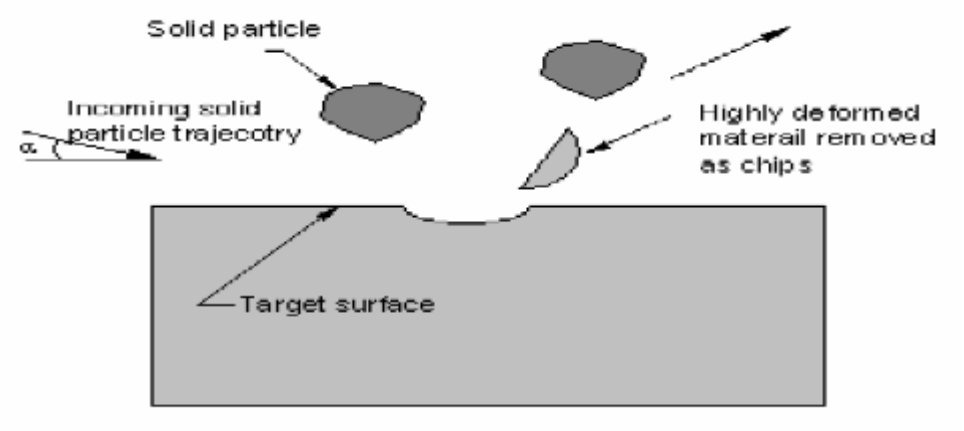

Figure 1.7 Cutting erosion mechanism

1.4.2 PLOUGHING EROSION

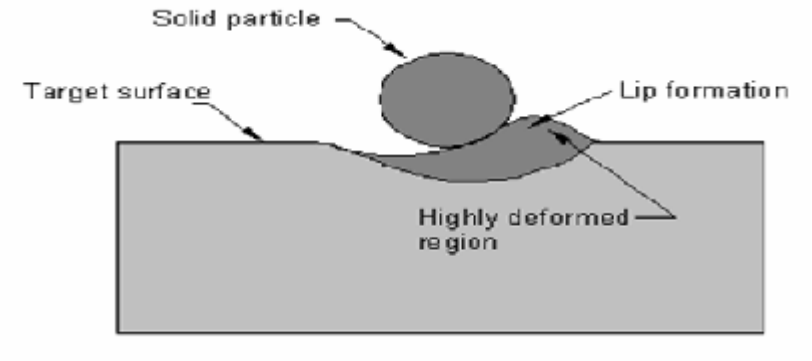

Figure 1.8 Ploughing erosion mechanism

Ploughing erosion is a two stage process involving localized plastic deformation of the surface from rounded particle impacts In first start stage process, particle impacts form surface caters with plastic flow of the surface occurring around the particle edges during impact. As a result of the particle collision, an extruded shear lip is formed. The second stage process involves repeated particle impacts causing fatigue of the extruded shear lip regions. The shear lips fail and are broken off

1.4.3 EXTRUSION AND FORGING MECHANISM

This mechanism is also known as platelet mechanism. The impact of a solid particle spreads the target material over the adjacent crater in the direction of impact. This spread material gets further flattened and extended to develop a platelet. A proposed sequence of particle impacts that could cause the material removal due to platelet mechanism is shown.

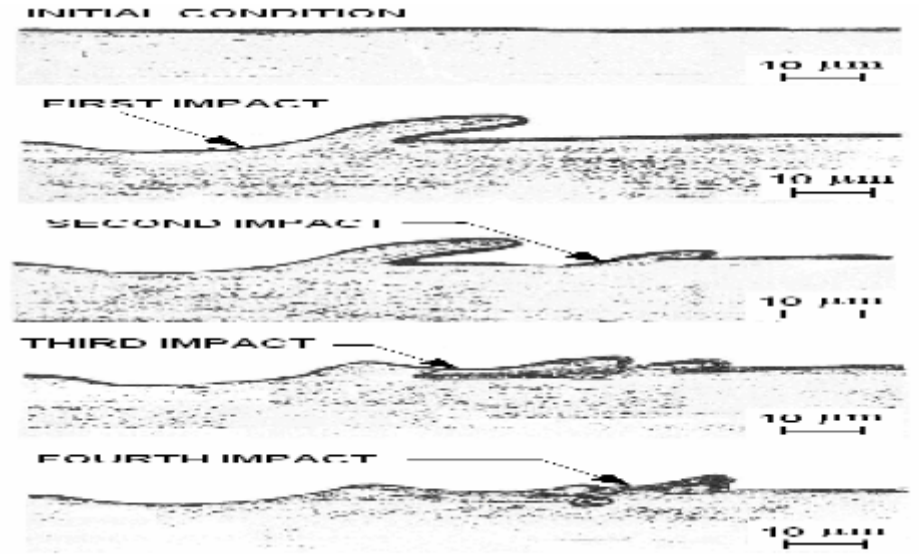

Figure 1.9 Extrusion and forging mechanism

1.4.4 SUBSURFACE DEFORMATION AND CRACKING

A blunt particle striking the target surface at high velocity causes localized plastic deformation at the point of contact, which develops cracks leading to wear by brittle fracture. This type of wear mechanism is known as subsurface deformation or cracking. As the particle moves over the surface, small increment in the plastic strain takes place and the residual stresses develop in the deformed layer. Since the ratio of particle size to contact asperity size is 100:1, the material experiences cyclic loading and unloading as it moved over the surface. This leads the anisotropy

in the surface layer and subsequent crack generation. When cracks generated from various parts of the solid link together through crack propagation, loose eroded material is formed. The ploughing process also causes subsurface plastic deformation and may also contribute to the generation and propagation of subsurface cracks. When subsurface cracks propagate, the target material loses out as small wear particles causing loss of material from the surface. Thus the solid particle striking at large impact angles causes brittle fracture and the material is removed from the surface by the formation and intersection of cracks.

1.5 PARAMETERS AFFECTING EROSION WEAR:

CONCENTRATION OF PARTICLES IN LIQUID: Higher concentration produces greater erosion wastage per unit of time, but the effect is not linear. When measured per unit of erodent mass, higher concentration reduces erosion damage. At very high concentrations particle interaction increases and this decreases the particles striking velocity on the striking surface.

SLURRY FLOW SPEED AND PARTICLE IMPACT SPEED: Speed of the particles strongly effect the erosion wear rate of the particle. Higher the speed of the flow of the slurry and particle impact speed higher is the erosion wastage, with exponents reported between 2 and 4.

IMPACT ANGLES OF PARTICLES ON WEARING SURFACE: Impact angle is the angle at which the particle strikes the target surface. The effect if impact angle is different for different materials. For ductile materials maximum erosion occurs at 20-30 degrees and for brittle materials maximum erosion occurs at 90 degree impact angle.

PARTICLE SIZE: The impact of larger particles produces more erosion than the impact of smaller particles, erosion being proportional to particle diameter. Bottom ash shows more erosion than fly ash because of the larger particle size.

PARTICLE DENSITY: Particles of higher density give higher density give rise to greater energy dissipation at impact and give rise to more damage per particle impact.

PARTICLE SHAPE: Sharp, jagged particles are more effective in producing waste than rounded or spherical particles.

PARTICLE AND TARGET SURFACE HARDNESS: The more the hardness of the erodent particles the more is the material eroded from the target surface. The increase in the hardness of the target surface shows more resistance to erosion.

NATURE OF SUSPENDING LIQUID: The liquids of low density and low viscosity are associated with higher erosion rates.

COATING: Coatings are coverings that are applied to the surface of a material called substrate to improve its properties like corrosion resistance, erosion resistance, appearance, adhesion, friction resistance etc.

1.6 THERMAL POWER PLANTS:

A modern pulverized coal-fired electricity generation facility that uses the most commonly employed rankine cycle based thermodynamic system. The majority of the thermal power plants still relies on the heat produced by combustion reactions and its fuels such as, pulverized coal fuel oil or natural gas have been used for more than a century. All thermal power plants convert heat energy into mechanical energy, and then into electricity. This is done by using heat to turn water into steam and then directing the steam at a turbine. The steam turns the turbine blades, converting heat into mechanical power. This in turn runs the generator, which creates electricity.

Thermal Power Plants – status in India (as of 12/2008)

• Current installed capacity of Thermal Power is 93,398.84 MW which is 64.7% of total installed capacity.

• Current installed base of Coal Based Thermal Power is 77,458.89 MW which comes to 53.3% of total installed base.

• Current installed base of Gas Based Thermal Power is 14,734.01 MW which is 10.5% of total installed base.

• Current installed base of Oil Based Thermal Power is 1,199.75 MW which is 0.9% of total installed base.

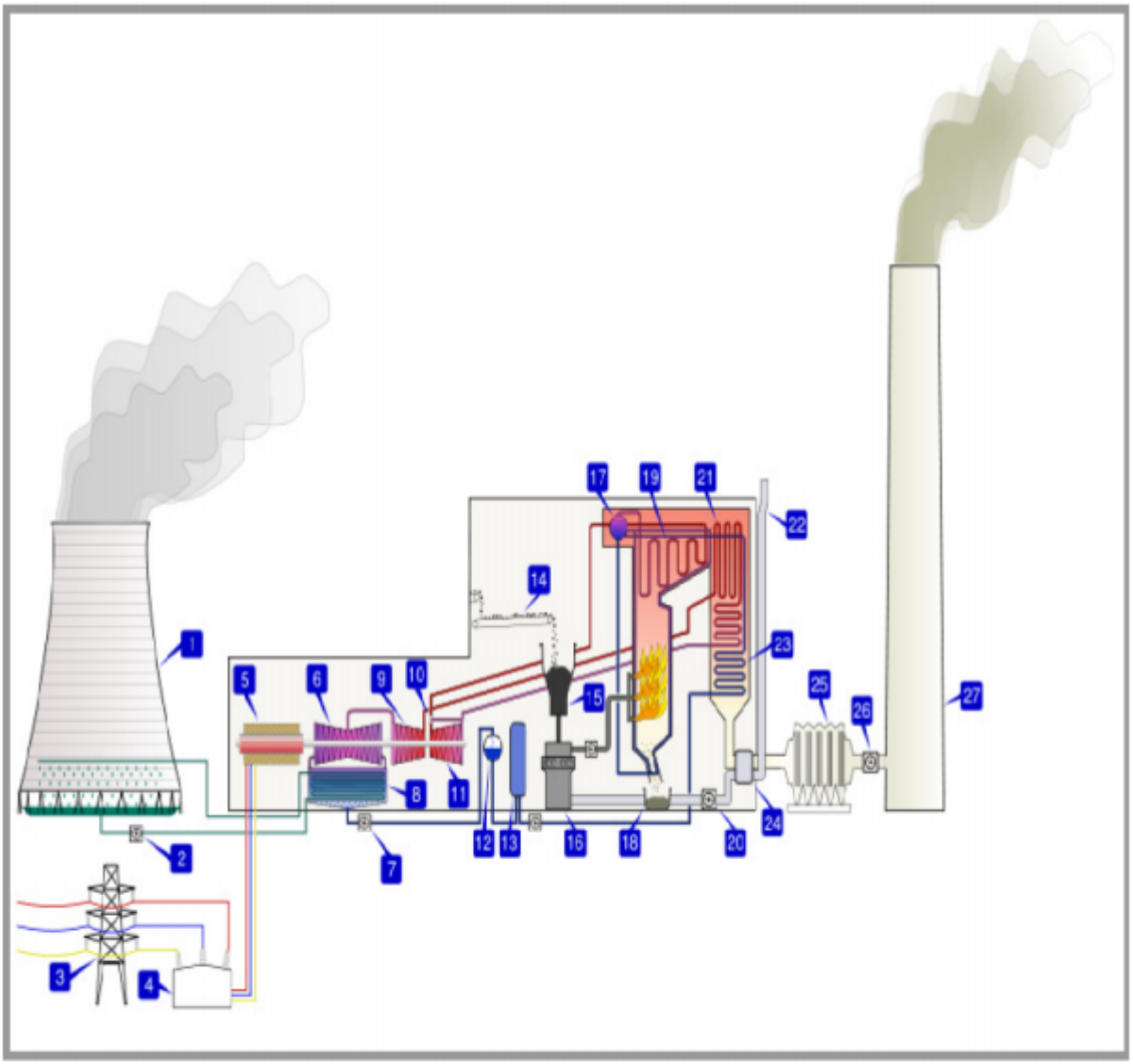

Figure 1.10 Schematic of coal fired thermal power plant

1. Cooling tower
2. Cooling water pump
3. Transmission line
4. Unit transformer
5. Electric generator
6. Low pressure turbine
7. Boiler feed pump
8. Condensor
9. Intermediate pressure turbine
10. Steam governor valve
11. High pressure turbine
12. Deaerator
13. Feed heater
14. Coal conveyor
15. Coal hopper
16. Pulverised fuel mill
17. Boiler drum
18. Ash hopper
19. Superheater
20. Forced draught fan
21. Reheater
22. Air intake
23. Economiser
24. Air preheater
25. Precipitator
26. Induced draught fan
27. Chimney Stack

1.7 ASH TRANSPORTATION:

Ash disposal in thermal power plants is a highly environmentally sensitive issue. India is currently producing in excess of 100 million tonnes of coal ash. Currently fly ash and bottom ash are mixed together and transported hydraulically to ash ponds. The end uses of fly ash and bottom ash are different as their properties are different. Mixing them during transportation would affect the end usage of both forms of ashes.

1.7.1 ALTERNATIVE FORMS OF ASH TRANSPORTATION:

1) Dry disposal as ash mounds

2) Wet transportation for disposal in ash ponds

1.7.2 WET DISPOSAL CAN BE CLASSIFIED INTO THREE CATEGORIES:

1) Low concentration slurry disposal (LCSD)(10% to 30%)

2) Medium concentration slurry disposal (MCSD)(40% to 50%)

3) High concentration slurry disposal (HCSD)(60% to 70%)

1.8 BASIC SLURRY TRANSPORTATION SYSTEM:

The basic slurry transportation systems consists of three sub-system

(1) Slurry preparation facility
(2) Pipelines and pumps
(3) Terminal facility

In the slurry preparation sub-system, the solids are reduced to powder form and are stored in the storage place. Then water or the liquid is added to the powdered solid to make slurry and is pumped with the help of pumps. The pumped slurry is then transported to the next station using pipelines. Pipelines can transport the slurry to longer distances easily. The next station is the

dewatering station where water is removed from the slurry and the powdered form is transported for further utilization or it is sent to the dumping yard far away.

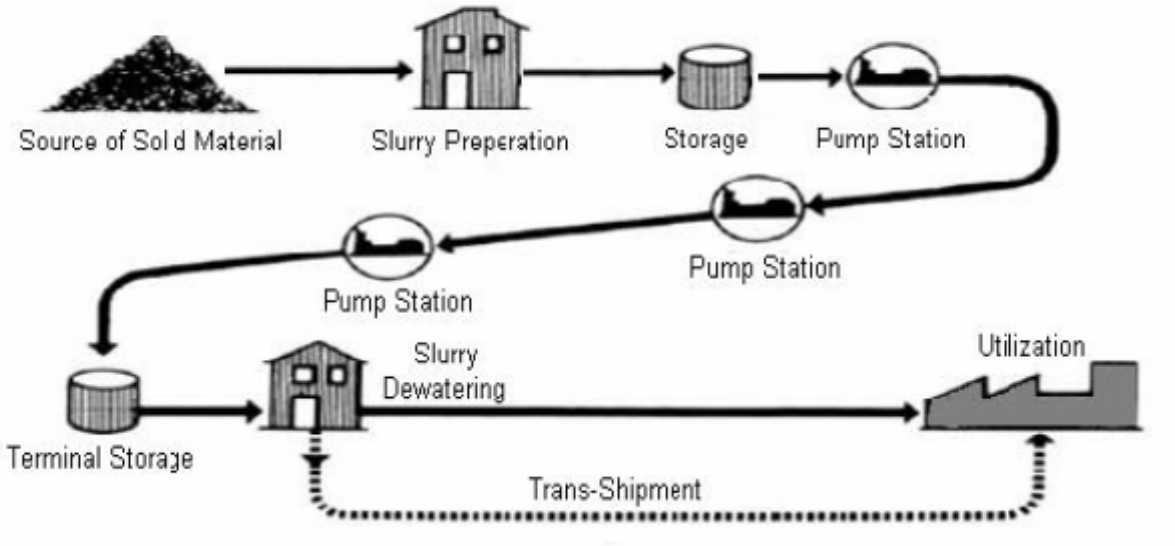

Figure 1.11 A slurry transport system

1.9 SLURRY PIPELINES:

Slurry pipelines have been accepted by various industries as an extremely safe and attractive mode of solid transportation because of its low maintenance, round the year availability and being eco-friendly. Slurry pipelines are used to transport solid materials using water or any other liquid as carries fluid either for long distance transportation of bulk materials, like mineral ore to processing plants, coal to thermal power plants or for disposal of waste material like fly ash, tailings materials etc. to the disposal sites. The economic benefit derived from increasing the erosion resistance of material used for wear protection in materials processing, handling and transport by hydraulic means lies mainly in less frequent failure of critical components leading to reduced maintenance costs and plant downtime. The ability to assess accurately the erosion resistance of materials for industrial use by means of laboratory testing would thus be most valuable in product selection and in the prediction of service life.

1.9.1 ADVANTAGES OF SLURRY PIPELINES:

1) Simple to install and small space requirement

2) Low manpower requirement for installation, operation and maintenance

3) Distance and volume of transportation is increased

4) Ease of crossing both natural and artificial obstacles

5) High efficiency and reliability

6) Traffic and air pollution reduction

7) Saving on energy consumption

1.10 WEAR IN SLURRY PIPELINES:

Wear in slurry pipes takes place because of two mechanisms, namely corrosion and erosion. These mechanisms are quite different in nature. Corrosion of a metal is an electro-chemical phenomenon and in slurry pipeline it is generally due to the dissolved oxygen in the slurry. Corrosion can be controlled by passivating either the anodic or the cathodic reactions of the pipe wall. Elimination of dissolved oxygen and the adjustment of slurry pH can also reduce the corrosion rate. Erosion of metal occurs due to the dynamic action of the moving particles on the pipe wall and is generally more pronounced than corrosion in slurry pipeline systems. It usually takes place through two mechanisms, namely ‘deformation wear’ (impact) and ‘cutting wear (sliding). The high kinetic energy of the impinging particles causes deformation wear (impact) and can be attributed to the creation of high local stresses. The oblique impact of particles causes a cutting wear (sliding) on the pipe surface. For horizontal pipelines, the cutting wear dominates the overall wear, whereas deformation wear is more significant in case of pipe bends, pumps etc. The erosion wear pattern is also influenced by the type of particle movement (sliding rolling or saltation) along the pipe surface, a phenomenon determined by the type of flow regime. Hence, it is difficult to forecast which form of erosion (sliding or impact) will be dominant for any given situation.

Erosion wear is very complex phenomenon and controlled experiments are required to identify the important parameters affecting it as well as to quantify the effects of each one of them. Once these effects have been quantified, it may then perhaps, be possible to increase the life span and hence reduce the effective cost due to inevitable wear. The rate of erosion in a slurry pipeline is affected by large number of parameters. The parameters that affect erosion wear in pipelines are:

a) Characteristics of solid particles

- Size (maximum and minimum) and size distribution
- Hardness
- Density
- Shape
- Composition
- Attrition

b) Characteristics of carrier fluid

- Corrosiveness
- Density
- Viscosity

c) Slurry properties

- Concentration
- Viscosity
- Density

d) Condition of flow

- Laminar/ Turbulent
- Heterogeneous/ Homogeneous
- Velocity of flow

e) Characteristics of pipe material

Strength

Ductility

Hardness

The dependence of erosion wear on such a large number of parameters makes the erosion phenomenon quite complicated. Wear in a pipeline is a strong function of velocity of flow. Several investigators have shown that wear rate is proportional to V^n and suggested different values n. in general, value of n can lie anywhere between 1to 3.5. The effect of solid concentration on local wear rate is more complicated. However, overall wear rate increases with increasing solid concentration. For horizontal slurry flows, impact angle is small ($< 20^0$) and thus is not important variable for slurry flow through horizontal pipelines. Particle size and particle hardness also are known to affect wear rate considerably. It has been reported that there is a strong dependence of wear rate on particle size until a critical size is reached. Above this size wear rate is independent of particle size. It has also been reported that wear rate increases with increasing hardness of the particles. It was also found that wear rate increases drastically with reduction in viscosity. As for the pipe characteristics it has been mentioned that harder the pipe more resistant it will be.

It has been observed that wear rate is dependent on velocity and concentration of solids apart from other variables mentioned above. In slurry flow through horizontal pipes, studies on local wear becomes important due to non-uniformity in velocity and concentration fields, which results in uneven wear of the pipe. Hence, for a horizontal slurry pipeline overall wear as well as maximum local wear need to be considered for determining the life span of the pipeline. Quantitative studies on this aspect of wear showed that erosion rate varies around the periphery for a given velocity of flow. The maximum wear rate was found to be at the bottom of the pipe and minimum at the top of the pipe. It was also reported that local wear rate is dependent on local concentration of solid particles and their size. An empirical correlation for wear rate as a function of local velocity, concentration and particle diameter has been proposed. This correlation is applicable for the same slurry and pipe material as hardness effects of the solid particles and pipe material have not been considered.

CHAPTER-2

LITERATURE REVIEW

Tavares et al[1965] conducted experiments in a pilot plant test loop to study the wear characteristics of steel tubes using equalized iron ore-water slurry. Using two equal sized iron-ore samples (325 mesh and 200 mesh) they established the effect of particle size on wear for o fixed velocity and concentration. They concluded that wear increases with the increase in particle size, but could not propose any relation regarding the variation of wear with particle size. They also conducted experiments to identify the effect of attrition on wear rate and found that wear rate decreased with time. This was attributed to particle attrition.

Tarjan et al[1972] had proposed a mechanism for estimating the expected wear in a pipe line before hand if specific wear is known. They have defined specific wear as the loss of pipeline thickness during one unit of displacement. To determine the specific wear, they developed a pilot plant test loop to smaller scale and called it a semi plant test loop. They tested three pipes materials with sand slurry at three concentrations and different velocities in the range of 2 m/s to 3.5 m/s and found that weight loss was directly proportional to the flow rate and density of pipe material for a given concentration and velocity. They also found that specific wear had a linear dependence on pipe diameter, velocity and concentration for a given pair of materials.

Hutchings et a[1974] studied the mechanism of metal removal by impacting the metal targets at an oblique angle by metal balls at velocities up to 250 m/s. They suggested that the initial stage of metal removal is the formation of lip at the exit end of the crater, caused by shearing of the surface layers. Above a critical velocity, this lip is detached from the surface by the propagation of ruptures at the base of the lip.

Karabela[1978] conducted uneven erosion wear studies in pipes using multisized sand-water slurry in a 3.56cm ID stainless steel loop. He measured the erosion rate by means of brass coupons mounted flush with the pipe surface and these were located at 0^0,90^0 and 180^0 with respect to the vertical pipe diameter. His studies were conducted for slurries with weighed mean

diameters lying between 30 μ and 140 μ at the concentration of c_v=30%. The velocity was varied between 2.29 m/s and 4.12 m/s and the run time was 15 hours. His results show that erosion rate varies around the periphery for a given velocity, the maximum being at the bottom of the pipe and the minimum at top of the pipe, they also found that erosion rate increased with mean velocity along the surface with the power of velocity varying between 2.32 and 3.27 from top to the bottom of pipe. Encouraged by his findings, he proposed an empirical relation for erosion wear as, $E=6.1\ d_{wm}^{2.15}\ V^{3.27}$, where E= erosion rate, mm/yr , d_{wm}= weighted mean diameter, mm V= mean slurry velocity, m/s

Haas et al[1979] conducted experiments under controlled conditions with equisized angular coarse silica sand particles [d_{50} =500 μ] slurry for two pipe materials. The specifically chose a much larger size than that used by most of the previous workers and these particles were chosen to have angular shape so that resulting wear could be high. Their test runs were anywhere between 3 and 6 weeks duration and the slurry war periodically changed to minimize the effect of particle attrition. The concentration of slurry chosen by them was 20% by volume and velocity was varied between 2m/s to 4m/s. They concluded that for slurries of coarse, angular particles, the increase in erosion rate with velocity is much less as compared to finer particles. A possible explanation of this interesting observation could be that for sliding wear processes, the wear per unit distance travelled is independent of velocity and if expressed in terms of wear per unit time would imply wear rates proportional to velocity. Hence the lower exponent of velocity also found the maximum erosion takes place at the bottom of the pipe.

Shook et al[1981] conducted the erosion wear studies for different pipe materials using multisize sand–water slurry. The material tested were high density polyethene, mild steel etc (d_{wm}=0.1555 μ to 0.94 μ)at a constant concentration of 20% by volume in the velocity range of 2m/s to 5.5 m/s. they replaced the slurry regularly to minimize the effect of particle attrition during the 6-week run for each test. Expressing their findings in term of specific wear rates, E, the following relation has been given, $E = 4M/(D^2VC_v \rho_s)$ Where, M= annual erosion rate, mm/yr, V = velocity of flow, m/s, ρ_s=solid density, C_o= concentration of volume. They have concluded

that specific wear rates for sand-water slurry are insensitive to slurry velocity and concentration. This conclusion is valid for low stress abrasive wall wear rather than impingement wear which occur in fitting, bending etc. They have further concluded that high density polyethylene are more wear resistant than steel for fine particles, slurries but less resistance to coarse particles. They have also expressed that particles shape may be important for determining wear rates.

Tsai et al[1981] developed a slurry pot tester for the determination of erosion wear of three steal alloys (A-53 mild steal, 304 SS and 316 SS) using coal and silicon carbide (SiC) suspensions in kerosene in an accelerated manner. The effects of various parameters including velocity, concentrations, hardness on erosion wear has been investigated by them using equisized coal ($24\,\mu$) and silicon carbide ($150\,\mu$) suspensions in kerosene tests were conducted with velocity ranging from 6.1 to 12.2 m/s and concentrations between 30% to 50% by volume . Results with coal–kerosene slurry for all the three alloys showed that erosion wear increases rapidly with increase in velocity thereby indicating a strong dependence of erosion wear on velocity. The results also showed that the rates of erosion for all the three steels wear nearly same. Results with $150\,\mu$ SiC suspensions in kerosene depicted the rates of corrosion to be about 40-100 times more than the rates for coal-kerosene slurry. However, the rates of erosion for all the three steels were not found to be same in this case- as it was observed to be higher for the A 53 mild steel. The substantial increase in the erosion rate y SiC slurry, according to them was not only due to in particle size, hardness and angularity but also because of an increase in density of slurry relative to coal-slurry. Regarding the effect of concentrations on erosion wear, they observed that erosion wear increases with the increase in concentrations and follows a non-linear curve. However, the effect of concentrations on erosion wear in much less than that due to velocity.

Li et al[1981] developed a liquid-solid jet rig to stimulate erosion in slurry pipeline system. The conducted experiments to study the erosion of pipe materials, namely copper, aluminium and mild steel using three slurries, wiz. Coal suspensions in kerosene, aluminium oxide (Al_2O_3) in water and silicon carbide (SiC) suspensions in water, the varied velocity from 12 m/s to 40 m/s by wt. Based on their experiments, they found that the JIT was capable of producing using

erosion data in a short span of time. They established the effect of slurry hardness on erosion rate of different pipe materials and found that slurries of harder particles (Al_2O_3 and SiC) produced erosion to orders higher than softer slurries (Coal-Kerosene). From their extensive experimental investigation, erosion wear was found to be approximately proportional to the square of velocity and had approximately a linear dependence on concentration up to 30% by wt. beyond which the rate of increase reduced, erosion wear increased with increasing impingement angle.

Steward et al[1992] studied the erosion wear of different pipe materials used for slurry transportation. A closed loop pipeline rig was used with jet impact to find the effect of erosion wear on different pipeline materials. They tested three types of materials which were: (1) Steels (2) Elastomers (3) Polymers. The material tested were high density polyethene, polyvinyl chloride, Polyurethane with different hardness rubber, basalt. gold tailings and crushed gold quartz were used as slurry. A ranking in the wear resistance of pipeline materials for the transportation of solids was made, even though the wear rates differ according to solids transported and the transport parameters

Gupta et al[1994] studied the effect of parameters like particle velocity, particle size and concentration on erosion wear of pipe materials. The pipe materials used were mild steel and brass. The experimental work was carried out in a pot tester. It was concluded that for a given concentration, erosion wear increases significantly with increase in velocity but for a given velocity, the increase in erosion wear with increase in slurry concentration is much smaller as compared to increase with increase in velocity. It was also concluded that erosion wear decreases with decrease in particle size of the erodent.

Wang et al[2000] studied the erosive wear in an alkaline slurry containing alumina particles of mild steel BS 6323 (Fe-C), the AISI 410 stainless steel (Fe-Cr-C), and the AISI 304 stainless steel (Fe-Cr-Ni), was carried out, by means of rotating cylinder, three-electrode erosion-corrosion test, with a view to investigation into the roles of the typical elements and the

mechanical and chemical properties in the erosive wear under simultaneous controlled corrosion. The total weight loss of erosion-corrosion was obtained. the result was compared and interpreted, for each material, by a full microscopical examination of the erosion-corrosion scars using scanning electron microscopy (SEM). It was found that the overall performance under erosion-corrosion in an descending order was the stainless steels AISI 304, AISI 410, and the mild steel. The individual contribution of each erosion and corrosion process was thus further separated through corrosion charge conversion using the Faraday's second law and the results were interpreted by discussion, on basis of the experimental and microscopical evidences, of the main factors that influenced the mechanical and wear behavior, in conjunction with those influencing corrosion and passivity

O.P.Modi et al[2000] studied the erosion wear performance of a high-carbon steel in coal and bottom ash slurries. The slurry was made mixing bottom ash and coal ash in water separately. The samples were tested in a sample rotation method tester with fixed linear velocity of 5m/s for different traversal distances. The steel was hardened by hardening and annealing treatments to analyze the effect of hardness on erosion wear. They concluded that the erosion wear increased with increase in traversal distance. They also concluded that hardened steel showed lower erosion wear when compared with steel in an annealed condition. Samples showed higher erosion wear in bottom ash as compared to coal ash slurry. Higher rate of erosion wear in bottom ash is due to the more efficient transfer of kinetic energy of moving bottom ash particles to the specimen surface than in case of softer coal particles.

Clark et al[2001] studied the slurry erosion performance of 11 commercially available wear resistant plate and pipeline steels. The hardness of the material surface was chosen upto 750VHN. A Coriolis tester was used for experimental analysis. The tester was operated at 5000rpm, slurry concentration of 10% wt and particle size of 200-300μm silica sand slurry. It was concluded that hardened steel showed more erosion resistance than non-hardened, carbon steel line pipe material.

Moore et al[2002] conducted experimental work to evaluate the performance of thermal spray coatings as corrosion barriers when applied to interior pipe walls. The ability to apply these coatings has recently been developed. They attempted to validate the suitability of these coatings with aggressive geothermal fluids, as well as identify the procedures necessary to assure a successful coating application. Carbon steel pipe with inconel 625. It was anticipated that a coated steel pipe will replace the cement lined or nickel alloy piping currently used.

A.K.Jha et al[2002] studied the erosion wear of commercial aluminium in sand water slurry. They found the effect of impingement angle and rotator speed on the erosion wear rate of the material. Samples were mounted at various angles and rotated at various speeds. The sample size was taken of 25mm*25mm with hardness HV 40. Tester used was DUCOM TR 40. Microstructure investigation was carried out in order to reveal the nature of damage of the specimen using SEM. Specimens were positioned at 0,30 45 90 degree angles with respect to its rotating direction. Speeds were maintained at 300,400,500,600,700 revolutions per minute. Wear rate was calculated using mass loss measurement. The result show that the wear rates increase with increasing impingement angle up to 90 degree. Contrary to the conventional understanding of maximum loss of ductile material at about 45 degree impingement angle, Maximum wear rate was observed in case of aluminium sample fixed at 90 degree. However increasing rotation speed of the sample results in exponential increase in wear rates. Findings are sustained with metallographic study of worn surfaces.

Mbabazi et al[**2004**] investigated the effect of ash particle impact velocity and impact angle on the erosive wear of mild-steel surfaces through experiments. The experimental data were used to calibrate a fundamentally-derived model for the prediction of erosion rates. This model incorporates the properties and motion of the ash particles as well as target metal surface properties.

Machio et al[2005] studied the erosion wear of WC-12Co, WC-17CO and experimental WC-10VC-12Co and WC-10VC-17Co coatings. The coatings were deposited on stainless steels

substrates using a high velocity oxy-fuel (HVOF) thermal spray process. The slurry used was silica sand in water. It was concluded that WC-VC-Co coatings exhibit higher erosion resistance then commercial WC-Co coatings. In slurry erosion, the best performance of the VC-containing coatings is as good as that of the commercial WC-Co coatings. They found that erosion resistance of the WC-VC-Co coatings was similar to that of the commercial grades. This may be due to the (V,W)C grains being less resistant to impact fracture because of high hardness. They also found that coatings with higher cobalt content showed higher wear rate

Tian et al[2005] have observed the erosive wear of some metallic materials such as high chromium white iron and aluminium alloy using Coriolis wear testing approach. In the present study, the correlation between wear rate and particle size on the tested materials is discussed. Factors, which should be considered in wear modeling and prediction, have also been addressed. It can be seen that larger solids particles resulted in higher mass loss in all test materials. Although the wear rates at smaller particle sizes were relatively close within each material group, the wear rate difference was significantly widened with larger particle sizes. The tested high-Cr white irons showed a wear resistance some 27–140 times higher than that of the aluminium alloys in the Coriolis test conditions Both flow rate and solids concentration of slurry affected the wear results of the test materials. The higher the flow rate, the higher the wear rate of test materials.

Gandhi et al[2006] have developed a methodology to determine the nominal particle size of multi-sized particulate slurry for estimation of mass loss due to the erosion wear. The effect of presence of finer particles (less than 75 micron) in relatively coarse particulate slurry has also been studied. They have observed that addition of particles finer than 75 micron in narrow-size or multi-sized slurries reduce the erosion wear. In addition, the effective particle size for narrow-size particulate slurries can be taken as the mean size whereas the weighted mass particle size seems to be a better choice for multi-sized particulate slurries. The reductions in erosion wear due to addition of fine particles decreases with increase in the concentration of coarse size particles.

Huanga et al[2010] developed a comprehensive phenomenological model for erosion of material in slurry pipeline flow is developed. This model captures the effects of particle shape, particle size, slurry mean velocity, pipe diameter, fluid viscosity and properties. This model shows that the erosion rate has a power-law relation with slurry mean velocity, particle size, pipe diameter, fluid viscosity and solid concentration. They also concluded that erosion rate depends strongly on slurry mean velocity and weakly on pipe diameter and fluid viscosity. The exponent of slurry mean velocity varies in a range of 2-3.575. The model also elucidates that the effect of particle size on erosion rate depends on the particle shape, flow condition and erosion location on periphery of a pipe. This model was developed by combining the single particle erosion model developed previously with additional information about the nature of abrasive particles, target material and the liquid flow.

Rateick et al[2006] compared the solid particle erosion of tungsten carcide/cobalt cermet and hardened stainless steel 440C. Angular Al_2O_3 abrasives were used as erodent. The affect of parameters like impact angle (20°, 50° or 90°); erodent velocity (60 or 120 m/s); erodent nominal diameter (63 or 143 μm). They concluded that for all the test conditions stainless steel eroded faster than the cermet. Scanning electron microscopy of both the materials was done which showed that the erosion mechanism were similar for both the materials. Analysis of weight loss data was also done for both the materials. Both exhibited significant plasticity when impacted, but the stainless steel response to impact was ductile in nature

Mann et al[2006] compared the erosion behavior of WC-10Co-Cr, armcore ‘M’, satellite 6 and 12 high velocity oxy-fuel coatings and TiAlN PVD coatings. Impact angle 60° and velocity 20m/s constant for all experiments. Mineral sand was used as solid particles of slurry. It was concluded that WC-10Co-4Cr high velocity oxy-fuel coatings show best performance against slurry erosion. They also evaluated the corrosion performance and found that WC-10Co-4Cr high velocity oxy-fuel coatings corroded significantly. WC-10C0-4Cr high velocity oxy-fuel coatings gave very good erosion resistance but not corrosion resistance

Oka et al[2007] proposed a practical, predictive equation for estimating erosion damage caused by solid particle impact, which can be utilized under any impact conditions and for any type of material. The impact parameters taken into consideration were impact velocity, impact angle and size and shape of particles impacting. The material properties are mechanical properties such as material hardness. The effect of impacting parameters on the correlative equation was investigated for aluminium, copper, carbon steel and stainless steel specimens. The impact angle dependence of erosion damage to these materials was also discussed. It was concluded that material hardness was an essential parameter and should be a dependent variable in terms of impact velocity dependence and impact angle dependence in the practical, predictive equations. It was also concluded that impact velocity and particle size were independent of each other, that is, particle size did not affect the impact velocity dependence of erosion damage and the impact velocity did not affect the particle diameter dependence of erosion damage.

Santa et al[2009] studied the slurry and cavitation erosion resistance of six thermal spray coatings in laboratory and compared their performance with uncoated martensitic steek. Nickel, ,chromium oxide and tungsten carbide coatings were applied by oxy-fuel powder process. Chromium and tungsten carbide coatings were obtained by high velocity oxy-fuel (HVOF) coating process. The microstructure of the cotings was analyzed by optical microscope and scanning electron microscope. The x-ray diffraction (XRD) analysis was also done of the specimens. The slurry erosion tests were carried out in a modified centrifugal pump in which the samples were placed to guarantee grazing incidence conditions, as well as high velocity jet erosion testing machine was used for experimental work. It was concluded that slurry erosion can be improved by approximately 16 times by thermal spray coatings. On the other hand none of the specimens showed better cavitaion resistance than uncoated steel in experiments. Microcutting and microploughung was main wear mechanism observed in micrographs.

Gandhi et al[2009] conducted experiments on the effect of particle size on erosion wear of aluminum alloy 6063 (AA 6063) in a pot tester. Narrow sized particulate slurry of quartz with mean size varying in the range of 37.5-655µm were used at 3m/s velocity for 20% wt.

Concentration of solids at 30°-90° orientation angles. Further it was concluded that there exists minimum kinetic energy of the particles, which changes mechanism of material removal from erosion to three body abrasion. Due to three body abrasion, the wear due to smaller sized particles is little higher compared to the bigger size particles

Liu et al[2010] studied the improvement in erosion wear of thermally sprayed WC-10Co-4Cr by high velocity oxy-fuel by addition of nano-WC-12Co powder to it. 15% nano-WC-12Co was added Sub-micron WC-10Co-4Cr powder in order to improve its hardness. It was noted that the addition of the nano-WC-12Co powder improved the hardness of the thermal spray coatings. Sliding wear test and slurry erosion tests were carried out. It was concluded that the wear and erosion resistance of coatings increases with the addition of WC-12Co powder. The result showed that 15% addition of WC-12Co to WC-10Co-4Cr based AC-HVAF coating has the best wear and erosion resistance. In addition, this also demonstrated that it is possible to fabricate the nanostructured WC–10Co–4Cr coating with low porosity and high hardness by AC-HVAF spray deposition with reasonable thermal spraying parameters

Patil et al[2011] studied the erosion wear of aluminium in sand-water slurry. The aim of the present study is to analyze the parametric dependence of erosion wear of aluminium in sand water suspension. The effect of parameters like particle velocity, particle size , impact angle and solid concentration on erosion wear of aluminium has been evaluated. The experimental work was carried out in a pot tester with a capacity of 6.6 liter. The wear rate in mm/year was obtained from the data points. Also a correlation was developed from the data points which agreed with the experimental values in an error band of ±16%.

$E_w=0.075\theta^{0.12}C_w^{1.09}V^{3.55}d^{1.37,}$ where, θ= Impact angle in degree, C_w= Concentration by weight in %, V= Velocity in m/sec, D= Particle size in mm

Kumar et al[2011] studied the comparison of erosion wear performance of plasma and flame thermal spray coatings. Major components of the turbine and pumps get eroded in the hydro

power stations. Different coating techniques have been implemented but thermal spray techniques have shown improvement in performance under erosion wear conditions. Thermal coating techniques can be differentiated in low and high kinetic energy sprays depending upon spray velocity. In this paper the two of the low kinetic energy methods used for protection against erosion wear has been discussed along with their resulting effects on different types of coatings. From the experiments conducted previously they concluded that plasma sprayed coatings perform better because of lesser defects and better microstructure as compared to flame spray coatings.

Ramesh et al[2011] studied the effect of lnconel-718 coatings on slurry erosion wear of material. Mild steel was coated with lnconel-717 powder by thermally spraying using air plasma thermal spraying facilities. The surface hardness of developed coatings was higher than of the substrate and increases with increase in coating thickness. Slurry erosion tests were carried on both coated and uncoated samples using a slurry erosive wear tester. Effect of concentration, velocity, time and impact angle were calculated on mild steel and different thickness coated mild steel. It was concluded that under all test conditions studied, lnconel-718 coatings exhibited improved slurry erosive wear resistance compared with uncoated mild steel and wear resistance increases with increase in coating thickness

Goyal et al[2012] studied the erosion wear of steels used in turbines in hydraulic power plants. The material used was CF8M turbine steel. The steel was coated with WC-10Co-4Cr and Al_2O_3+13TiO_2 by High velocity oxy-fuel thermal spray coating process. The coated and uncoated steels were studied with regards to their performance under slurry erosion conditions. High speed erosion test rig was used for the erosion tests and effect of parameters namely average particle size, speed(rpm) and slurry concentration on slurry erosion of these materials was investigated. The bare steel followed ductile mechanism and Al_2O_3+10TiO_2 coating followed brittle mechanism under slurry erosion, whereas the WC-10Co-Cr coating followed mixed behavior (mainly ductile). WC-10Co-4Cr coatings improved the erosion resistance of the steels remarkably. SEM micrographs were taken before and after the erosion tests to know the effect of slurry erosion on microstructure of the materials

Goyal et al[2012] Slurry erosion wear of coating on turbine steels was evaluated. Cr_2O_3 coatings were deposited on CF8M and CA6NM turbine steels by high velocity oxy-fuel (HVOF) spray process. In a high speed erosion test rig the performance of the coated material was analyzed under slurry erosion conditions. The effect of parameters like average particle size, Speed(rpm), and slurry concentration on slurry erosion of these materials were investigated. SEM micrographs were taken on the surface of samples, before and after slurry erosion tests to know the effect on the microstructure of the eroded material. The result showed HVOF sprayed coated steels better erosion resistance than the uncoated steels which may be due to the higher hardness of the coated steels because of the HVOF-sprayed Cr_2O_3 coatings.

.

.

CHAPTER 3

PROPERTIES OF FLY ASH AND BOTTOM ASH

3.1 FLY ASH

Fly ash is one of the residues generated in combustion of coal in thermal power plants, and it comprises the fine particles that rise with the flue gases. Depending upon the source and makeup of the coal being burned, the components of fly ash vary considerably, but all fly ash includes substantial amounts of silicon dioxide (SiO_2) (both amorphous and crystalline) and calcium oxide (CaO) . They get collected at several locations like economizer, air preheater, mechanical dust collector, electro-static precipitators (ESP) and chimney in the thermal power plants.

3.2 BOTTOM ASH

Bottom ash refers to part of the non-combustible residues of combustion. It comprises of coarse particles and it does not rise during of coal and stays at bottom. This is the ash that gets collected at the ash hoppers in the bottom of the boilers. They are in the form of lumps and are generally crushed into a coarse form.

Out of total ash produced in any thermal power plant approximately 15-20% is bottom ash and the rest is fly ash.

3.3 BENCH SCALE TEST

The bottom ash and fly ash were procured from Guru Hargobind thermal power plant Lehra Mohabbat, Bhatinda, Punjab. Different bench scale tests were performed on the ash to determine the various characteristics of both the ashes such as particle size distribution, specific gravity, pH value of both the ash at different concentrations used in the experimental analysis, static settling characteristics. The different tests conducted on the ashes were useful in selecting the parameters for the erosion wear tests. The data of the different tests conducted on both the ashes is presented here.

3.3.1 pH VALUE

The pH value of the fly ash and bottom ash was calculated at the chemistry lab in Thapar University chemistry department. A pH meter was used to calculate the pH value of fly ash and bottom ash at different concentrations of 10, 20,30,40,50 and 60 percent by weight. For the calculation of pH value of ash the electrode of the pH meter was moistened with distilled water and calibrated with a buffer solution of known pH value. The sample of the ash slurry was made in beaker with required concentration of the ash by mixing it in the distilled water with a stirrer. The electrode was dipped into the beaker containing the slurry and the pH suspension was noted when equilibrium value was reached. Same procedure was calculated for slurry at different concentrations for both the slurries.

C_w,%	10	20	30	40	50	60
pH(Fly ash)	7.23	7.21	7.20	7.19	7.15	7.13
pH(Bottom ash)	7.54	7.48	7.48	7.45	7.45	7.43

Table 3.1 pH value of fly ash and bottom ash slurries

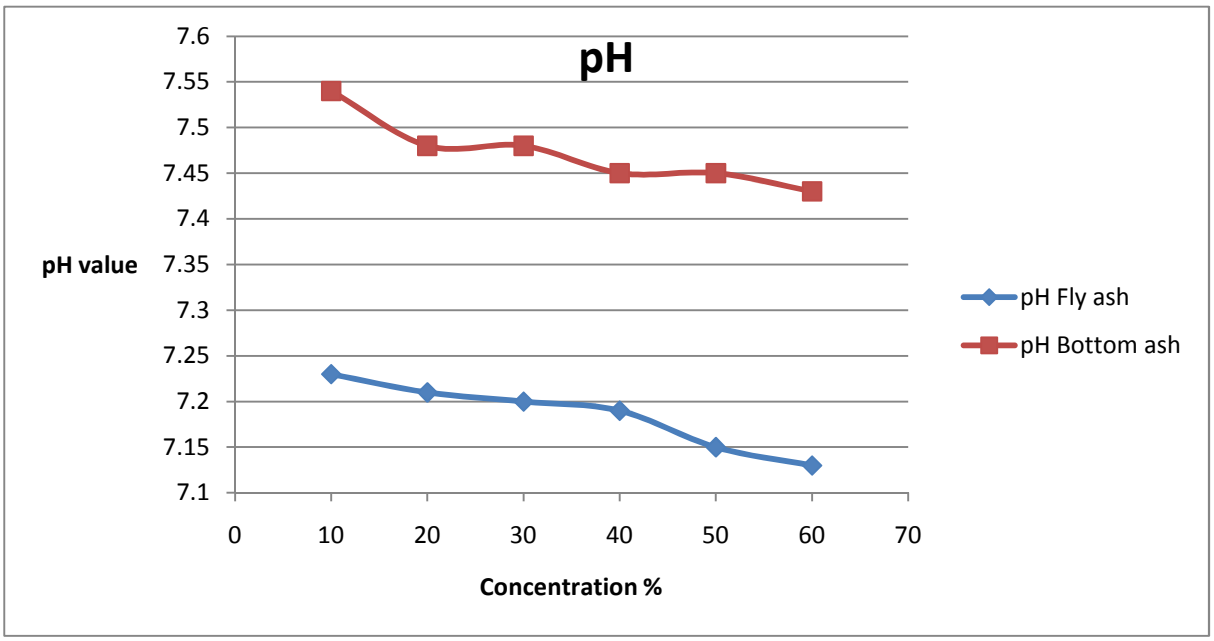

Fig 3.1 pH value vs concentration plot for fly ash and bottom ash

3.3.2 STATIC SETTLING CONCENTRATION

The static settling concentration depends on density and viscosity of carrier fluid and specific gravity, shape and size distribution of solids and it decides the highest limit of solid concentration, which can be achieved by gravitational settling. The optimum concentration for solids transportation is around 5 to 10% lower than the static settled value. The static settled concentration is measured by allowing it to settle in a graduated measuring jar till the level of solids become constant. The slurry sample is prepared of intermediate concentration of 20% (by weight). The slurry levels at regular intervals of time were recorded during the process to determine the settling rate of slurry. The value of the solid concentration in the settled portion of slurry is the static settled concentration.

Time(Minute)	0	1	2	3	4	5	15	30	60	120	180	240	480
Conc. Fly ash (%C_w)	20	25.32	26.18	30.43	32.91	44.87	53.90	54.04	54.49	55.70	55.98	57.39	57.39
Conc. Bottom ash(%C_w	21.14	29.14	34.28	44.37	47.54	49.66	50.39	50.57	50.88	50.97	51.26	51.77	51.77

Table 3.2 Static settling concentration of fly ash and bottom ash

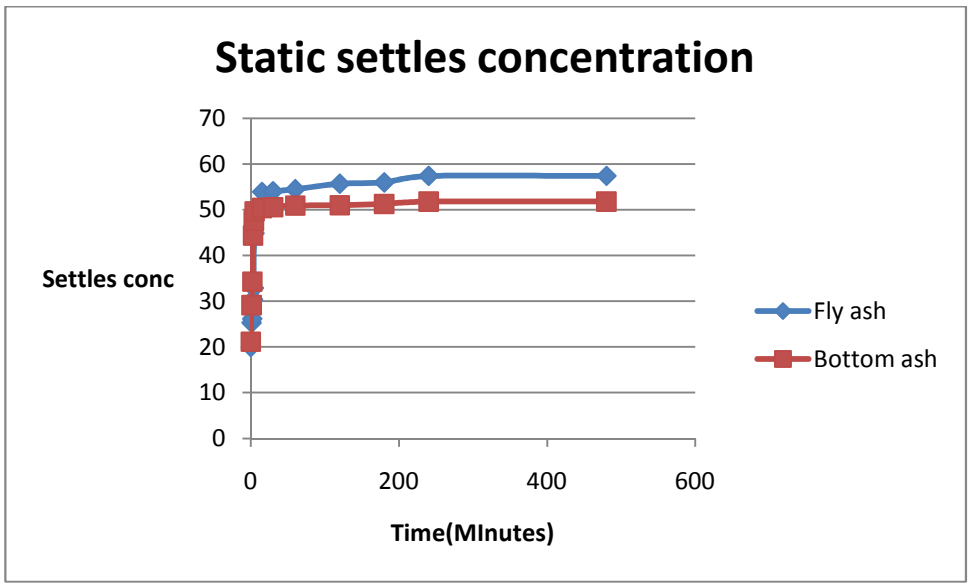

Fig 3.2 Static settled concentration vs time plot for fly ash and bottom ash

3.3.3 SPECIFIC GRAVITY

The specific gravity is determined by using fixed volume bottle. 50ml fixed volume bottle was taken and cleaned thoroughly, and was kept in the oven in order to remove moisture from the bottle. Bottle was kept in the oven for 2 hours and after taking it out of the oven was allowed to cool down. The weight of the dry bottle was taken (W_b). After weighing some solids which were oven dried were put in the bottle (about 30 grams) and weighed (W_{bs}). After this distilled water was slowly poured in the bottle so that no air is entrapped in it and, shake well and keep on pouring the water. It is shaken well each time till the solid get wet. Fill $3/4^{th}$ of bottle with water and put the thumb on the mouth of the bottle and shake it well for 5 minutes. Keep it for at least two Hours, so that air bubbles get out from the bottle. Then the bottle is filled with water and corked. Bottle is cleaned with cloth/tissue paper and weight it. Weght is noted down(W_{bsw}). Now remove the solids from the bottle and clean it, Thoroughly, Dry it and fill it with distilled water. Note down the weight (W_{bw}). Calculate the specific gravity of solids as given below

Specific Gravity of solids= $(W_{bs}-W_b)/ \{W_{bw}-W_{bsw}+(W_{bs}-W_b)\}$

Where W_b = Weight of beaker

W_{bs} = Weight of beaker and solid

W_{bw} = Weight of beaker and water

W_{bsw} = weight of beaker, solid and water

Specific gravity of fly ash = 2.04 Specific gravity of bottom ash = 2.11

3.3.4 PARTICLE SIZE DISTRIBUTION (PSD)

The particle size distribution tells the percentage of different sized particle and the variation in the size of particles in the solid sample. Pre-selected size ranges are determined to establish the particle size distribution (PSD). Sieve analysis is used for the evaluation of particle size distribution. In the present study a known weight (100 grams) of the solid sample was taken. It was washed over B.S mesh 200 (75mm) and then particulate material are dried in the over. The

dried particulates are then sieved through a set of standard sieves. The sample retained on each sieve is retained and properly weighed and percentage retained on each sieve is calculated using the standard procedure.

FLY ASH PARTICLE SIZE DISTRIBUTION:

Sieve openings(μ)	500	355	250	150	106	75	53
% finer	100	99.16	92.37	80.98	69.40	48.94	27.76

Table 3.3 Particle size distribution of fly ash

BOTTOM ASH PARTICLE SIZE DISTRIBUTION:

Sieve openings(μ)	2000	1000	710	500	355	250	150	106	75	53
% finer	100	99.59	99.04	97.47	96.59	88.11	67.65	51.49	32.22	3.54

Table 3.4 Particle size distribution of bottom ash

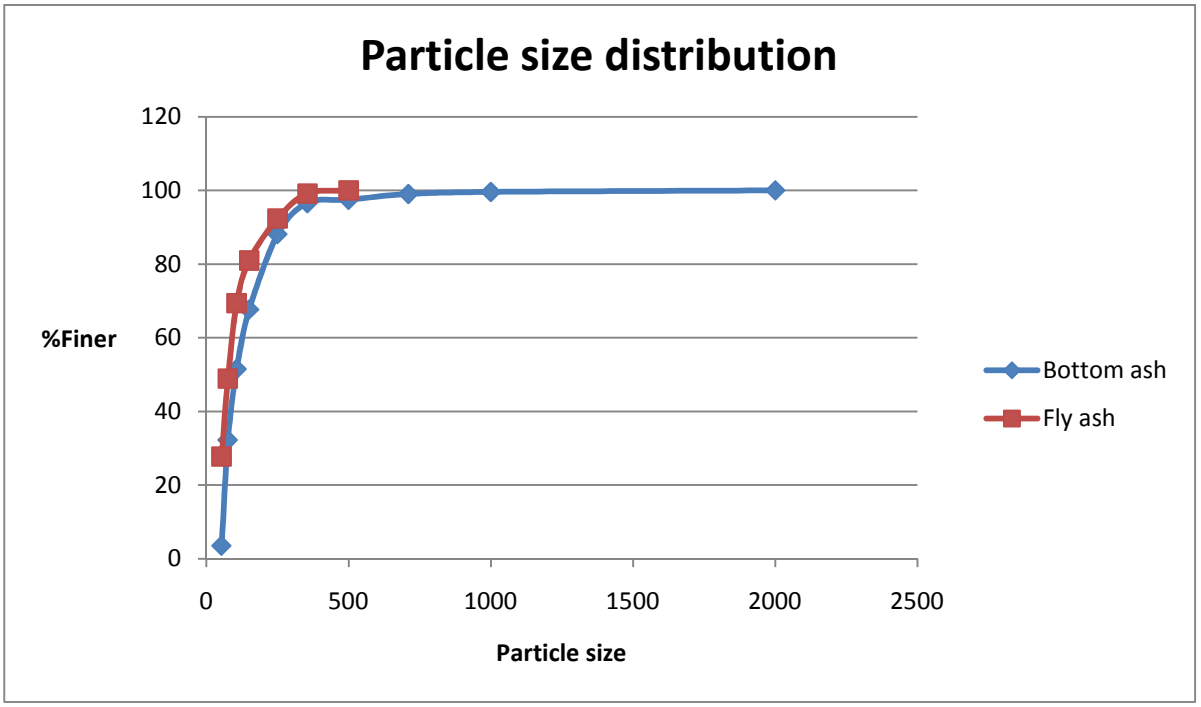

Fig 3.3 % Finer vs particle size distribution plot for fly ash

3.4 RHEOLOGICAL BEHAVIOR

One of the most important input data required to design of the slurry transportation system is the rheological behavior of the slurry at various concentrations and flow conditions. The rheological characteristics of slurry depends on several parameters such as shape, size particle size distribution, solids concentration, carrier fluid properties etc.

PREPERATION OF SAMPLE FOR RHEOLOGY

The sample is prepared by mixing 100ml of ash-water suspension by mixing required amount of ash with distilled water. The ash was accurately measured in electronic type single pan balance. The suspension was mixed gently taking care to avoid attrition of particles with the help glass rod. The mixture was stirred properly before taking the readings.

RHEOMETER

The standard Rheolab Q-C (Anton Paar, Germany) used to calculate the rheological characteristics of the slurries which is shown in figure 4.1. Co-axial concentric cylinder cup and bob geometry is used for measuring the rheological properties of bottom and fly ash mixture. Before conducting tests on rheometer, the bob and cup assembly is fixing using a locking device and slurry mixture is added into cup (cylinder) up to the particular mark. The shear stress value measured at the shear rate range from 50-225 s^{-1} at the constant temperature condition 26 °C with wide range of concentrations varying from 0 to 60% (by weight) for ash and water slurries. The rheological parameter shear stress, viscosity measured with the range of shear rate 50-225 s^{-1} for each sample.

Figure 3.4 Anton paar rheometer

Concentration (Cw) %	Yield stress (Pa)	Slurry viscosity(cP)	Water viscosity(cP)	Relative viscosity	Flow behaviour
0	0	0.995	0.995	1	Newtonian
10	0	1.02	0.995	1.025	Newtonian
20	0	2.53	0.995	2.542	Newtonian
30	0	7.05	0.995	7.085	Newtonian
40	0	22.5	0.995	---	Non-Newtonian

50	0	33.19	0.995	----	Non-Newtonian
60	0	67.8	0.995	----	Non-Newtonian

Table 3.5 Relative viscosity of fly ash at different concentrations

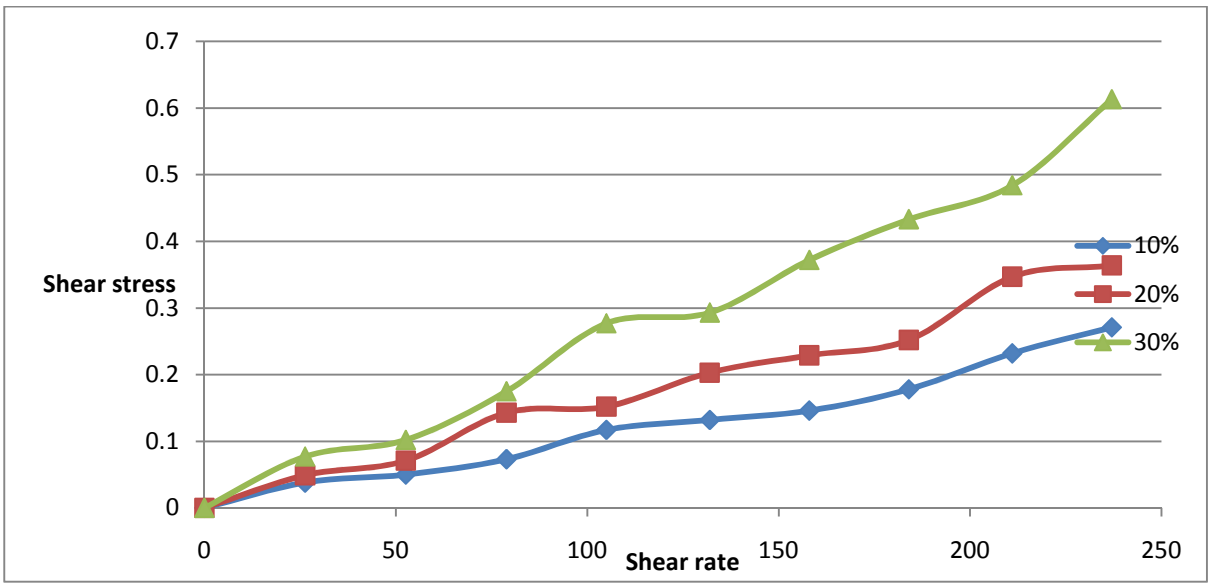

Fig 3.5 Shear rate vs shear stress plot for different concentration of fly ash

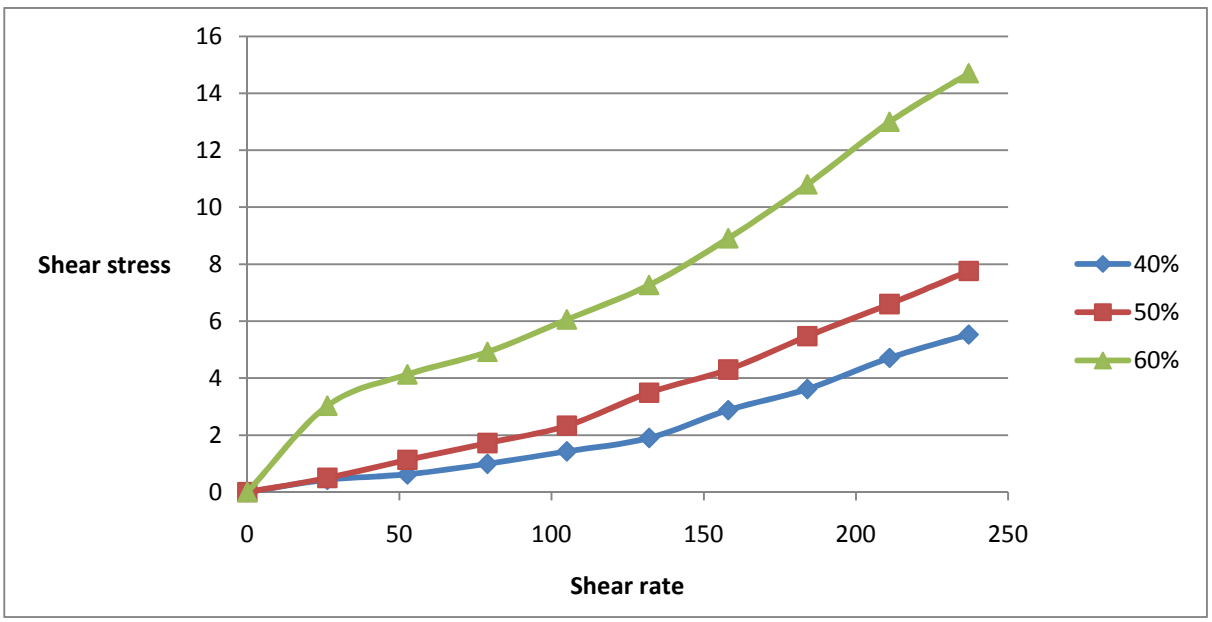

Fig 3.6 Shear rate vs shear stress plot for different concentration of fly ash

RELATIVE VISCOSITY OF BOTTOM ASH:

Concentration (Cw) %	Yield stress (Pascal)	Slurry viscosity(cP)	Water viscosity(cP)	Relative viscosity	Flow behaviour
0	0	0.995	0.995	1	Newtonian
10	0	1.01	0.995	1.02	Newtonian
20	0	1.6	0.995	1.61	Newtonian
30	0	2.2	0.995	2.21	Newtonian
40	0	4.3	0.995	4.32	Newtonian
50	0	5.6	0.995	5.62	Newtonian

Table 3.6 Relative viscosity of fly ash at different concentrations

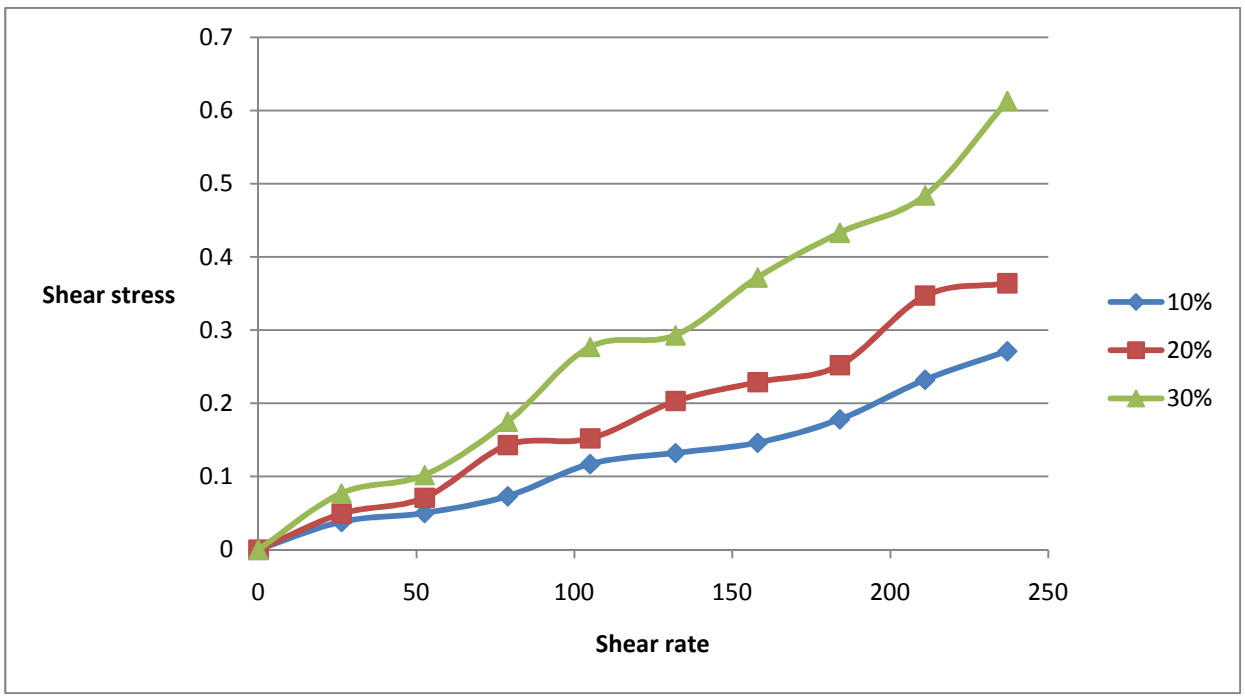

Fig 3.7 Shear rate vs shear stress plot for different concentration of bottom ash

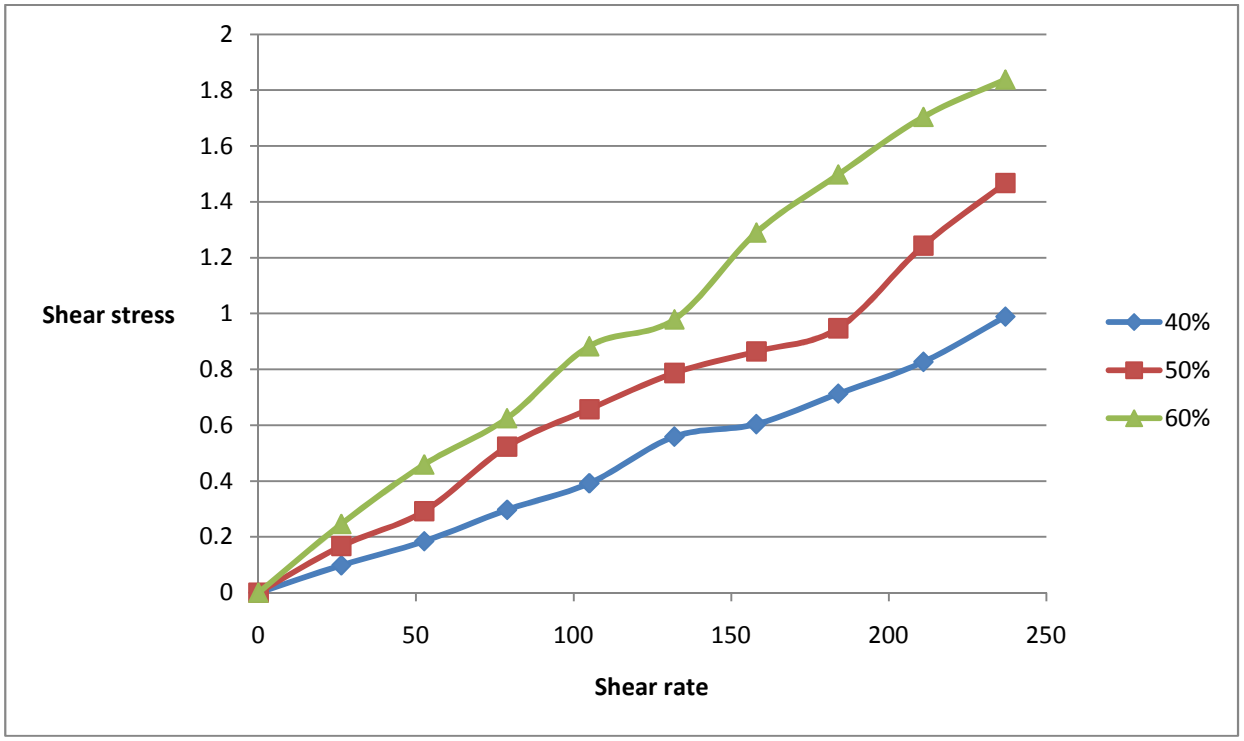

Fig 3.8 Shear rate vs shear stress plot for different concentration of bottom ash

3.5 SCANNING ELECTRON MICROSCOPY OF ASHES:

Fig 3.9 Scanning electron microscopy of bottom ash

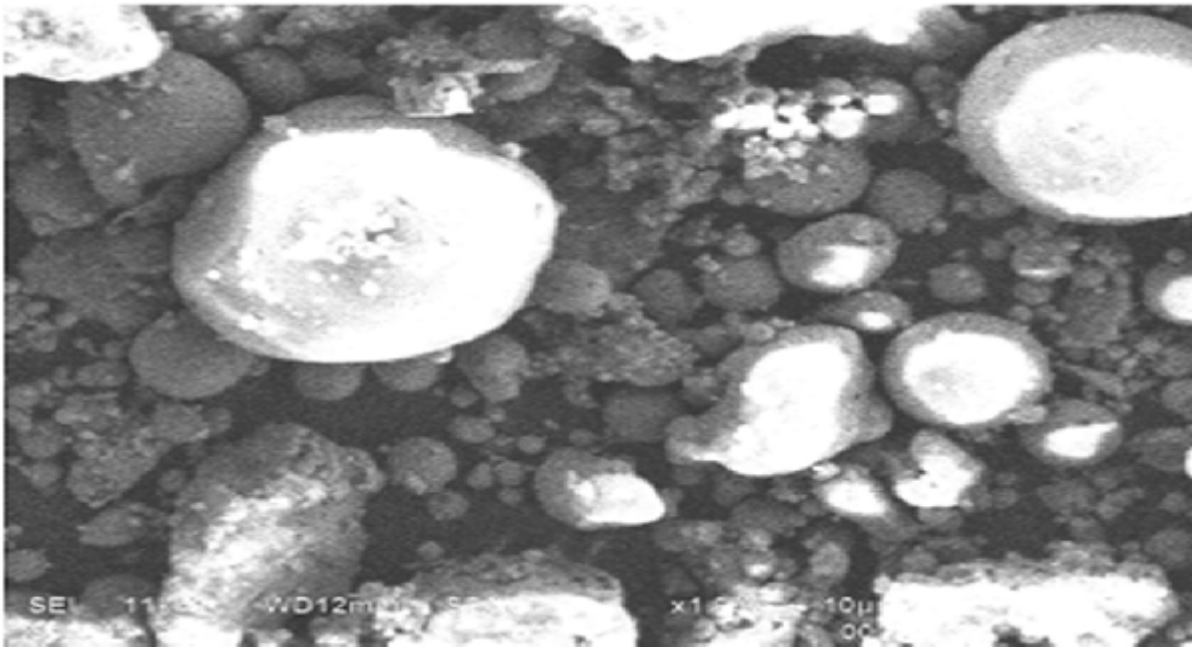

Fig 3.10 Scanning electron microscopy of fly ash

Scanning electron microscopy is done to check the size and the shape of the ash particles. Figure 3.9 shows SEM micrograph of the bottom ash. The sharp edge or angular shaped particles of irregular shape are visible in the micrograph. These sharp edges of the particles will cause erosion wear of the material.

In figure 3.10 SEM micrograph of fly ash can be seen. Micrograph shows mostly spherical or circular shaped particles. These particles will erode the material.

Chapter-4

Experimental setup

4.1 SLURRY POT TESTER :

The erosion tester consists of a cylindrical pot which contains the slurry. Slurry is kept in suspension by a rotating shaft connected to the motor. The specimen is connected to the rotating shaft by a fixture and is dipped into the pot carrying the slurry. The shaft rotates inside the pot with specimen fixed to it. The stirrer at bottom of specimen agitates the slurry to have uniform distribution at the striking portion of specimen. The relative motion between the specimen and the slurry causes erosion wear of the specimen. There is a container (jacket) in which slurry pot is placed and is fixed at the top of the tester cabin so that the slurry is not spilled. Cold water is poured inside the container carrying the pot so that temperature of the pot and slurry inside is not raised. The rpm of the shaft can be adjusted from the display panel with maximum rpm of 1500. Effect of various parameters like velocity, concentration, time, particle size can be evaluated. The test rig is small in size, easy to operate, simple in design and can be used to generate experimental data at accelerated rate. The test duration and specimen rotation speed are varied. Specimens are weighed before and after test and the loss in mass is recorded, mass loss is calculated. Capacity of the slurry pot = 1.2L

Fig 4.1 Ducom pot tester

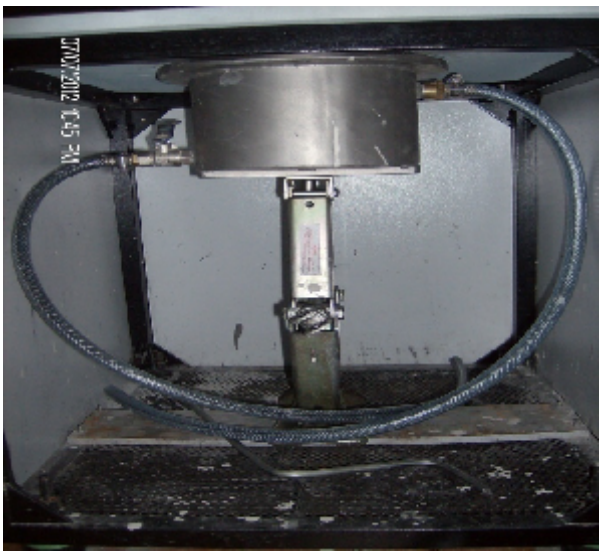

Fig 4.2 Inside of the pot tester

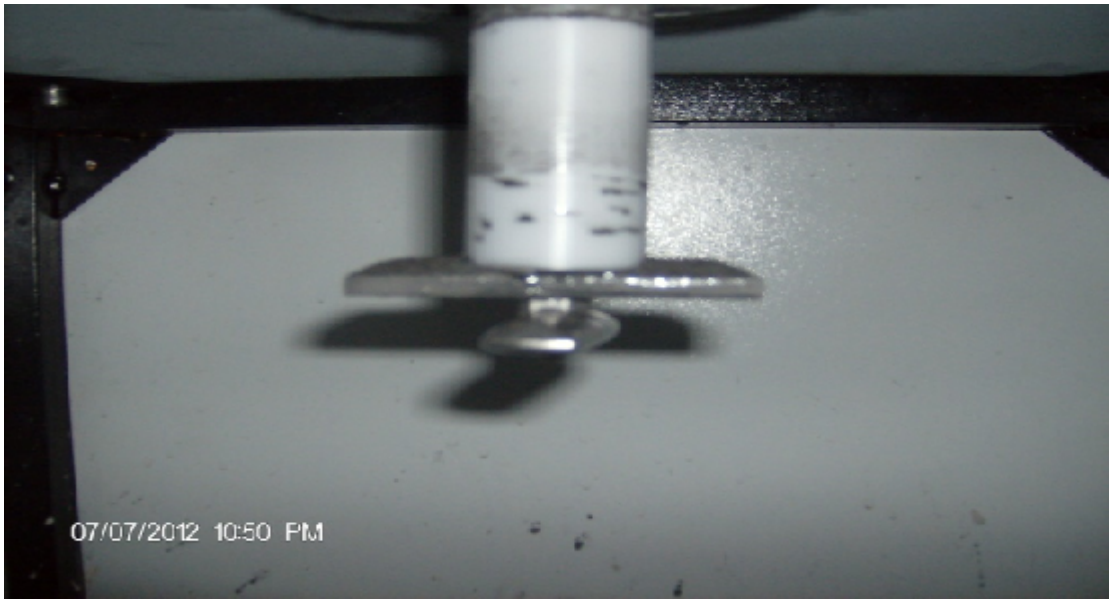

Fig 4.3 Shaft and fixture for specimen inside tester

4.2 EXPERIMENTAL PROCEDURE:

Erosion wear experiments are performed through a sequence of steps, in which most of the observations are recorded manually and graphs are plotted according to the observations or data point collected. Mass loss of the specimen after each test is the measure of the erosion wear. The steps to perform the experimental procedure are:

1) Thoroughly clean and rinse the slurry chamber to remove the remnants of slurry from previous test.

2) Weigh the abrasive and fill inside the slurry vessel.

3) Fill the vessel with water.

4) Weigh specimen to the nearest 0.0001gm and record the value.

5) Locate specimen on the slot of each spindle and tighten with stirrer.

6) Connect inlet port to water source and outlet drain.

7) Switch On MCB supply power to tester to allow 1 min for stabilizing the circuits.

8) Press start push button on control panel and slowly rotate the set RPM knob till the speed display on module show 1000rpm.

9) Press STOP to arrest spindle rotation, but retain the position of SET RPM knob.

10) Place the slurry vessel inside the water jacket.

11) Clean the top surface of the vessel and base plate with cloth.

12) Slowly rotate the handle to raise the water jacket till it presses the base plate with sufficient pressure to prevent leakage of slurry.

13) Set the test duration.

14) Specimen rotates, the direction of rotation is clockwise, the stirrer agitates slurry, slurry rotates along the direction of rotation, the slurry rotation is arrested/deflected by vertical fins to propel it towards specimen.

15) Motor will be switched off automatically after elapse of preset revolutions.

16) Slowly lower the handle to lower the cooling tank to the bottom most level, Taking care not to spill any slurry on the surface.

17) Clean the surface of each specimen with cloth to remove slurry..

18) Rinse to clean and dry specimen.

19) Weigh each specimen and compute mass loss.

4.3 PIPE MATERIAL USED IN THERMAL POWER PLANTS IN INDIA:

Table 4.1 Pipe material used in thermal power plants in India

Thermal power plant	Pipe material used
Kothagudem Thermal power station , (1 x 67.5 MW), Andhra Pradesh	Slurry pump and Mild Steel piping are provided for slurry disposal
National Fertilizers Limited captive Power plant(1 x 210 T/hr.Boiler) Bathinda.	Mild Steel piping (400 NB) and slurry pump having capacity 1000 cu.m/hr with discharge pressure for 5kms is used for slurry disposal
National Fertilizers Limited captive Power plant (1 x 210 T/hr.Boiler), Panipat	Mild Steel piping (350 NB) (6 Kms) with slurry pump of the capacity of 700 cu.m/hr per series for slurry disposal
Nellore Thermal Power Station (1 x 35 MW) Andhra Pradesh	Cast Iron piping and slurry pump is used for slurry disposal
Southern Generating Station (2 x 67.5 MW) CESC Limited	Mild Steel piping up to disposal area
Gandhinagar Thermal Power Station (2 x 210 MW) Gujarat	MIld Steel piping upto slurry pump and slurry disposal
Shriram Fertilizers and Chemical Captive Power Plant (1 x 35 MW) Kota	Mild Steel piping used for slurry disposal
Kota Thermal Power Station Stage-3, (1 x 210 MW) Rajasthan	Slurry transfer system is through Cast Iron (300 NB) disposal piping
Guru Hargobind Thermal Plant Bathinda, (2 x 210 MW) Punjab	Mild Steel piping (300 ND, 2.5 Km) upto slurry pump and slurry pump to disposal area
Sanjay Gandhi Thermal Power Station, Unit # 3 and 4 (2 x 210 MW)	Slurry disposal piping of Mild Steel (300 NB, 6 km)
Guru Gobind Singh Super Thermal Plant, Ropar (6 x 210 MW) Punjab	Slurry disposal piping of Mild Steel

4.4 TESTING MATERIAL:

1) Mild Steel

2) Steel 202

4.4.1 MILD STEEL:

Mild steel is the most common form of steel because its price is relatively low while it provides material properties that are acceptable for many applications. Mild steel contains 0.16–0.29% carbon; making it malleable and ductile, but it cannot be hardened by heat treatment. Mild steel has a relatively low tensile strength. It is often used when large quantities of steel are needed, for example as structural steel. The density of mild steel is approximately 7.85 g/cm^3(7850 kg/m^3 or 0.284 lb/in^3) and the Young's modulus is 210 GPa (30,000,000 psi).

4.4.2 STEEL 202:

Steel 202 belongs to the austenitic series the 200 series of steels. 200 series austenitics are typically used to replace types 304 and 301 as well as Carbon steels. This contains lower nickel than the 300 series which is replaced by manganese. Thus, lower cost than the 300 series. They have similar mechanical and physical properties to 300 series. It has corrosion resistance similar to steel 304 and is stronger than steel 304. Steel 202 can replace steel 304 and carbon steels in the slurry transport systems.

4.5 CHEMICAL COMPOSITION OF MATERIALS USED:

The chemical composition of Mild Steel and Steel 202 were determined by the spectrometer analysis. A spectrometer is a device used to measure chemical composition of ferrous materials. The chemical composition is measured by the light intensity produced by arc. A spectrometer is used in spectroscopy for producing spectral lines and measuring their wavelengths and intensities. Spectrometer instruments that operate over a very wide range of wavelengths, from gamma rays and X-rays into the far infrared.

Fig: 4.5 Foundary master spectrometer

Components	Percentage Composition
Fe	99.1
C	0.129
Si	0.144
Mn	0.415
S	0.0345
Cr	0.0171
Mo	0.0050

Table 4.2 Chemical composition of mild steel

Components	Percentage Composition
Fe	74.3
C	0.106
Si	0.300
Mn	10.2

S	0.0126
Cr	13.5
Mo	0.0050

Table 4.3 Chemical composition of Steel 202

4.6 Sample preparation: Mild steel and steel 202 samples were cut from long bars using hacksaw. Then the specimens were grinded with the help of surface grinder to get the dimensions required for the testing. A hole was drilled in the centre of the specimen so that it can be held in the fixture.

Specimen specification: 76.2mm×25.4mm×6.35mm

Hole diameter: 8.5mm

4.7 Experimental parameters

Specimen Dimensions	76.2mm×25.4mm×6.35mm
Speed	700rpm, 1000rpm, 1400rpm
Slurry concentration	20%,40%,60% by weight
Time	$1,1^{1/2},2,2^{1/2}$,3 hours
Ash	Fly ash, Bottom ash
Material	Mild steel, steel 202

Table 4.4 Experimental parameters for erosion testing

4.8 COATING: Coatings are coverings that are applied to the surface of a material called substrate to improve its properties like corrosion resistance, erosion resistance, appearance, adhesion, friction resistance etc.

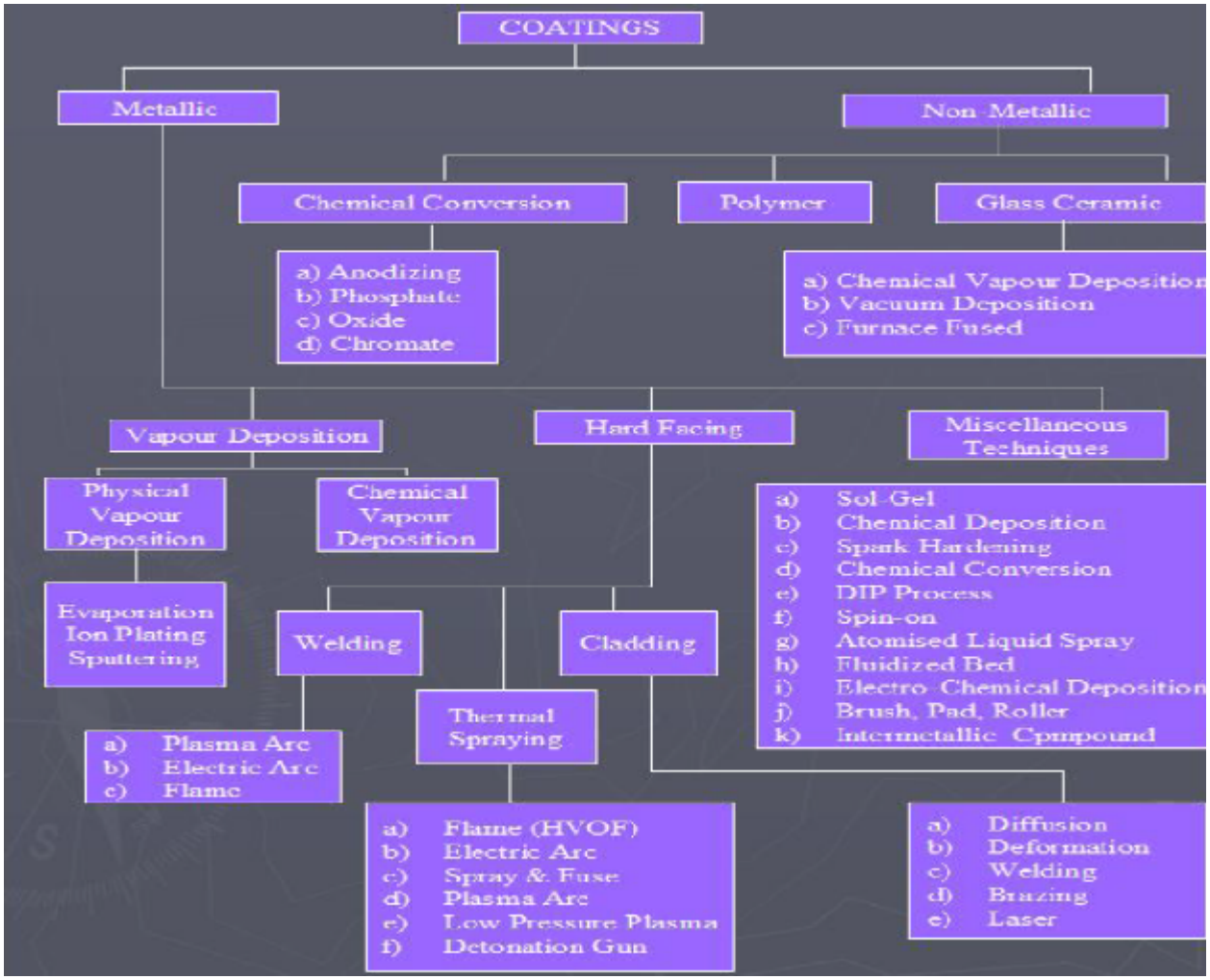

Fig 4.6 Types of coating methods

4.8.1 TYPES OF COATING METHODS:

1) Physical vapor deposition

2) Chemical vapor deposition

3) Electroplating

4) Thermal spray

4.8.1.1 PHYSICAL VAPOR DEPOSITION:

Physical vapor deposition is the evaporation of a coating metal source and condensation of the vapors on the substrate. The process is carried out at low pressure, typically at 10^{-1}Pa, in order to avoid oxidation of the metallic vapor. Virtually any coating metal can be applied by PVD and environmental concerns associated with liquid wastes can be avoided. Coatings upto 10μm are deposited, and deposition rates are controlled by the rate of heat input used to vaporize the coating metal source. Resistance and induction heating methods are often used, but the highest rates are obtained with electron beam heating.

4.8.1.2 CHEMICAL VAPOR DEPOSITION:

In chemical vapor deposition, a gas containing the coating metal is thermally decomposed on a heated substrate surface to form a deposit. Typical coating thickness cover a very wide range upto 100μm depending on the specific coating applied. Owing to the generally high temperature required for thermal decomposition, chemical vapor deposition deposits usually have good adhesion and density. Gases used include halides, hydrides, carbonyls and organometallics, nickel, tungsten and chromium are the most commonly applied CVD metal coatings.

4.8.1.3 ELECTROPLATING:

Electroplating is a plating process that uses electrical current to reduce cations of a desired material from a solution and coat a conductive object with a thin layer of the material, such as a metal. Electroplating is primarily used for depositing a layer of material for a desired property to a surface that otherwise lacks the property. The process used in electroplating is called electrodeposition.

4.8.1.4 THERMAL SPRAY COATING PROCESS:

Thermal spraying is a process in which molten or semi-molten or solid particles are deposited on a substrate. The spraying technique is a way of generating a stream of such particles. Coatings can be generated if the particles can plastically deform at impact with the substrate, which may only happen if they are molten or solid and sufficiently rapid. Their heating and/or acceleration are practical if they occur in a stream of gas. Thus an academic classification of the spray techniques is based on the way of generation of such streams.

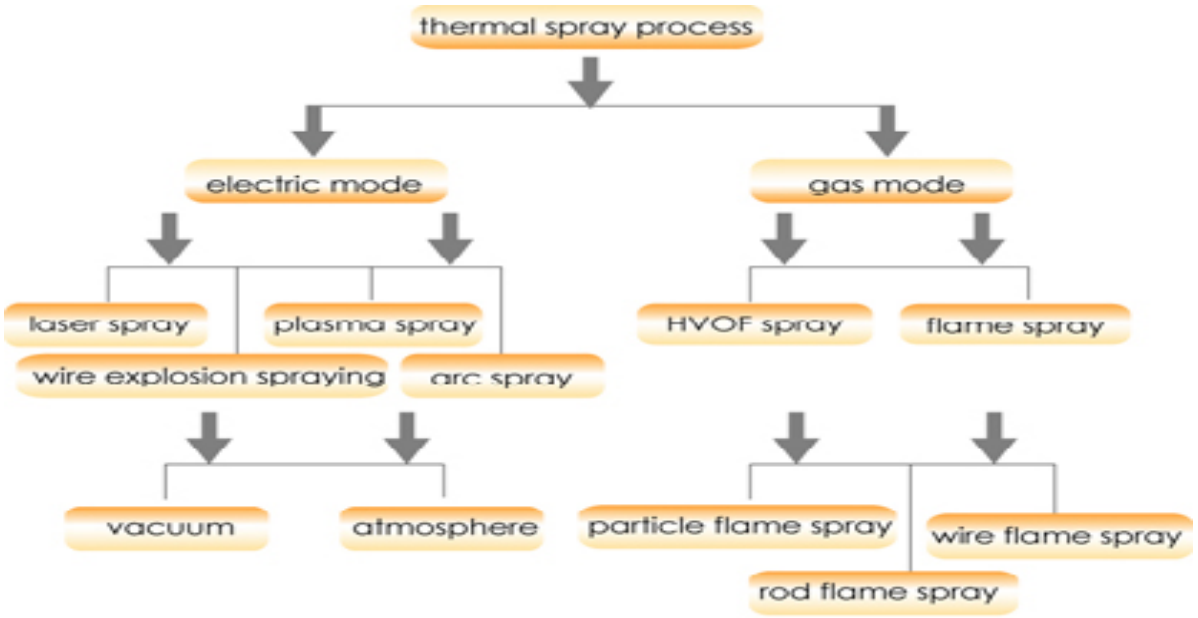

Fig 4.7 Types of thermal sprat processes

4.9 HIGH VELOCITY OXY-FUEL COATING PROCESS: the high velocity oxy-furl process is shown in the diagram. In this process a mixture of a fuel gas (hydrogen, propane, propylene, MAP or acetylene) and oxygen are mixed and burned in a combustion chamber. The expanding, high-temperature combustion product gases are allowed to escape through a nozzle at high velocity. The gas velocity is frequently supersonic. Powder particles are heated and accelerated by the high-temperature gas. Even though the gas velocity is supersonic, the particle velocities are far lower, usually in the range of 350 to 550 meters per second. Depending on the oxy-fuel ratio used, the combustion products maybe eaither oxidizing or carburizing relative to metallic or carbide coating materials. In addition, air is drawn into the effluent of the HVOF coatings produced using hydrogen suffer less oxidation than those produced using propane or propylene (it should be noted, however, that the cost of the hydrogen is usually higher than that of the hydrocarbon fuels). Most of the HVOF devices can be used to deposit metallic coatings or cermet coatings such as chromium carbide- NiCr or tungsten carbide-cobalt. The selection of an appropriate powder is crucial to the successful deposition of the carbides. Most of the HVOF

devices are not capable of producing adequate oxide coatings. Those using acetylene as a fuel gas may be more successful with the oxides.

4.9.1 TYPES OF HVOF PROCESSES:

a) Gas-Fuel HVOF
b) Liquid-Fuel HVOF

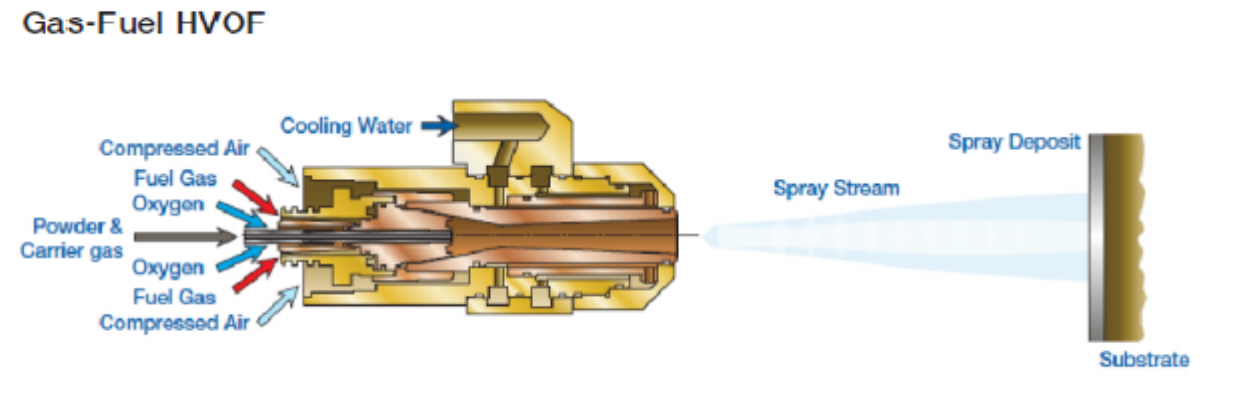

Fig 4.8 Gas-fuel high velocity oxy-fuel coating process

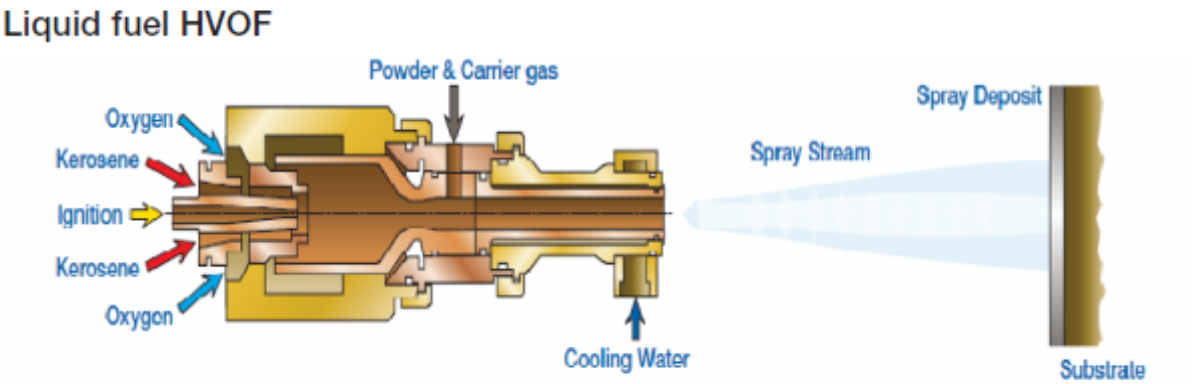

Fig 4.9 Liquid-fuel high velocity oxy-fuel coating process

Fig 4.10 Coated specimen Fig 4.11HVOF coating process used for the coating of specimen

4.10 COATING POWDER:

Composition	Total C=5.3-5.5, Fe < 0.1, Co= 11.5-12.5, W= Balance
Particle size	-53/+20µm, -45/+15µm, -38/+15µm

Table 4.5 Coating powder properties

4.11 ENERGY DISPERSIVE X-RAY SPECTROSCOPY:

Energy-dispersive X-ray spectroscopy (EDS or EDX) is an analytical technique used for the elemental analysis or chemical characterization of a sample. It relies on the investigation of an interaction of some source of X-ray excitation and a sample. Its characterization capabilities are due in large part to the fundamental principle that each element has a unique atomic structure allowing unique set of peaks on its X-ray spectrum. To stimulate the emission of characteristic X-rays from a specimen, a high-energy beam of charged particles such as electrons or protons , or a beam of X-rays, is focused into the sample being studied.

Element	Weight %	Atomic %
O K	27.81	78.31
Co K	7.71	5.89
W M	64.47	15.80
Total	100	

Table 4.6 Composition of coated surface of the specimen

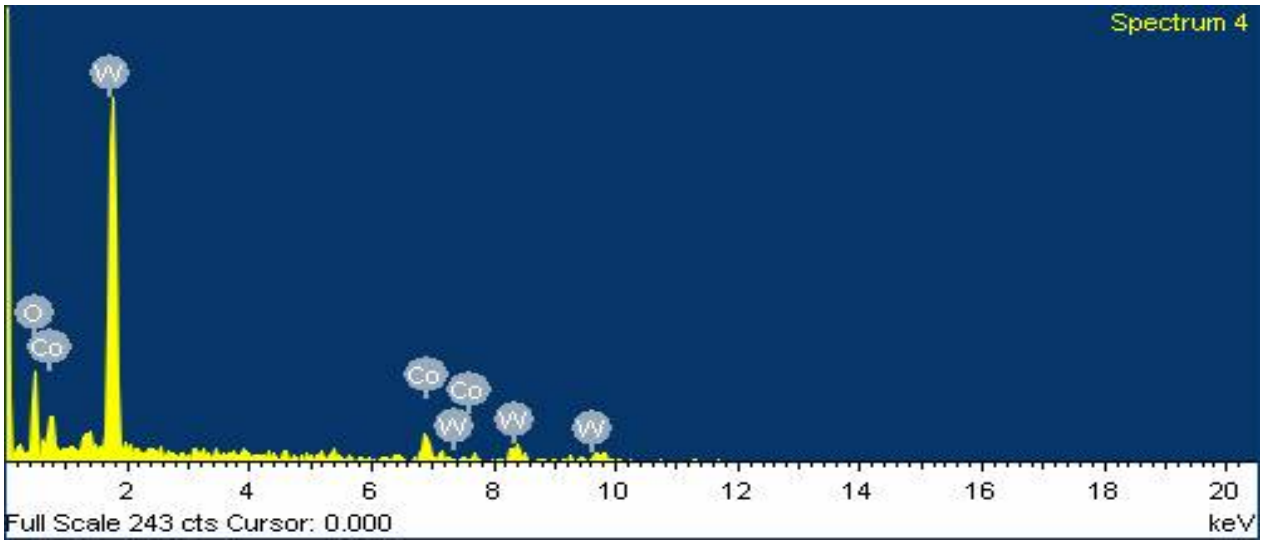

Fig 4.12 Energy dispersive X-ray spectroscopy of as coated specimen

The energy dispersive X-ray spectroscopy was done on as coated specimen. The test confirms the presence of tungsten and cobalt on the coated specimen

4.12 SCANNING ELECTRON MICROSCOPY OF WC-12C0 POWDER:

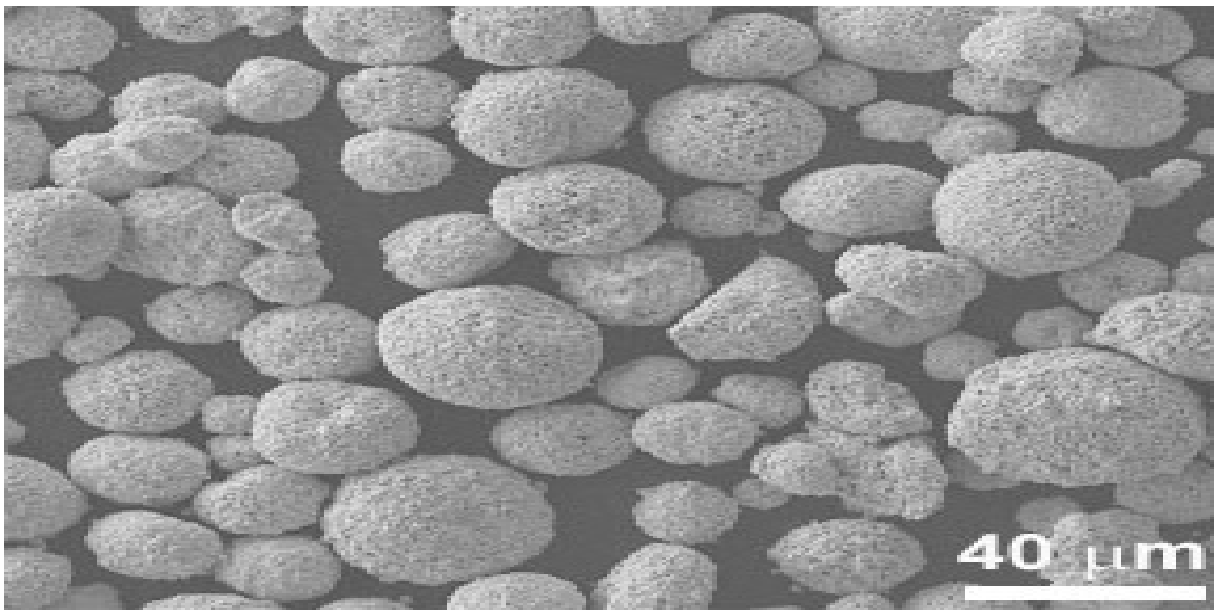

Fig 4.13 Scanning electron microscopy of WC-12Co coating powder

The scanning electron micrograph confirms the spherical morphology for the WC–12Co powder.

4.13 HIGH VELOCITY OXY-FUEL COATING PARAMETERS:

Coating thickness	200-250µm
Spraying distance	20cm
Spray gun temperature	2600°
Particle velocity	1050m/s
Oxygen pressure	10kg/cm^2
Fuel pressure	6.5kg/cm^2
Air pressure	5.5kg/cm^2

Table 4.7 High velocity oxy-fuel coating parameters

4.14 MICROHARDNESS OF MATERIALS:

Material	Hardness (VHN)
Mild steel	102
Stainless steel 202	198
Mild steel Coated with WC-12Co	810
Stainless steel coated with WC-12Co	860

4.15 CALCULATION OF WEIGHT LOSS:

Erosion wear was calculated in terms of specific mass loss. To calculate the area of every specimen a digital micrometer with accuracy of 0.01mm was used. The total surface are of the specimen was calculated. The formula used for calculation of specific mass loss is:

Specific mass loss= (Mass loss)/(Peripheral area) g/m^2

CHAPTER-5

RESULTS AND DISCUSSION

Erosion wear tests of mild steel and steel 202 with and without high velocity oxy-fuel coating of WC-12Co were conducted at different parameters. The parameters varied were the concentration of the slurry used, speed of sample rotation in the pot tester and the time duration of the tests. By changing these parameters different data points were obtained which were plotted on the graph to compare the performances of the different materials used under accelerated erosion wear conditions. The results obtained are discussed in this chapter:

5.1 EFFECT OF CONCENTRATION OF FLY ASH ON EROSION WEAR:

Change in slurry concentration has effect on erosion wear. Erosion wear increases with increase in concentration keeping the velocity constant.

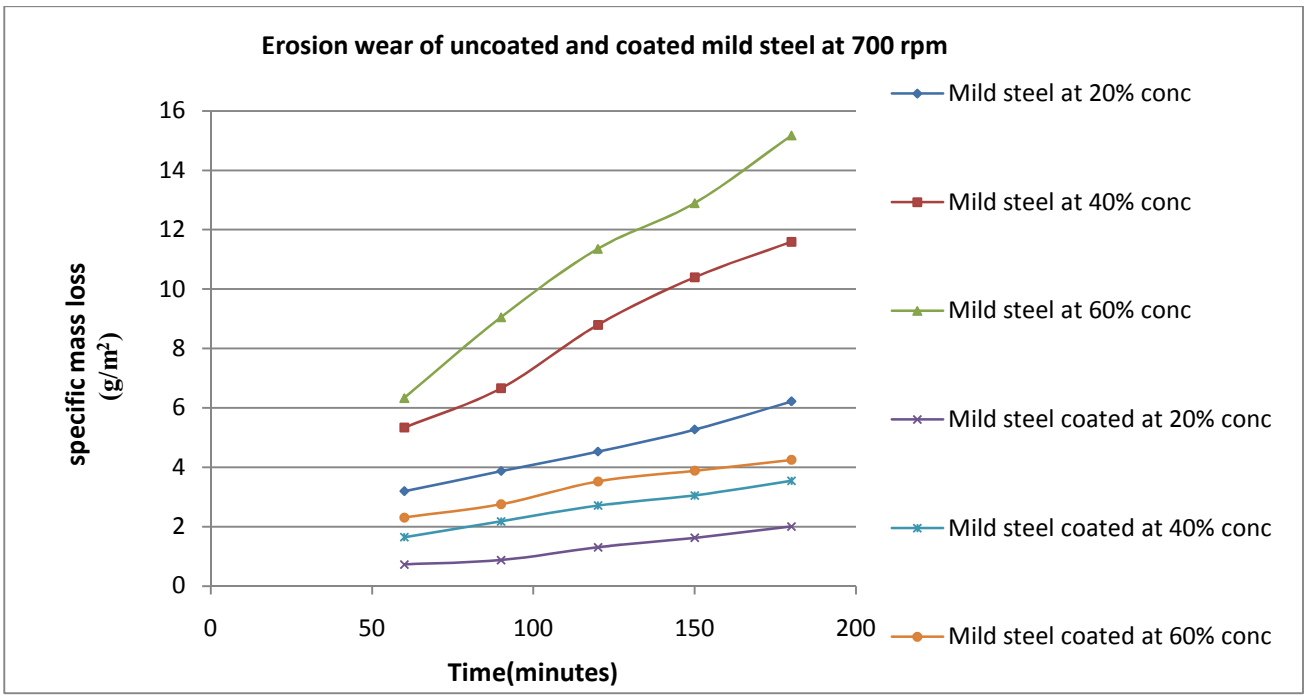

Figure 5.1 Erosion wear of mild steel coated and uncoated at 700rpm in fly ash

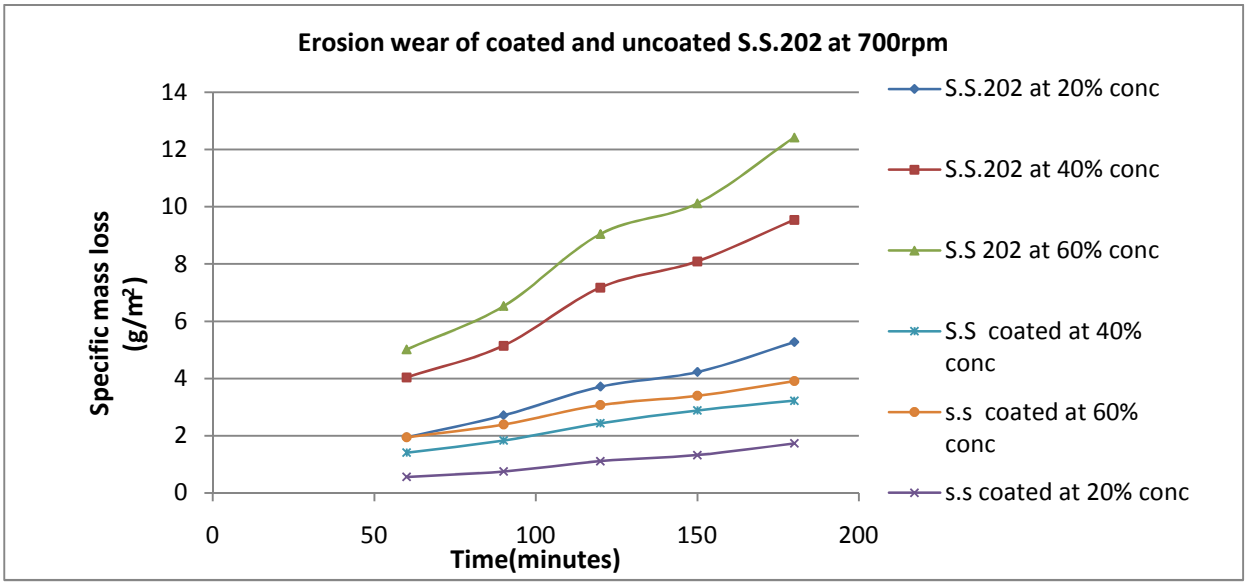

Figure 5.2 Erosion wear of coated and uncoated steel 202 at 700rpm in fly ash

Figure 5.1-5.2 shows the erosion wear of selected materials at 700rpm with varying fly ash concentration and time. In figure 5.1and 5.2 the erosion wear increases with increase in concentration from 20% to 40% more than from 40% to 60%. This can be due to the fact that at higher concentration the solid particles lose their sharp edges due to collision with each other. It is also clear from the figure 5.1 that erosion wear of coated mild steel is 2.87 to 3.7 times less at different points in the graph and from figure 5.2 the erosion wear of coated steel 202 is approximately 2.38 to 3.1 times less than uncoated steel 202. Figure 5.1 and 5,.2 also shows that that at lower concentration with variation of time of the operation more weight loss occurring as compared to higher concentration

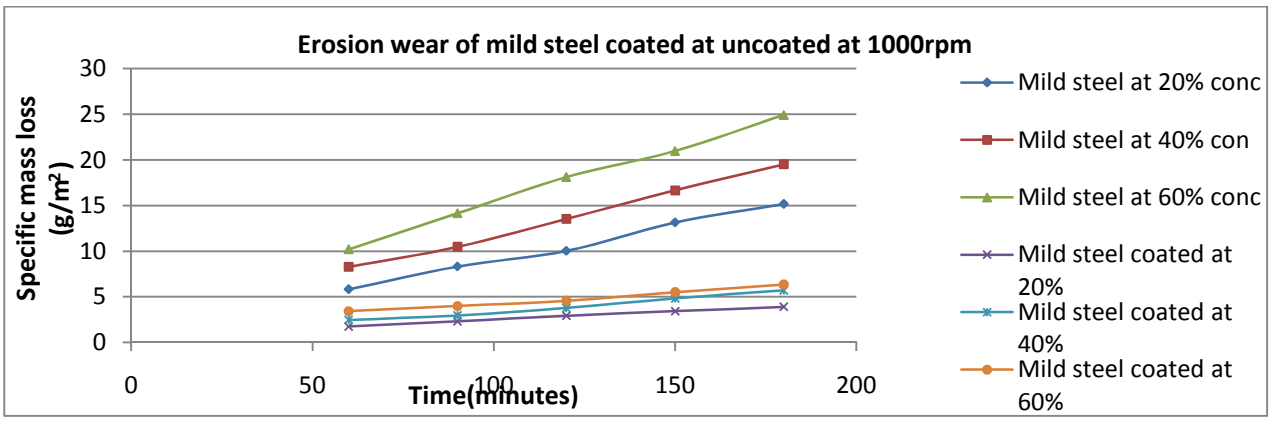

Figure 5.3 Erosion wear of mild steel coated and uncoated at 1000rpm in fly ash

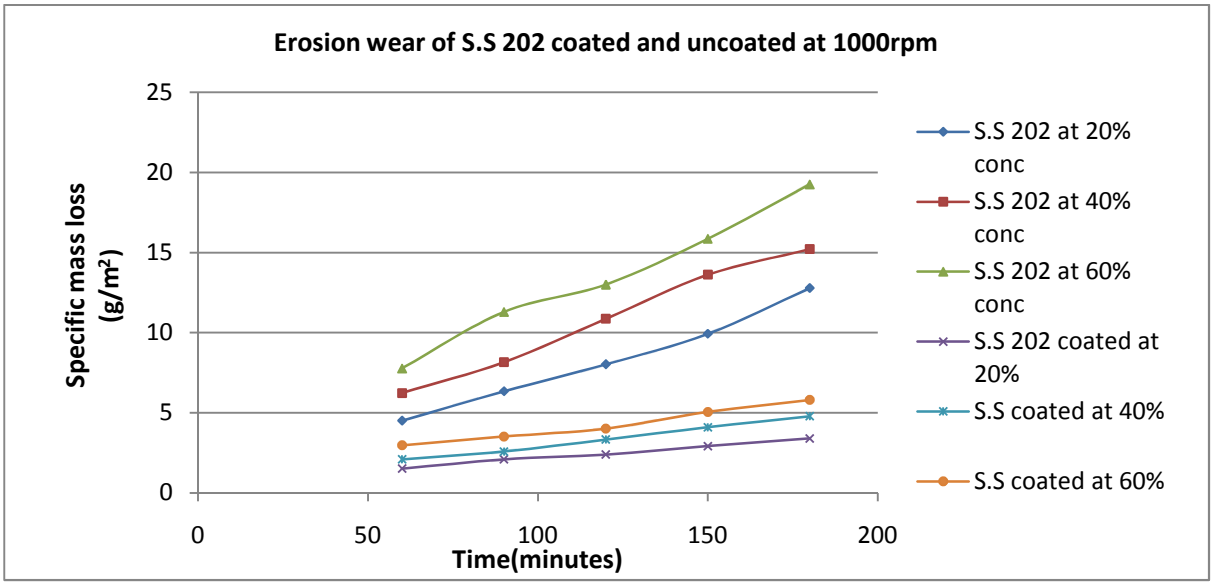

Figure 5.4 Erosion wear of coated and uncoated steel 202 at 1000rpm in fly ash

From figure 5.3 and 5.4 it can be seen that the erosion rate at 1000rpm of both the coated and uncoated materials increases than 700rpm at every concentration of fly ash. The increase in concentration does not have a big effect on erosion wear at this speed. In figure 5.3 the coated mild steel shows 2.9-3.9 times less erosion wear. In figure 5.4 the coated stainless steel 202 shows 2.6-3.4 times less erosion wear.

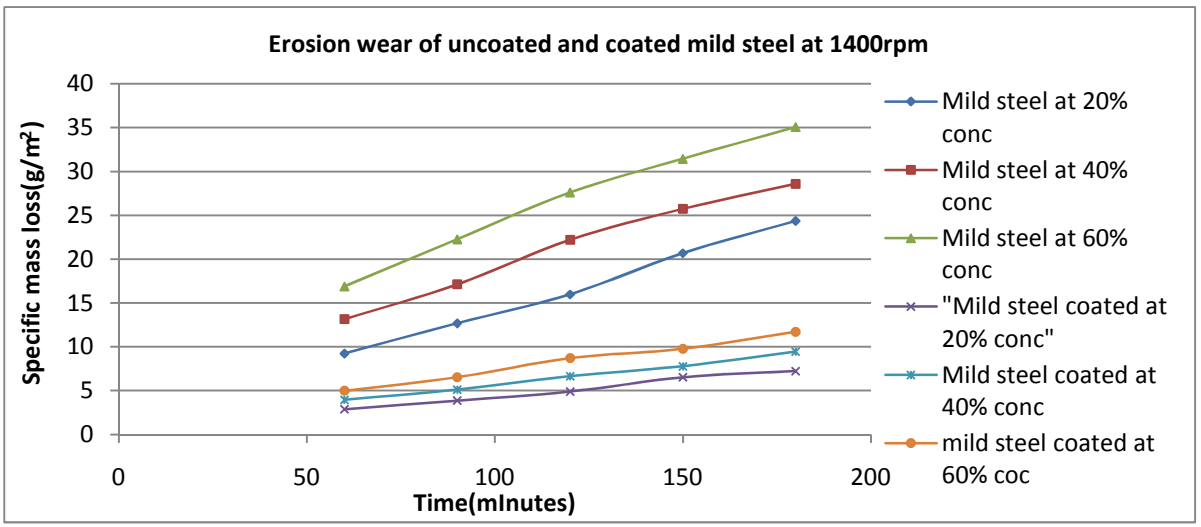

Figure 5.5 Erosion wear of uncoated and coated mild steel at 1400rpm

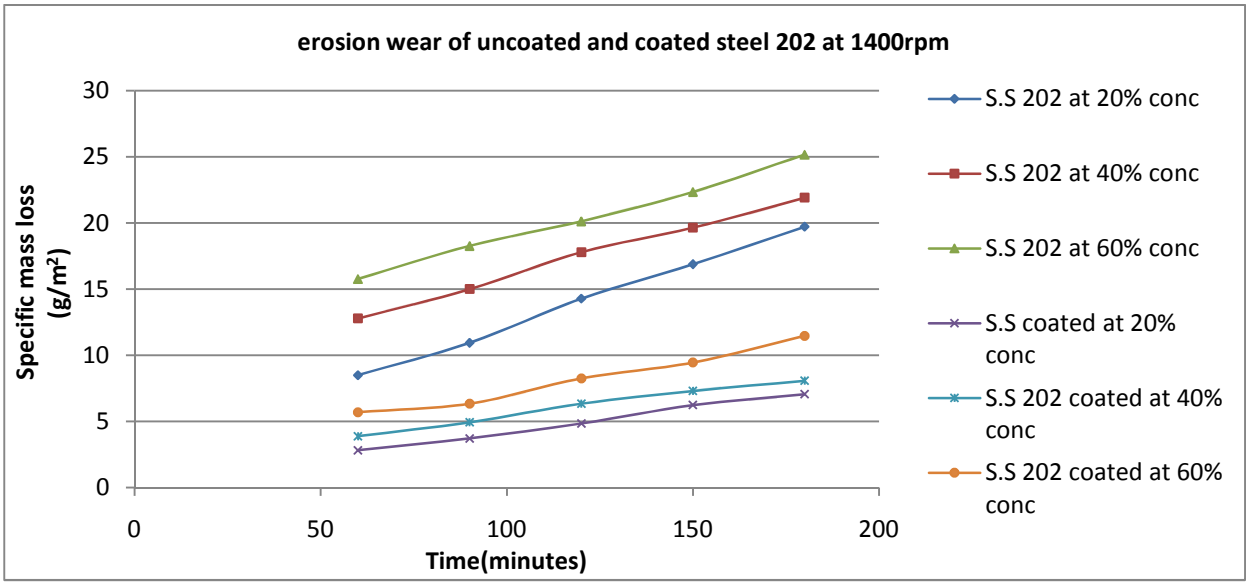

Figure 5.6 Erosion wear of uncoated and coated steel 202 at 1400rpm

In fig 5.5 and 5.6 the wear rate increases significantly due to increase in the concentration. The maximum erosion of the specimen can be seen at 1400rpm with 60% concentration of ash for both uncoated and coated materials. The erosion wear for coated mild steel in figure 5.5 is 2.9-3.7 times less than the bare mild steel at different data points and in figure 5.6 the erosion wear of coated steel 202 is 2.19-2.7 times less than bare steel 202

5.2 EFFECT OF SPEED ON EROSION WEAR:

Speed has a very significant effect on the erosion wear of material. The erosion wear of a material increases rapidly with increase in the speed of the slurry flow. The effect of increase in speed on the erosion wear of the materials tested is shown in the graphs:

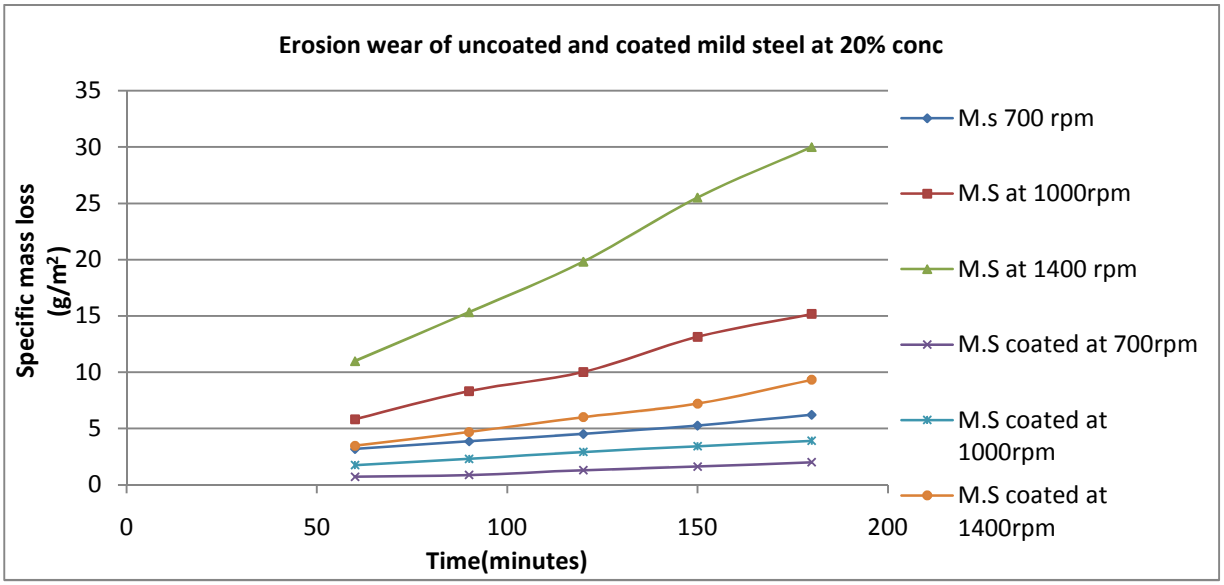

Figure 5.7 Erosion wear of coated and uncoated mild steel at 20% fly ash concentration

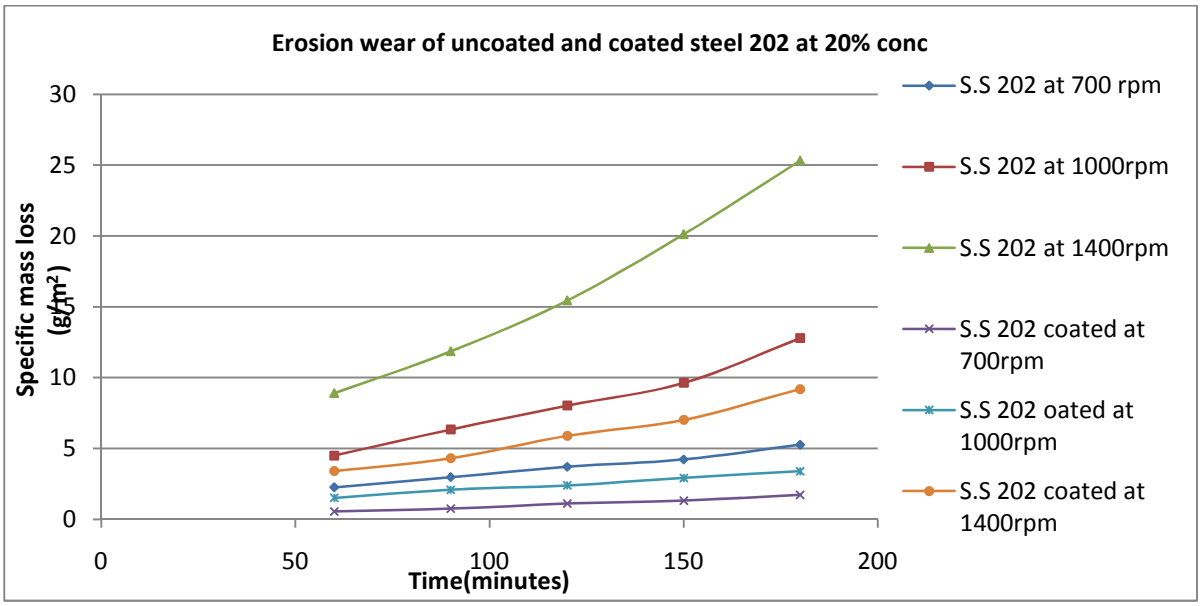

Figure 5.8 Erosion wear of coated and uncoated steel 202 at 20% fly ash concentration

Figure 5.7 shows erosion wear of uncoated and coated mild steel with increasing speed at 20% concentration of fly ash. The erosion wear rate is more from 1000rpm to 1400rpm than from 700rpm to 1000rpm for both uncoated and coated mild steel. This shows that change in speed of specimen effects the erosion wear more than change in concentration. The coated steel in figure

5.7 shows 3.17-3.8 times less erosion wear than bare mild steel. In figure 5.8 the erosion wear of steel 202 uncoated and coated shows similar behavior as that of mild steel uncoated and coated in figure 5.7. The wear rate increases with increase in speed keeping the concentration constant. with change in time. The erosion wear of coated steel 202 is 2.6-2.7 times less than the bare steel 202 in figure 5.8. The erosion wear rate is decreasing with increase in time for a given speed.

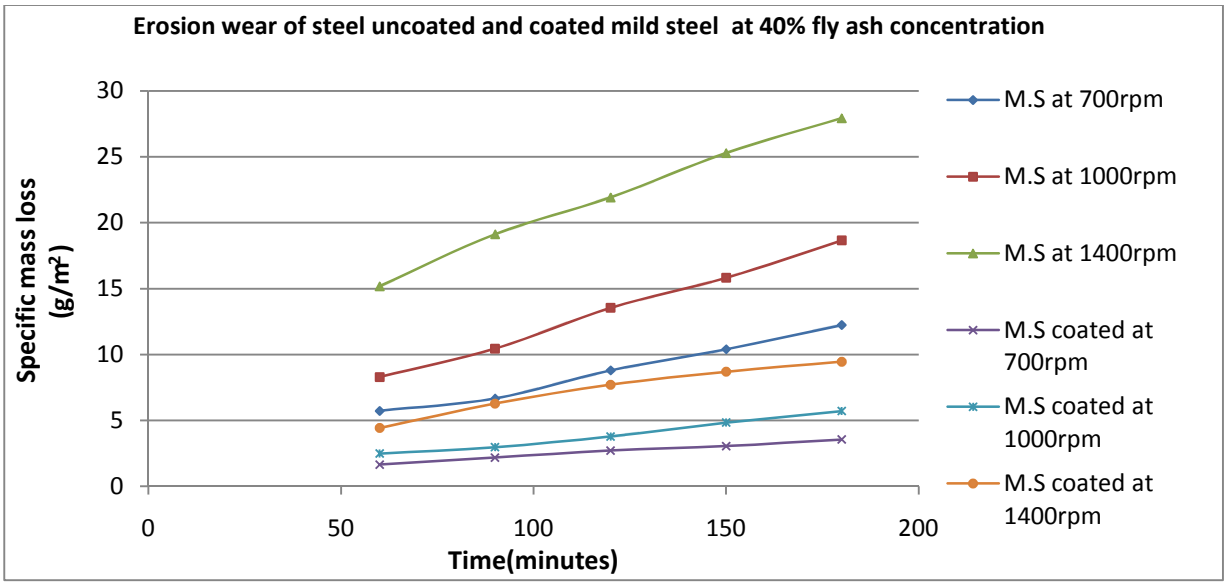

Figure 5.9 Erosion wear of coated and uncoated mild steel at 40% fly ash concentration

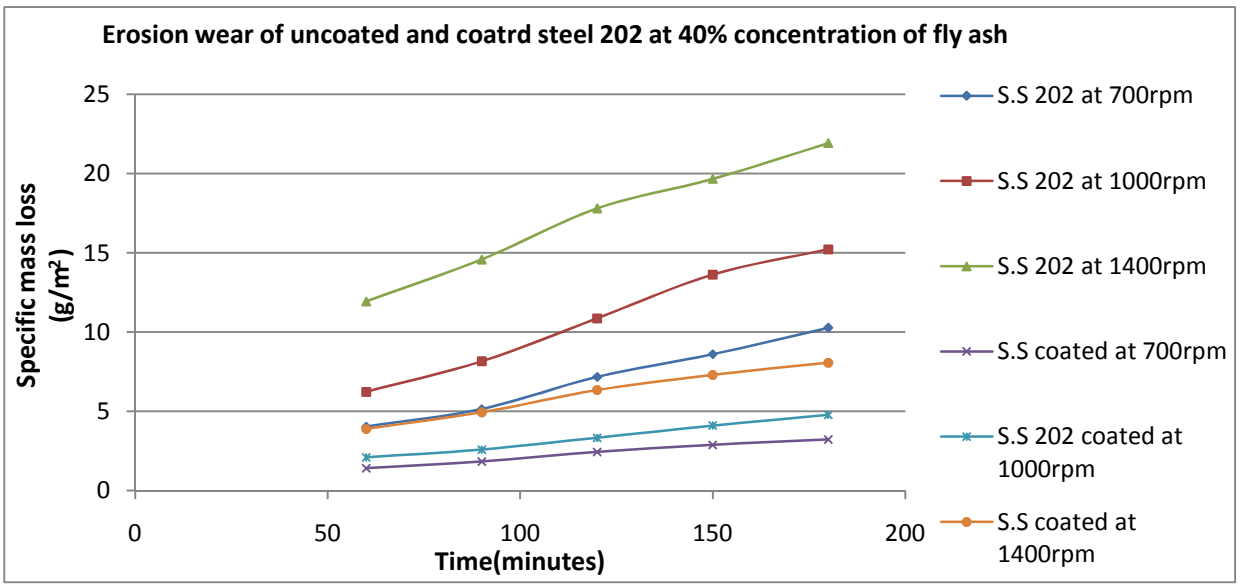

Figure 5.10 Erosion wear of coated and uncoated steel 202 at 40% fly ash concentration

In figure 5.9 the erosion wear rate for 1000rpm to 1400rpm is more than that of 700rpm to 1000rpm at 40% concentration of fly ash. The wear rate of uncoated steel at 700rpm is similar to that of the coated steel at 1400rpm. The erosion wear of coated steel is 2.97-3.64 times less than bare mild steel at different data points.

In figure 5.10 the wear of coated steel 202 for 1000rpm to 1400rpm increases with change in time. The erosion wear of coated steel 202 is 2.47 to 3.1 times less than bare steel 202.

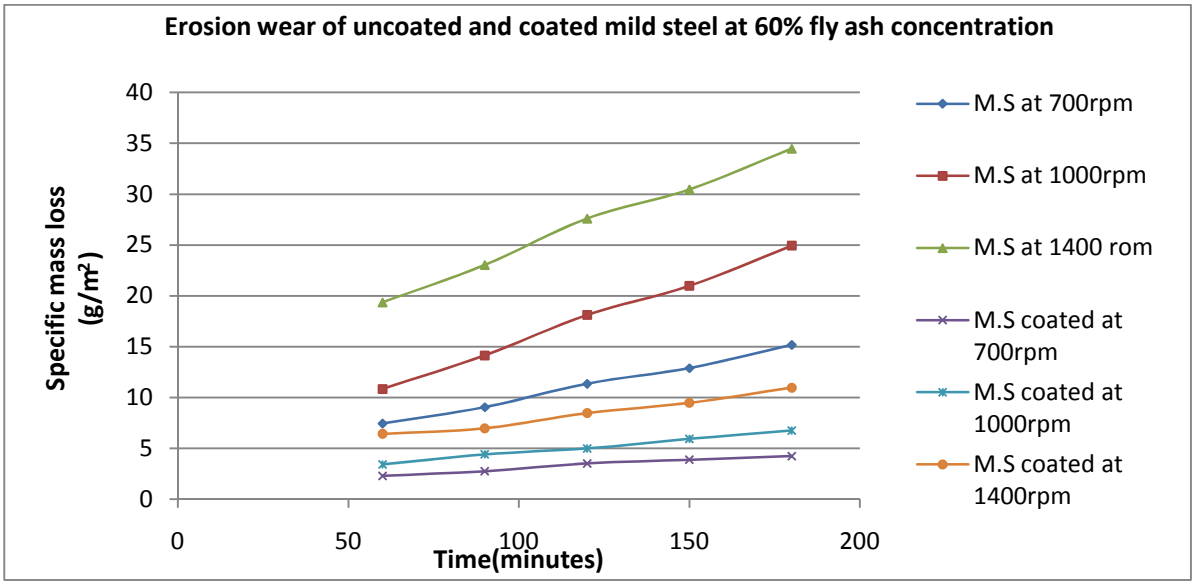

Figure 5.11 Erosion wear of coated and uncoated mild steel at 60% fly ash concentration

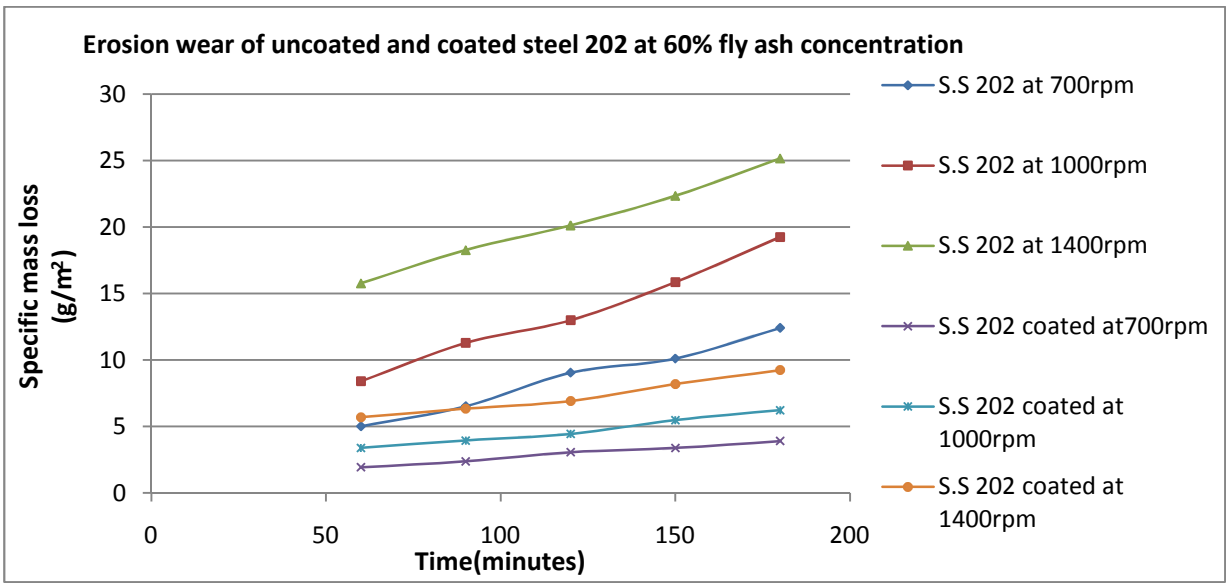

Figure 5.12 Erosion wear of coated and uncoated steel 202 at 60% fly ash concentration

In figure 5.11 the erosion wear rate for uncoated mild steel increases with increase in speed with change in time the erosion wear for coated mild steel is 3.3-3.7 times less than the bare mild steel at different data points in the figure. In figure 5.12 the increase in erosion wear for uncoated steel 202 and coated steel 202 is shown at 60% concentration. The maximum erosion occurs at 1400rpm. The erosion wear rate is different at different time interavals generally decreasing with increase in time.

BOTTOM ASH:

5.3 EFFECT OF CONCENTRATION OF BOTTOM ASH ON EROSION WEAR:

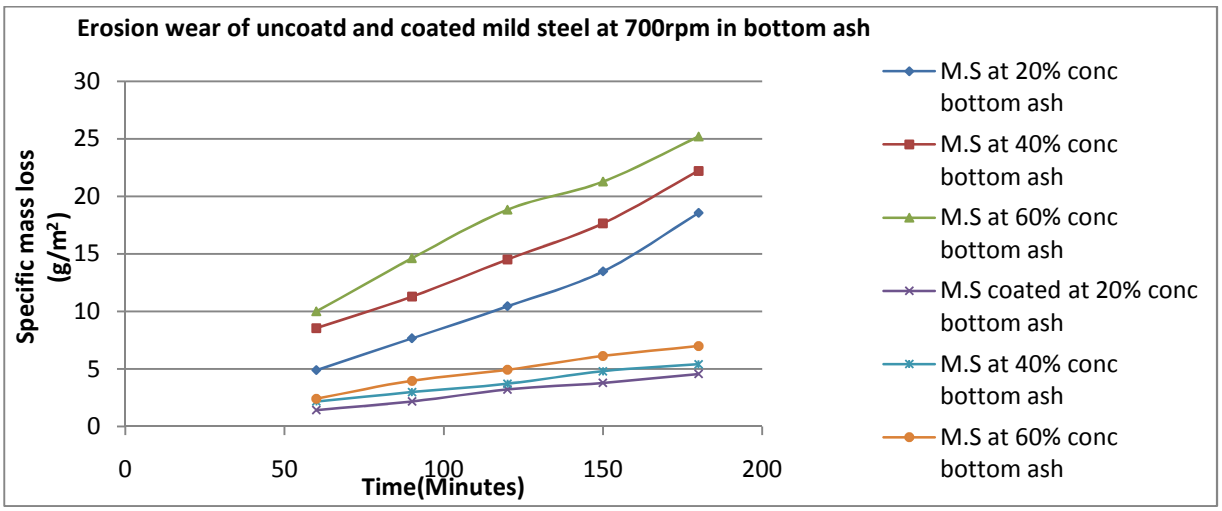

Figure 5.13 Erosion wear of uncoated and coated mild steel at 700rpm in bottom ash

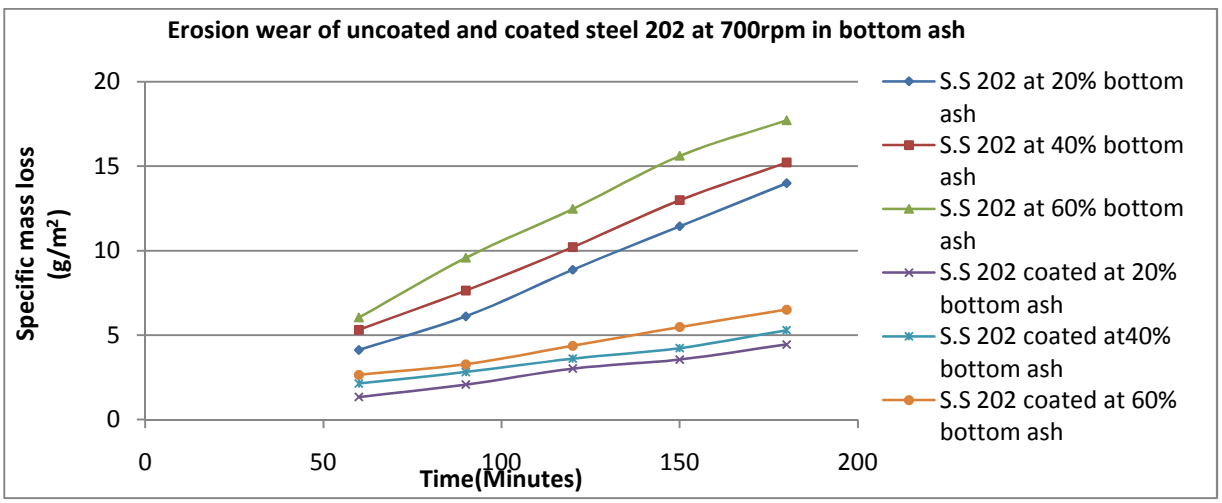

Figure 5.14 Erosion wear of uncoated and coated steel 202 at 700rpm in bottom ash

Figure 5.13 shows erosion wear of uncoated and coated mild steel at 700rpm with different bottom ash concentrations. The erosion wear with bottom ash is more than that of the fly ash. The erosion wear shows similar behavior for both uncoated and coated mild steel with wear increasing steadily with increase in concentration of bottom ash. The figure shows steady wear rate of coated and bare mild steel with time. The erosion wear of coated steel is 3.2-3.5 times less than bare mild steel at different data points. In figure 5.14 the erosion wear increases with increase in concentration at 700rpm. The change in concentration does not produce big change in wear rate of the material. The erosion wear of coated steel 202 is 2.4-2.7 times less than bare steel 202.

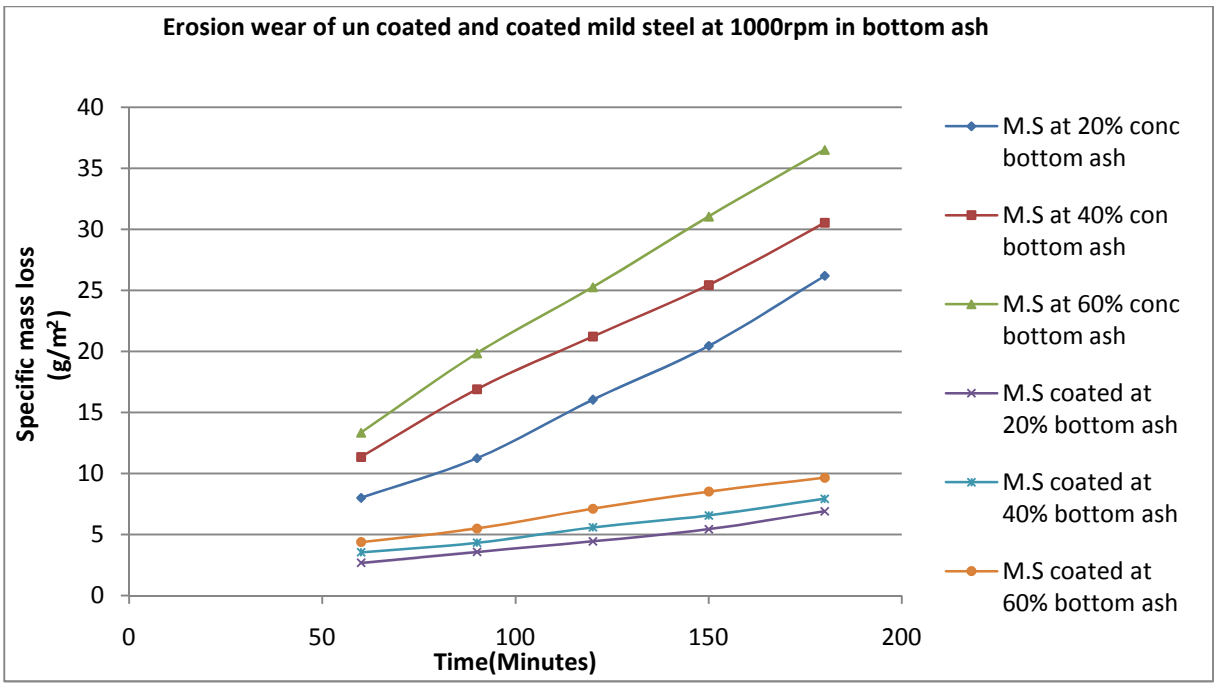

Figure 5.15 Erosion wear of uncoated and coated mild steel at 1000rpm in bottom ash

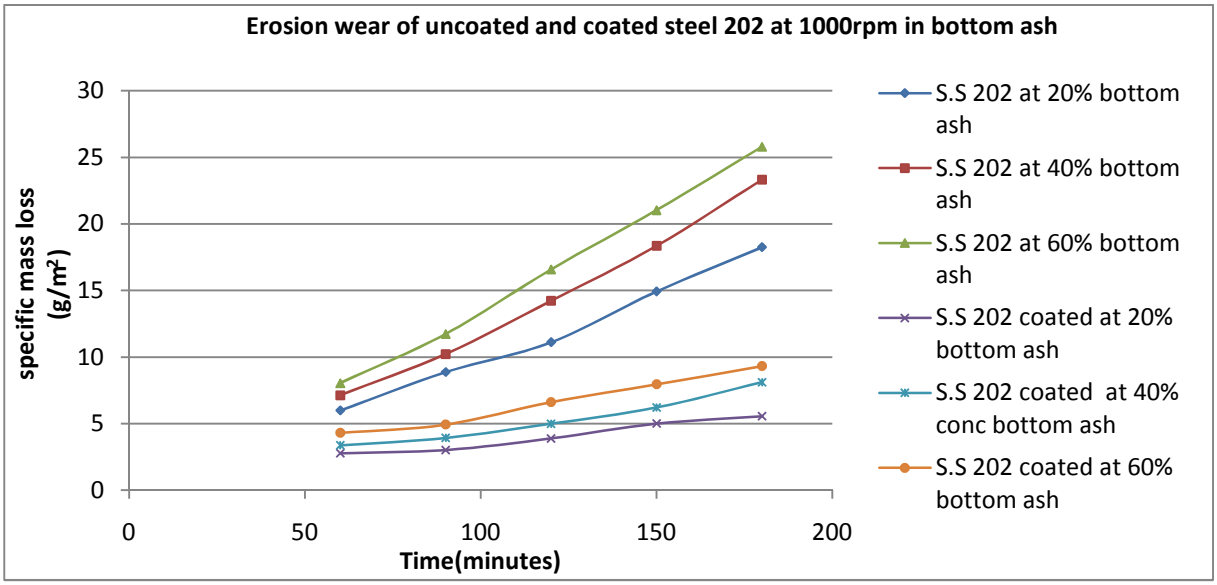

Figure 5.16 Erosion wear of uncoated and coated steel 202 at 1000rpm in bottom ash

In figure 5.15 and 5.16 the erosion wear at 1000rpm for different concentrations is shown. The erosion behavior of uncoated and coated specimens for both the materials is quite similar. Both the figures show steady erosion wear rate with change in time. The erosion wear of coated smild steel is 3.2-3.7 times less than the bare mild steel and erosion wear of coated steel 202 is 2.4-2.7 times less than uncoated steel 202 at different data points

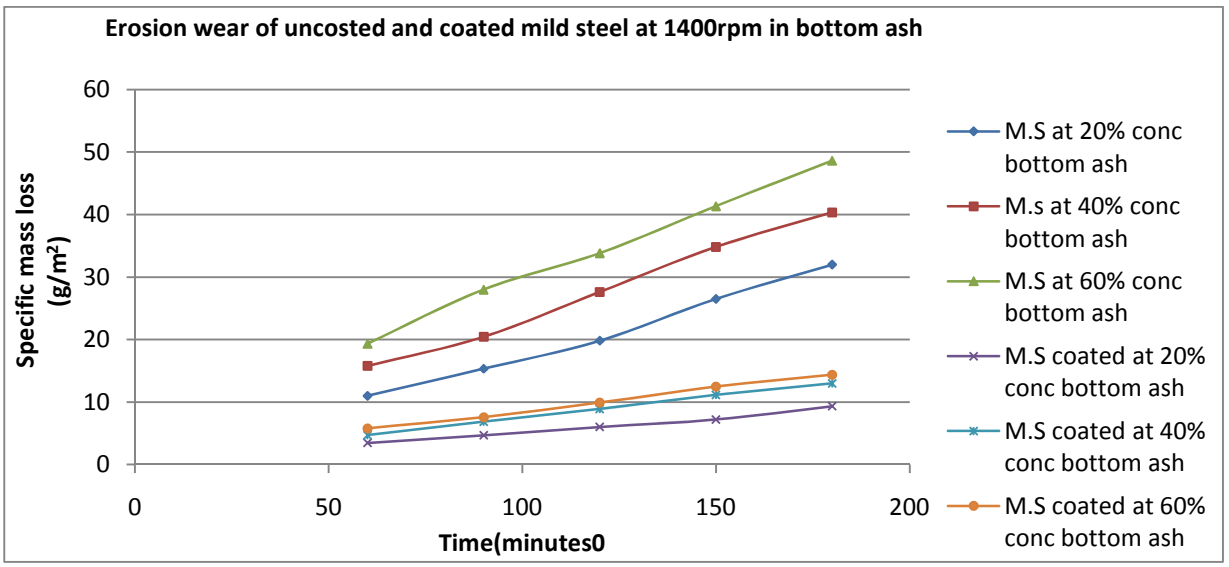

Figure 5.17 Erosion wear of uncoated and coated mild steel at 1400rpm in bottom ash

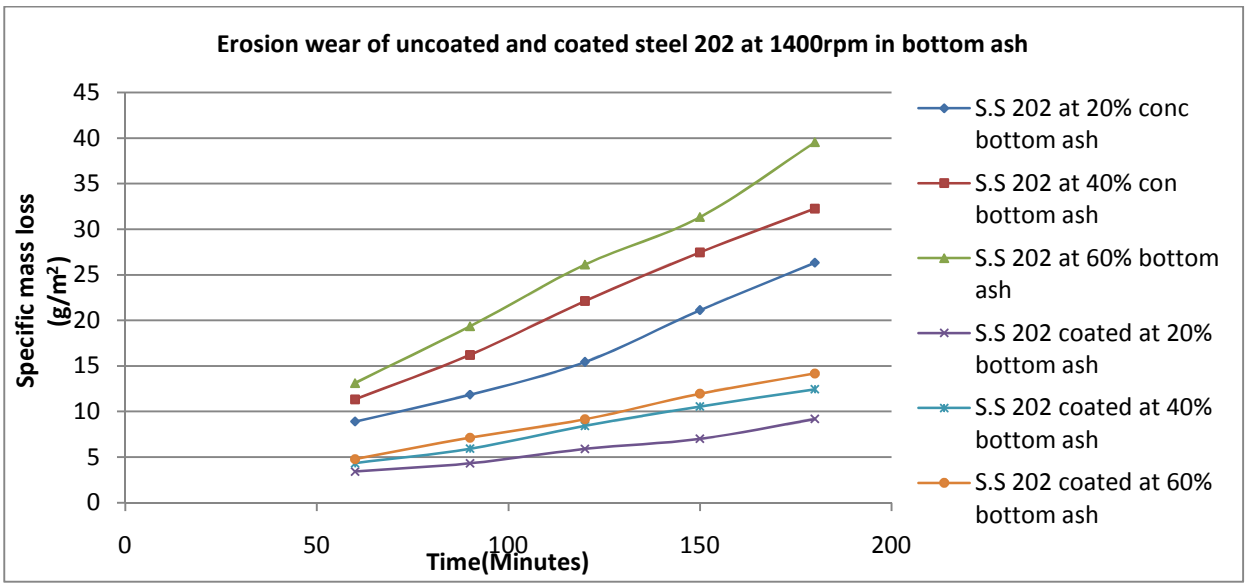

Figure 5.18 Erosion wear of uncoated and coated steel 202 at 1400rpm in bottom ash

Figure 5.17 and 5.18 shows erosion wear of materials at 1400rpm with different bottom ash concentration. High values for erosion wear are achieved at different concentrations for both the uncoated materials. The coated mild steel specimens show 3.5-4 times less erosion at different data points. In figure 5.17. The steel 202 coated specimens shows 2.4-2.9 times less erosion wear at different data points in figure 5.18.

5.4 EFFECT OF SPEED ON EROSION WITH BOTTOM ASH:

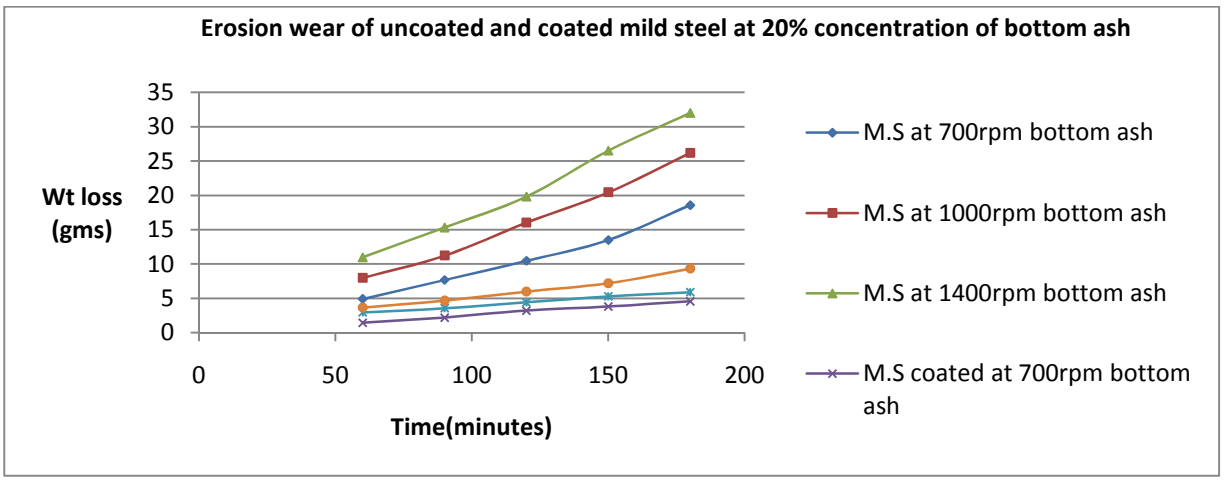

Figure 5.19 Erosion wear of coated and uncoated mild steel at 20% bottom ash concentration

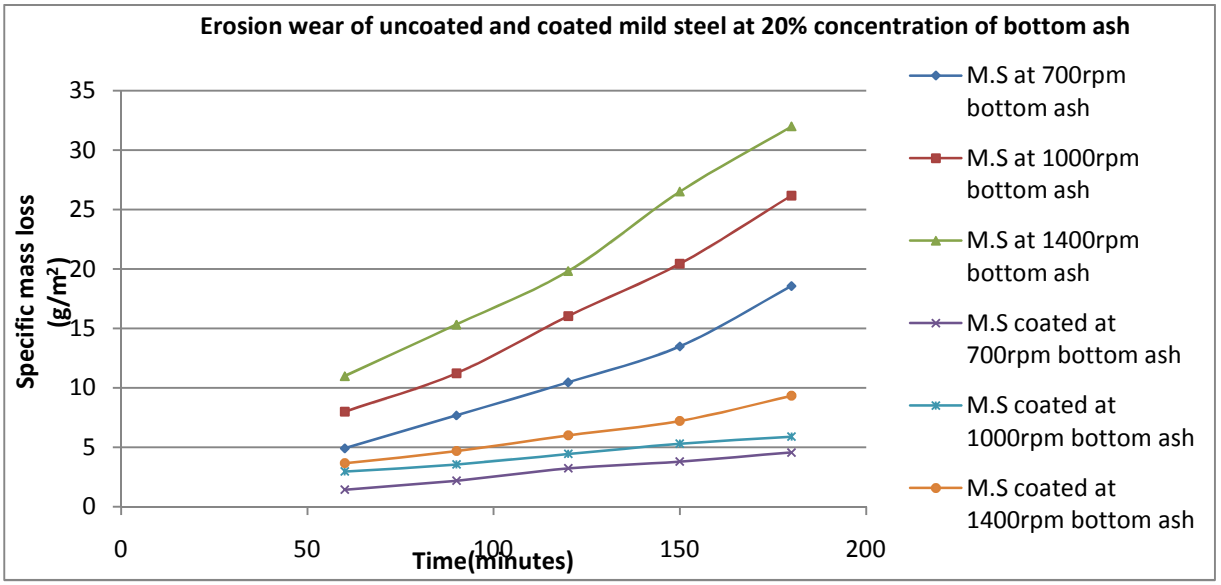

Figure 5.20 Erosion wear of coated and uncoated steel 202 at 20% bottom ash concentration

Figure 5.19 shows erosion wear at 20% bottom ash concentration with different speeds at different time intervals. The erosion rate increases with increase in speed and time at same concentration. The erosion wear of coated mild steel is 3.5 times less than bare mild steel in figure5.19

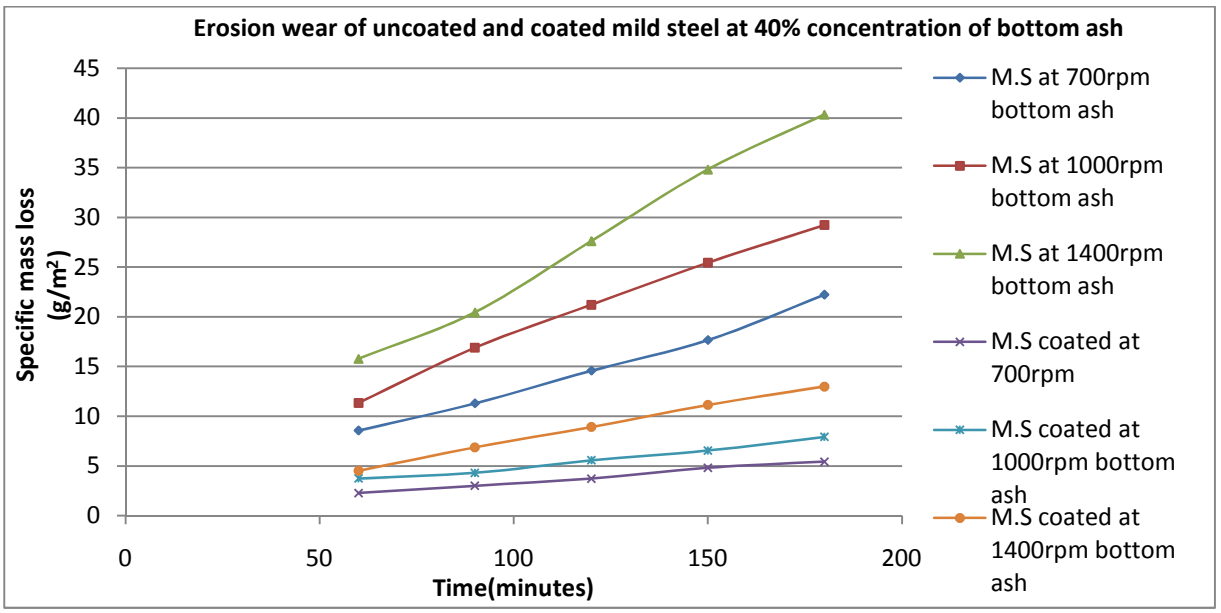

Figure 5.21 Erosion wear of coated and uncoated mild steel at 40% bottom ash concentration

In figure 5.20 the erosion rate of the uncoated and coated material increases with increase in speed.

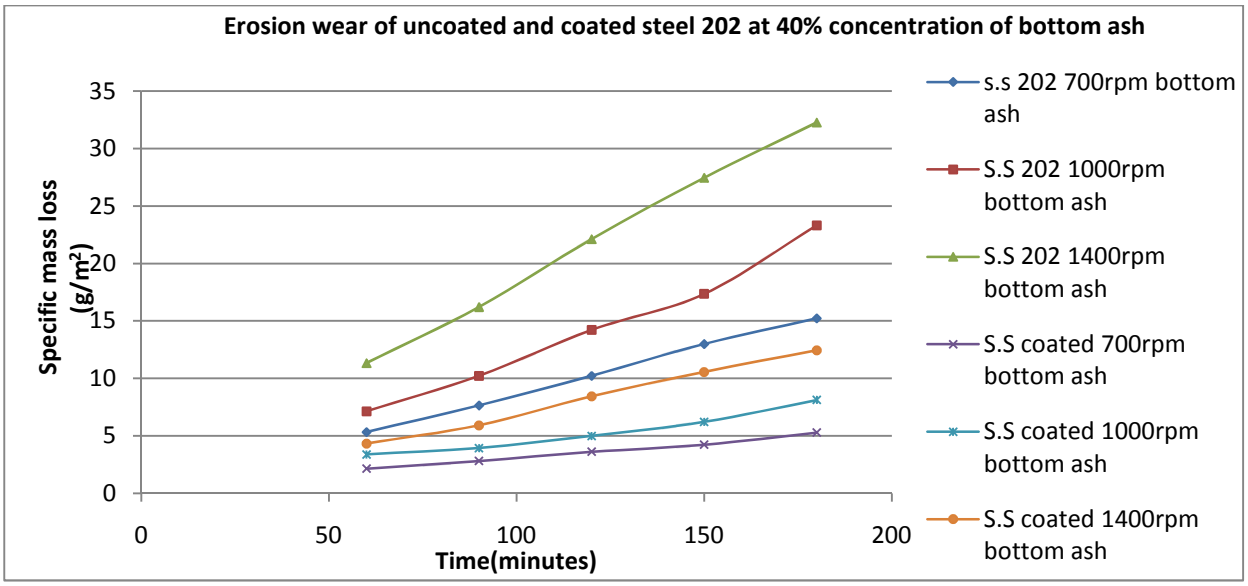

Figure 5.22 Erosion wear of coated and uncoated steel 202 at 40% bottom ash concentration

In figure 5.21 the increase in wear rate for mild steel is steady for all speeds. The maximum wear occurs at 60% concentration. The erosion wear is increasing with increase in time. The erosion wear of coated mild steel is 3.2-3.7 less than bare mild steel.

Figure 5.22 shows erosion wear of steel 202 at 40% concentration for different speeds at different time periods. The erosion wear is increasing with increase in speed and change in time. The erosion wear of coated steel 202 is 2.5 times less than bare steel 202.

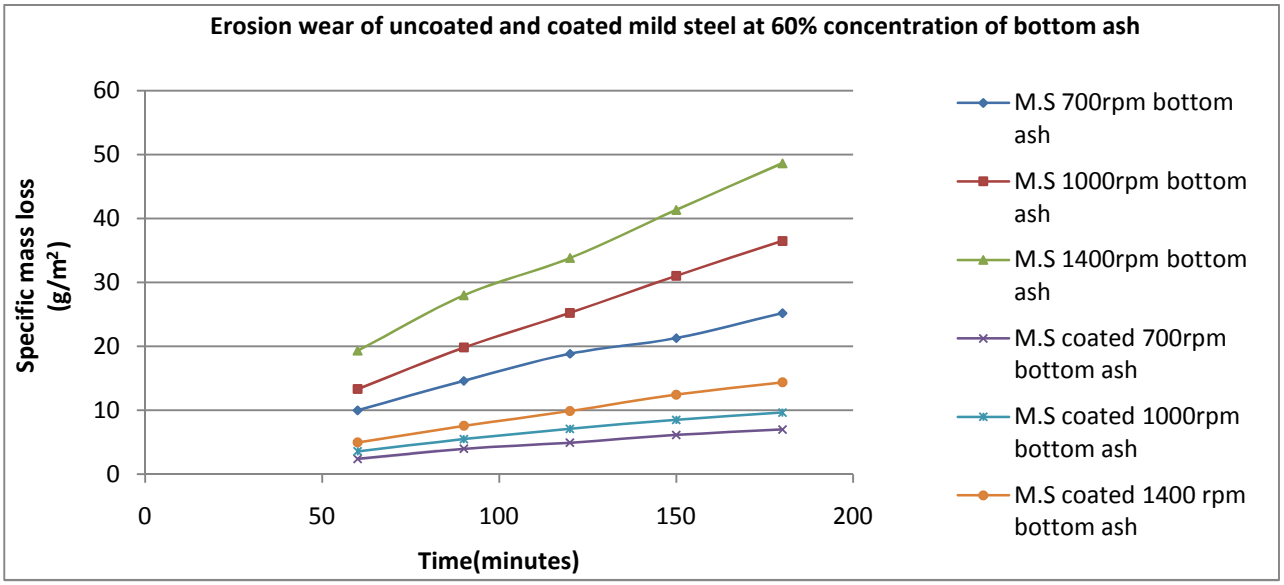

Figure 5.23 Erosion wear of coated and uncoated mild steel at 60% bottom ash concentration

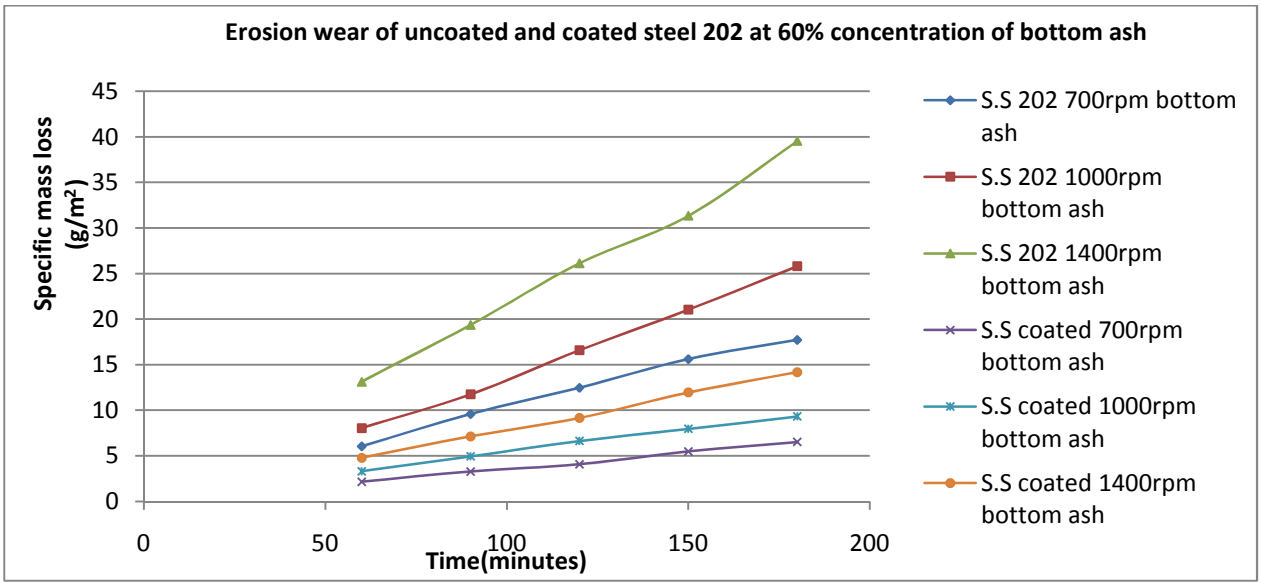

Figure 5.24 Erosion wear of coated and uncoated steel 202 at 60% bottom ash concentration

Figure 5.23 and 5.24 shows erosion wear of materials at different speeds with 60% concentration of bottom ash. The rate of erosion is increasing with increase in speed for all the materials. The maximum erosion can be seen at 1400rpm. Erosion of coated mild steel is3.5 times less than bare mild steel and erosion of coated steel 202 is 2.7 times less than coated steel 202.

5.5 SCANNING ELECTRON MICROSCOPY:

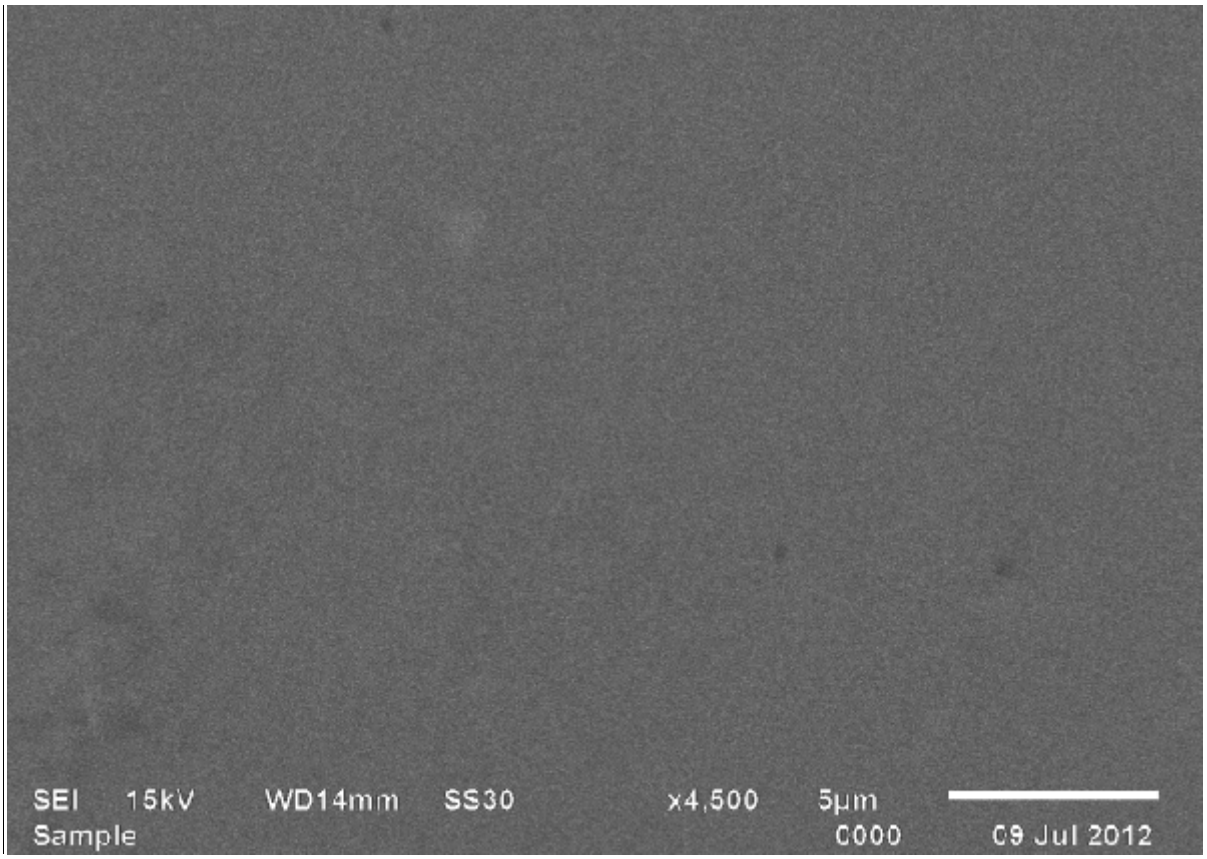

Figure 5.25 SEM stainless steel 202 before erosion at 4500X

Figure 5.25 shows SEM of stainless steel before erosion. Micrograph showing polished surface with no pits, cracks or deformation on the surface.

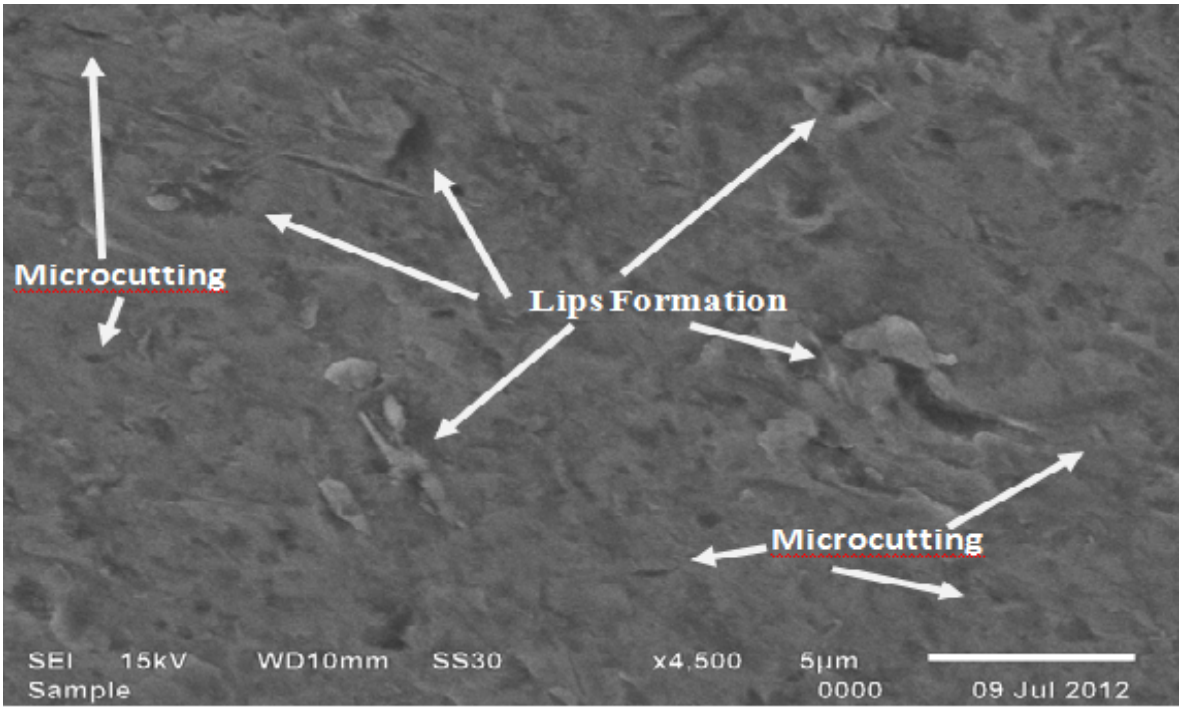

Figure 5.26 SEM of stainless steel 202 after erosion with bottom ash at 4500X

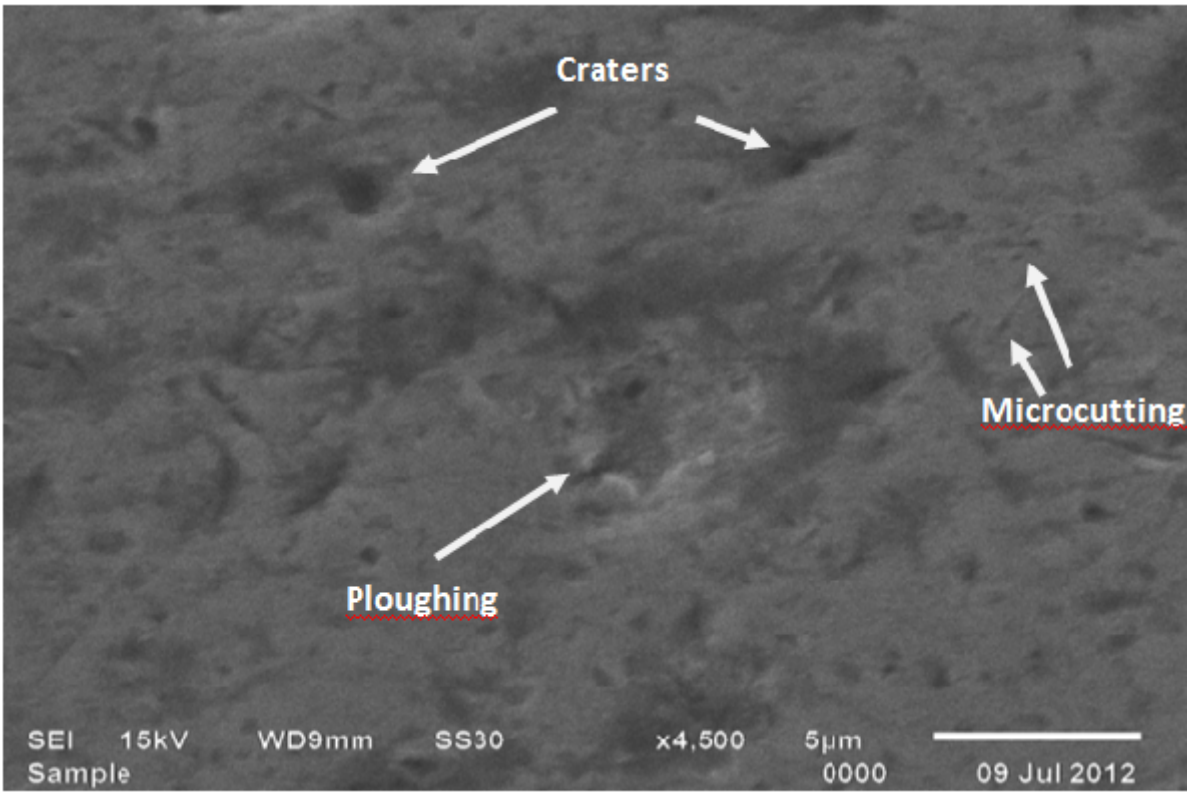

Figure 5.27 SEM of stainless steel 202 after erosion with fly ash at and 4500X

Figure 5.26 shows SEM of stainless steel 202 after erosion with bottom ash at 1400rpm, 60% concentration of bottom ash and 150 minutes run time. Micrograph shows lips formation, and microcutting at 4500X.

Figure 5.27 shows SEM of stainless steel after erosion with fly ash at 1400rpm, 60% fly ash concentration and 150 minutes run time. Micrograph shows microcutting and craters and ploughing action on the surface of the material.

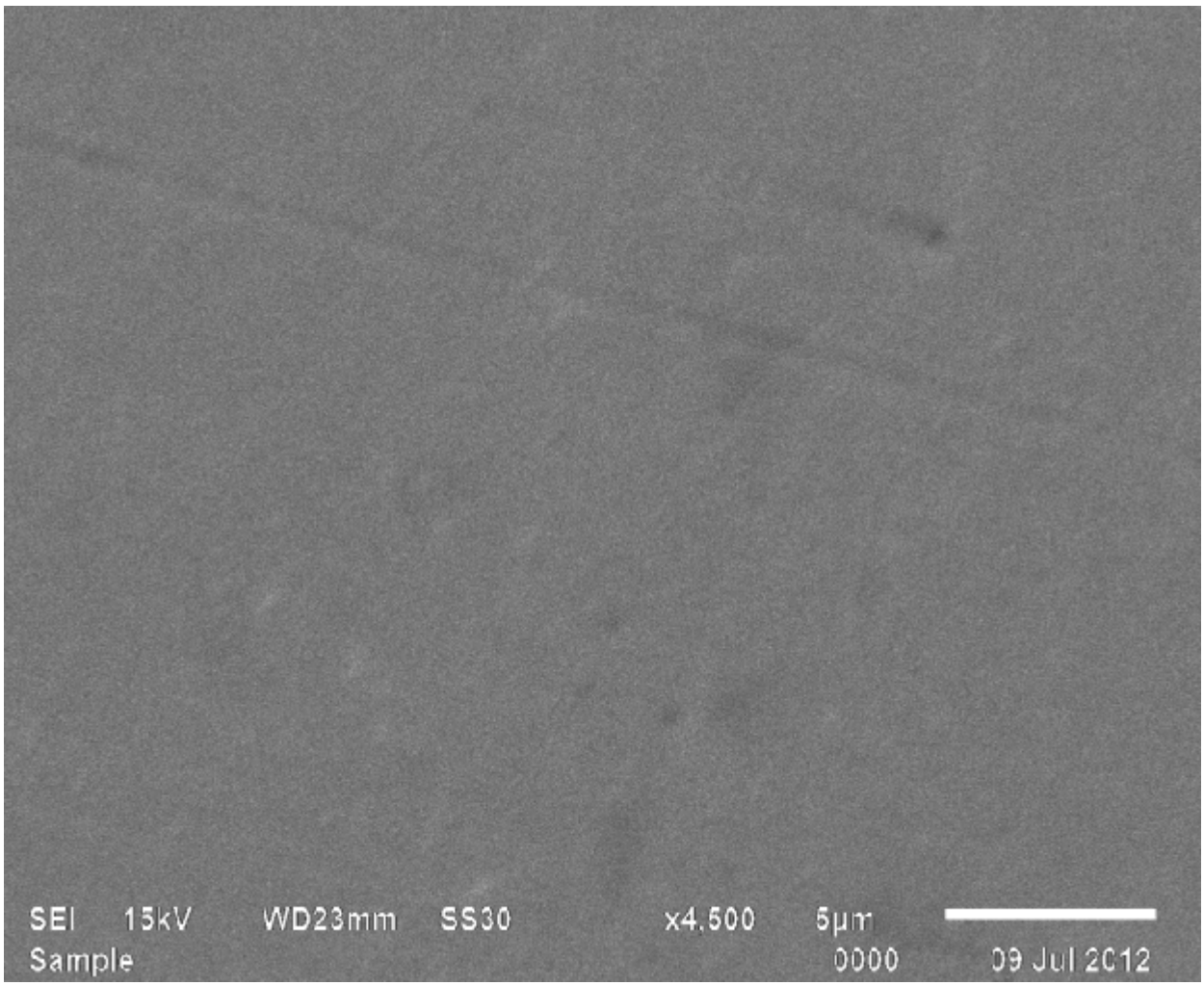

Figure 5.28 SEM of mild steel before erosion at 4500X

Figure 5.28 shows the SEM of mild steel before erosion. The micrograph shows polished surface with no microcracks, craters or any other surface deformation

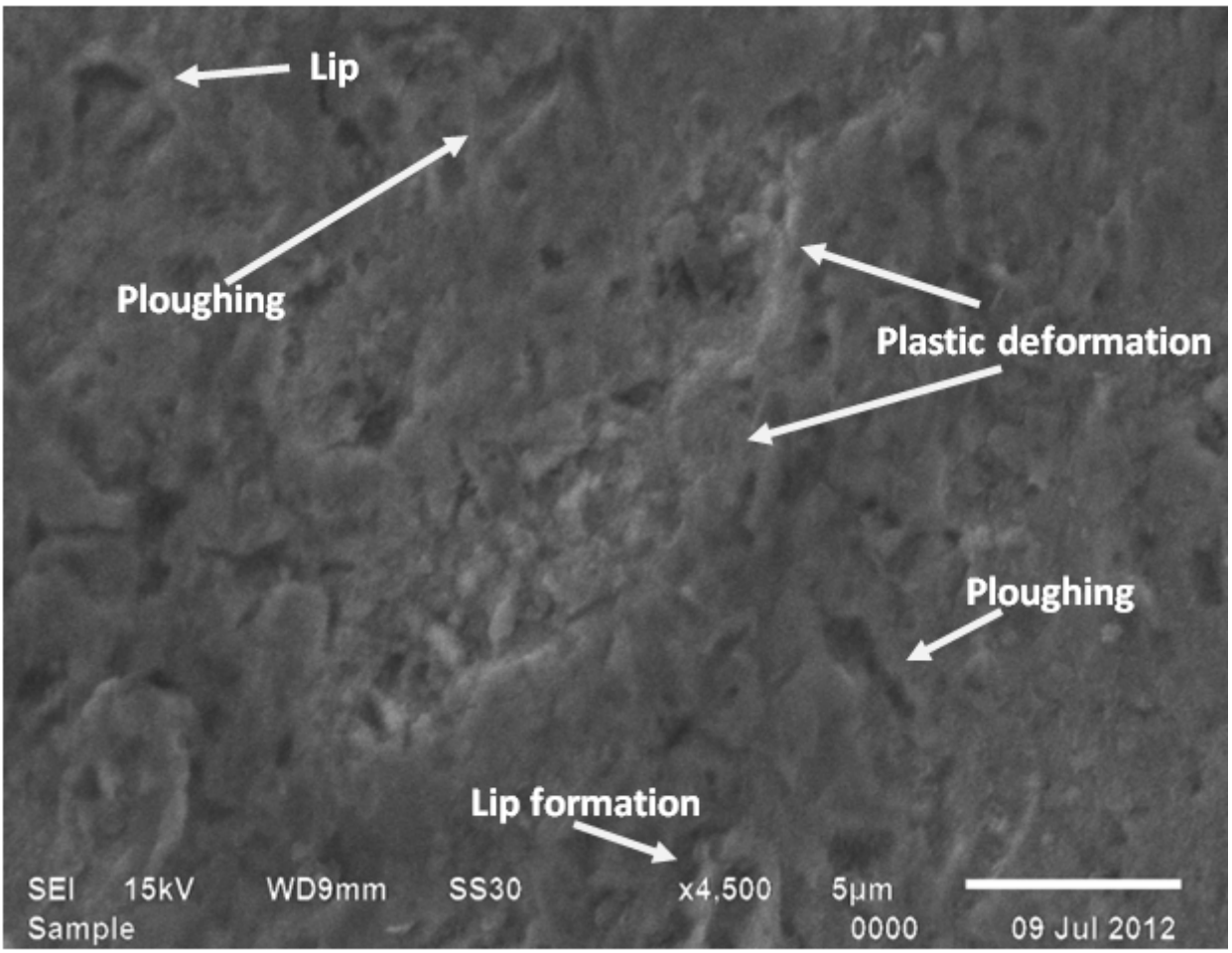

Figure 5.29 SEM of mild steel after erosion with bottom ash at 4500X

Figure 5.29 shows SEM of mild steel after erosion with bottom ash at1400rpm, 60% concentration of bottom ash and 150 minutes run time. The micrograph shows formation of microcracks and pits on the surface of the material formed due to the erosion of material by bottom ash slurry

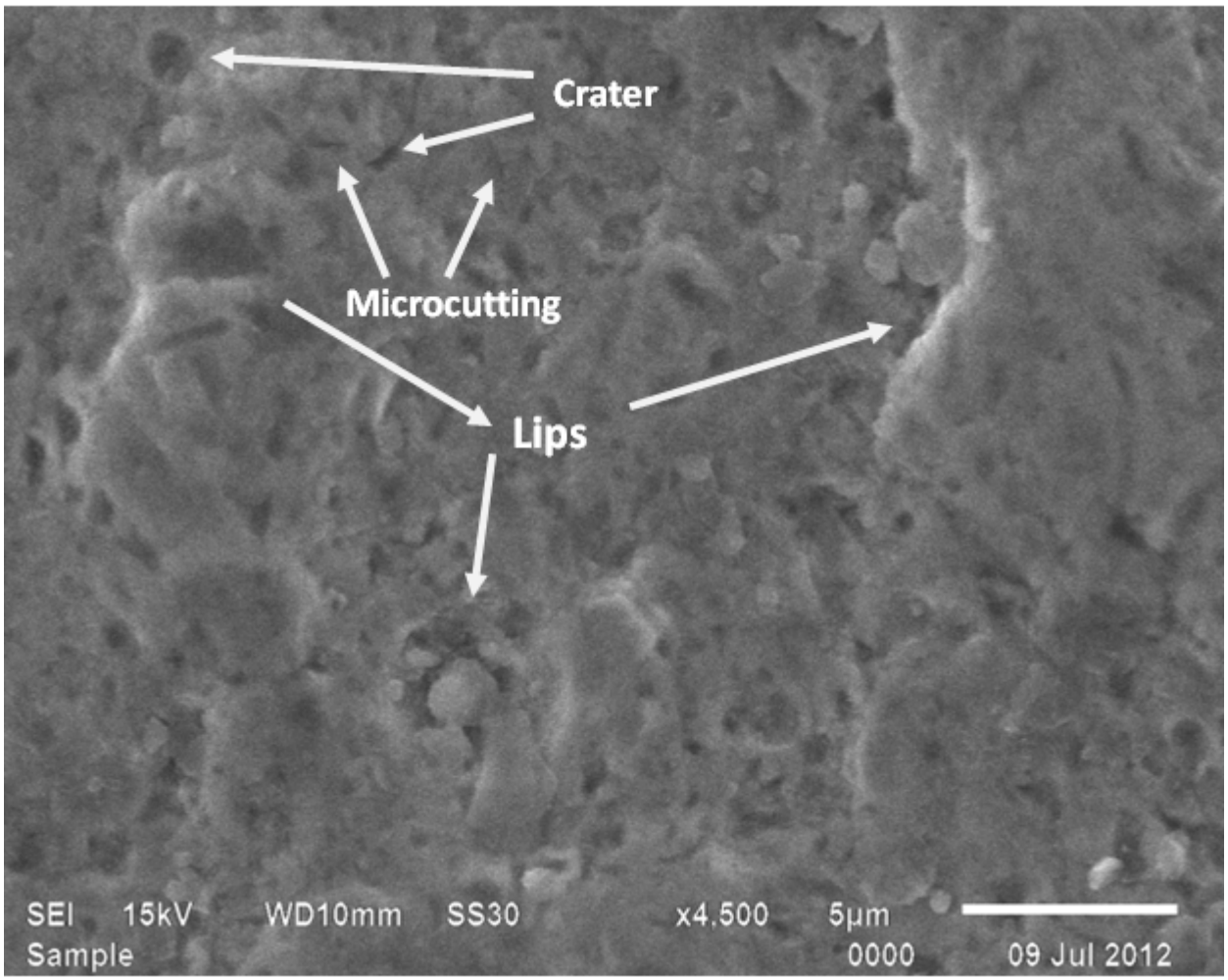

Figure 5.30 SEM of mild steel after erosion with fly ash at 1500X and 4500X

Figure 5.30 shows SEM of mild steel after erosion with fly ash at at1400rpm, 60% concentration of fly ash and 150 minutes run time. Micrograph of the sample shows damaged surface of the mild steel. Eroded surface showing microcracks.

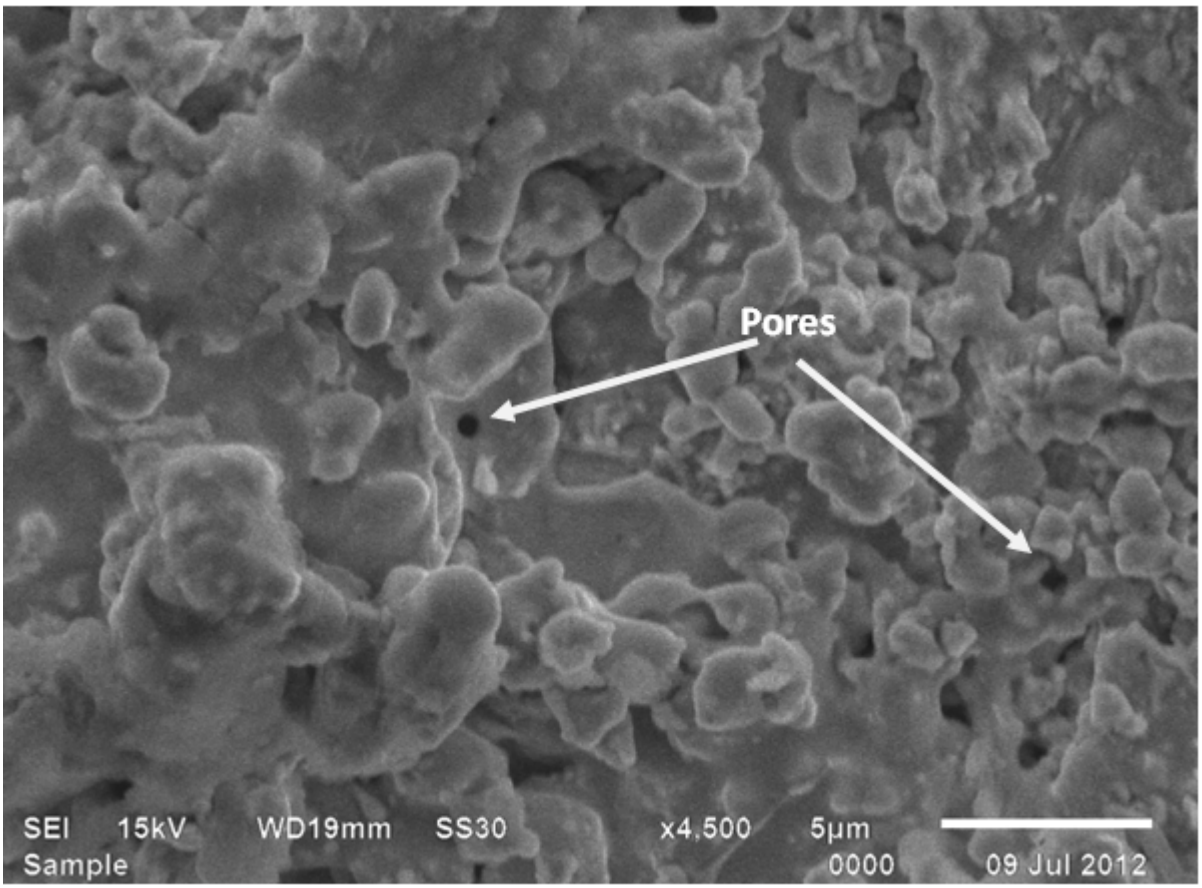

Figure 5.31 SEM of coated stainless steel 202 before erosion at 4500X

Figure 5.31 shows SEM of WC-12Co coated stainless steel 202 sample. Micrograph of the sample shows coated surface. Small pores can be seen on the surface of the sample. The micrograph is taken at 4500X.

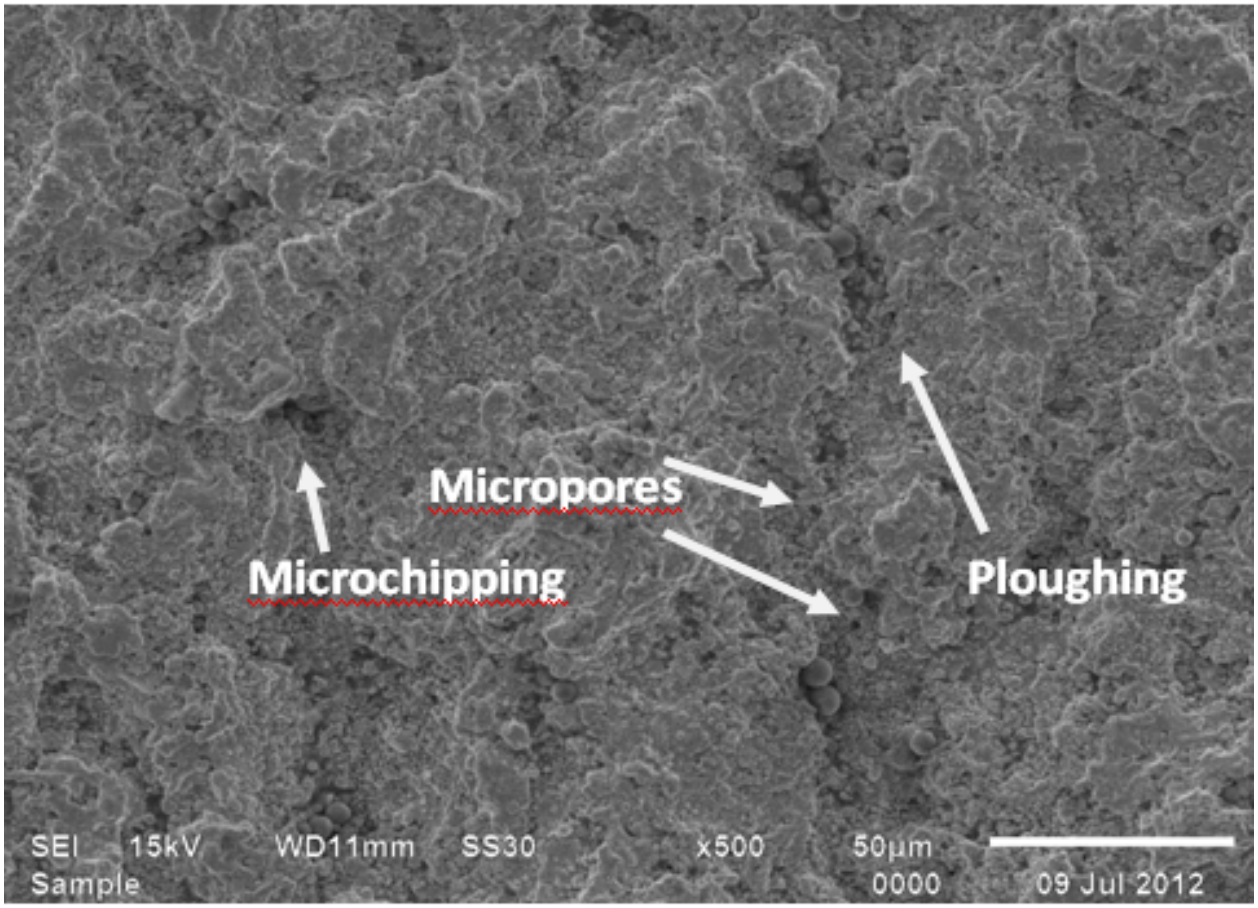

Figure 5.32 SEM of coated stainless steel after erosion with bottom ash at 500X

Figure 5.32 shows SEM of WC-12Co coated stainless steel after erosion with bottom ash at 1400rpm, 60% concentration of bottom ash and 150 minutes run time. The micrograph shows the microchipping, ploughing mechanism due to the displacement of the powder because of the eroding action of the bottom ash slurry.

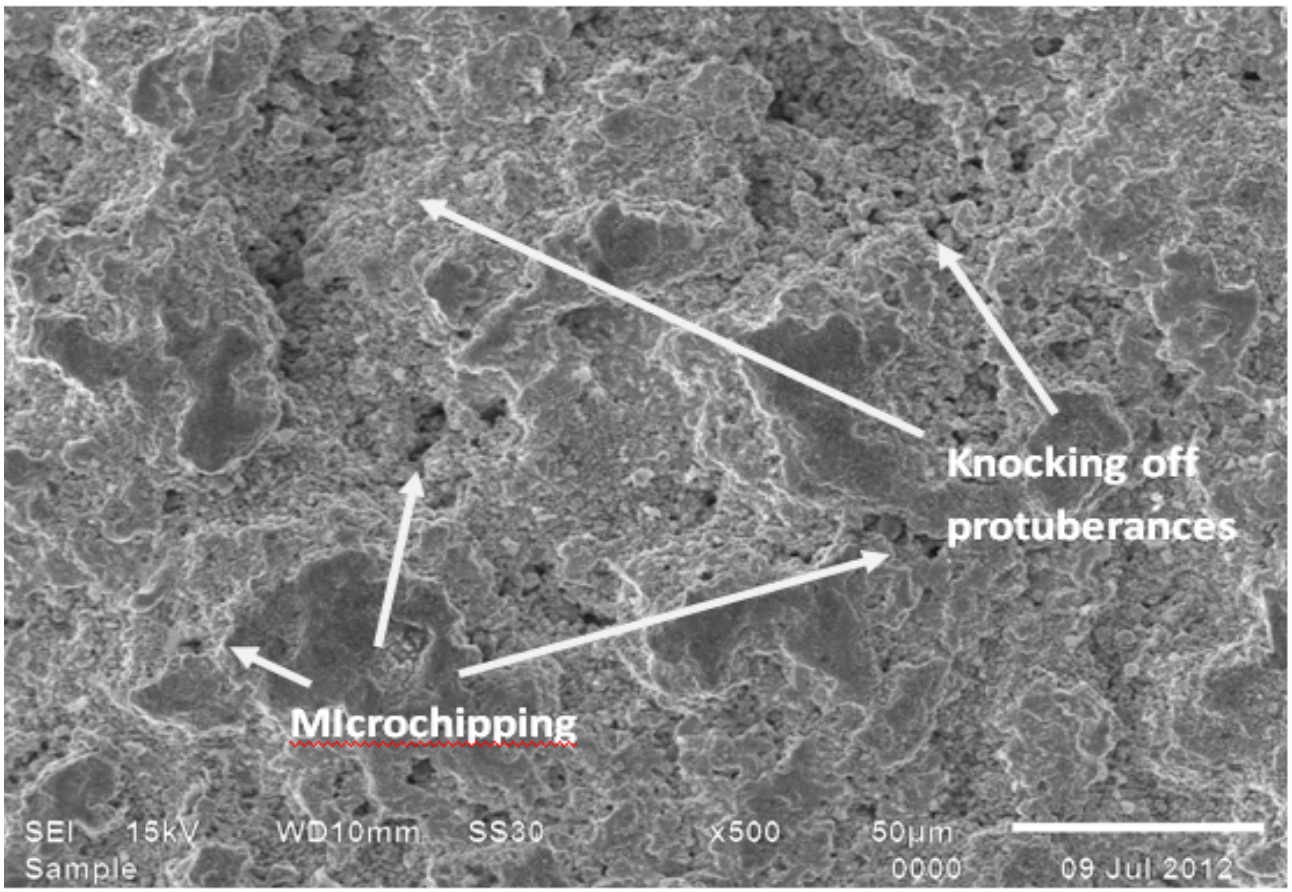

Figure 5.33 SEM of coated stainless steel after erosion with fly ash at 500X

.

Figure 5.33 is the SEM of WC-12Co coated stainless steel after erosion with fly ash at 1400rpm, 60% concentration of fly ash and 150 minutes run time. Micrograph shows microchipping on the surface of the coated specimen and knocking off protuberances.

CHAPTER-6

CONCLUSION

Erosion wear is a very common problem in the ash handling pipelines of the coal fired thermal power plants. Mild steel is most commonly used as the piping material in thermal power plants because of its low price and good mechanical properties. Therefore, mild steel was chosen as one of the test materials. Steel 202 was chosen as the second test material. Steel 202 is cheap and has better properties than mild steel. Moreover, high velocity oxy-fuel coating was done on with WC-12Co was done on these materials to further improve their properties and reduce erosion wear in pipes. Internal thermal spray coating of the pipes is possible these days. So, high velocity oxy-fuel coating was done on these materials. Experimental data was collected and the following conclusions have been drawn from the collected data.

- Bottom ash causes more erosion than fly ash
- Erosion wear resistance of steel 202 is better than mild steel for fly ash as well as bottom ash
- High velocity oxy-fuel produces coatings with excellent coatings on mild steel and steel 202 substrates
- Wc-12Co powder coating on mild steel and steel 202 increases their hardness significantly
- Erosion wear of mild steel is reduced approximately upto 4 times by the WC-12Co high velocity oxy-fuel thermal spray coating process
- Erosion wear of steel 202 is reduced approximately upto 3 times by the WC-12C0 high velocity oxy-fuel thermal spray coating process
- Ash handling pipelines can be internally coated with thermal spray processes to reduce erosion wear

FUTURE SCOPE

- Erosion wear can be evaluated using different materials
- Erosion wear can be evaluated using different coating techniques and coating powders
- The computational approach can be used to simulate the similar work with different operating conditions
- Different types slurries and testers can be used for erosion wear evaluation.

REFERENCES

1. Tavares h.l, aun p.e, maestrini a.a and magalhaes m.t(1965),"Pipeline wear in an iron ore transportation, proc.: 3rd Internayional conference, peaceful uses of atomic energy", session 42, pp. 341-344.
2. I.Tarjan. and E.Debreczeni (1972), "Theoretical and experimental investigation on the wear of pipeline caused by hydraulic transport", HT2, paper G1, pp. 1-14
3. I.M.Hutchings,R.E.Winter(1974)," Particle erosion of ductile metals: A mechanism of material removal" P.C.S, Cavendish Laboratoey, Madingley Road, Cambridge Gt.Britain.
4. A.J.Karabelas(1978)," An experimental study of pipe erosion by turbulent slurry flow", proc.HT-5, conference. paper E2, BHRA, cranfield
5. D.B.Hass, M.H.Small, W.H.W.Husband and C.A.Shook(1979)," An experimental study of wear in slurry pipelines using coarse particles" National Association of Corrosion Engineers, Clagary
6. C.A.Shook, D.B.Hass, W.H.W.Husband and M.Small(1981)," Relative wear rate determinations for slurry pipelines" Journal of Pipelines, vol.1, pp. 273-280
7. W.Tsai, J.A.C.Humphrey,I Cornet , A.V.Levy(1981),"Experimental measurement of accelerated erosion in a slurry pot tester" Wear, 68, pp. 289-303
8. K.K.S.Li, J.A.C.Humphrey, A.V.Levy(1981)," Wear of ductile metals by a particle-laden high velocity liquid jet" Wear ,73, pp.295-309
9. N.R. Steward , A.J.S. Spearing(1992)," Combating pipeline wear-an advancing technology" J. S. At,. Inst. Min. Metal/., vol. 92, no. 6.Jun. 1992. pp. 149-157
10. Rajat Gupta, S.N.Singh, V.Seshadri(1994)," Prediciton of uneven wear in slurry pipelines on the basis of measurement in a pot tester" Applied Mechanics Department, Indian Institute of'Technology, Hauz Khas, New Delhi-110016, India
11. H. W. Wang, M. M. Stack(2000)," The erosive wear of mild and stainless steels under controlled corrosion in alkaline slurries containing alumina particles" Corrosion and Protection Centre, University of Manchester Institute of Science and Technology, PO Box 88, Manchester M60 1QD, UK
12. O.P.Modi, Rupa Dasgupta, B.K.Prasad, A.K.Jha, A.H.Yogneswaran and G.Dixit(2000)," Erosion of high carbon steel in coal and bottom-ash slurries", Volume 9(5) October 2000, Journals of Material Engineering and Performance

13. H.McI. Clark, R.J. Llewellyn(2001),” Assessment of the erosion resistance of steels used for slurry handling and transport in mineral processing applications(2001)”, *Surface* Technology/Tribology Group, Innovation Centre, National Research Council, 3250 East Mall, Vancouver, BC, Canada V6T 1W5
14. Karen A Moore,Ronald E Mizia, Ray A. Zatorski(2002),” Internal Metallic Pipe Coatings for the Geothermal Industry” Zatorski Coating CompanyEast Hampton, CT 06424
15. A. K. Jha, R. Batham, M. Ahmed, A. K. Majumder, O. P. Modi, S. Chaturvedi, A. K. Gupta(2002),” Effect of impinging angle and rotating speed on erosion behavior of aluminum” Advanced Materials and Processes Research Institute, Bhopal-462026, India
16. J.G Mbabazi, T.J Sheer,R Shandu(2004),”A model to predict erosion on mild steel surfaces impacted by boiler fly ash particles”, School of Mechanical, Industrial and Aeronautical Engineering, University of the Witwatersrand, Private Bag 3, WITS 2050 Johannesburg, South Africa
17. C.N.Machio, G.Akdogan, M.J .Witcomb, S.Lyckx(2005),” Performance of WC-VC-Co thermal spray coatings in abrasion and slurry erosion tests”, Wear 258(2005) 434-442
18. Harry H.Tian, Graeme R.Addie,” Experimental study on erosive wear of some metallic materials using Coriolis wear testing approach”, Wear 258 (2005) 458-469
19. Cunkui Huanga, P. Minevb, Jingli Luoc, K. Nandakumard(2010),” A phenomenological model for erosion of material in a horizontal slurry pipeline flow”, Alberta Innovates – Technology Futures, 250 Karl Clark Road, Edmonton,
20. R.G. Rateick Jr. , K.R. Karasek , A.J. Cunninghamc, K.C. Goretta , J.L. Routbort,” Solid-particle erosion of tungsten carbide/cobalt cermet and hardened 440C stainless steel—A comparison”, Honeywell, South Bend, IN 46620, USA
21. B.S.Mann, VivekArya, A.K.Maiti, M.U.B.Rao and Pankaj Joshi(2006),” Corrosion and erosion performance of HVOF/TiAlN PVD coatings and candidate material for high pressure gate valve application. Wear, 75-82
22. Y.I.Oka ,K.Okamura, T.Yoshida(2005),” Practical estimation of erosion damage caused by solid particle impact. Part 1: Effects of impact parameters on a predictive equation”, Wear 93-101
23. J.F.Santa, L.A.Espitia, J.A. Blanco, S.A.Romo, A.Toro,” Slurry and cavitation erosion of aluminium alloy”, Wear(2009) 160-167

24. Jain S.C, Gandhi B.K, Desale G.R(2009),” Particle size effects on the slurry erosion of aluminium alloy”, Wear(2006) 1066-1071
25. S.L. Liu, X.P. Zheng, G.Q. Geng(2010),” Influence of nano-WC-12Co powder addition in WC-10Co-4Cr AC-HVAF sprayed coatings on wear and erosion wear behavior”, School of Materials Science and Engineering, Chang’an University, Xi’an 710061, PR China
26. Milind Suryaji Patil, Eknath R.Deore, Ramachandra S Jahagirdar ,Santosh V Patil,” Study of parameters effecting erosion wear of ductile material in solid-liquid mixture”, Proceeding of World Congress of Engineering 2011 Vol 4 july 6-8, 2011
27. Adarsh Kumar , Pawan Kumar Sapra, Sanjeev Bhandari,” A review paper on slurry erosion of plasma and flame thermal sprayed coatings”, national conference on advancements and futuristic trends in mechanical and materials engineering (oct. 7-8,2011)
28. C.S. Ramesha, D.S. Devaraja, R. Keshavamurthya, B.R. Sridharb,” Slurry erosive wear behaviour of thermally sprayed Inconel-718 coatings by APS process”, Department of Mechanical Engineering, PES Institute of Technology, Bangalore, India.
29. Deepak Kumar Goyal , HarpreetSingh , HarmeshKumar , VarinderSahni,” Slurry erosionbehaviourofHVOFsprayedWC–10Co–4CrandAl2O3þ13TiO2coatings on a turbine steel”,Baba Banda Singh Bahadur Engineering College, Fatehgarh Sahib140407 ,Punjab, India
30. Deepak KumarGoyal , HarpreetSingh , HarmeshKumar , VarinderSahni,” Slurry erosive wear evaluation of hvof-spray Cr_2O_3 coating on some turbine steels”, Baba Banda Singh Bahadur Engineering College, Fatehgarh Sahib140407 ,Punjab, India